THEORY, DESIGN AND IMPLEMENTATION OF TIME OPTIMAL DIGITAL POSITION CONTROL

THEORY, DESIGN AND IMPLEMENTATION OF TIME OPTIMAL DIGITAL POSITION CONTROL

By

BARNA SZABADOS

Diplôme E.N.S.I. Grenoble

M.Eng. McMaster University, Hamilton

A Thesis

Submitted to the School of Graduate Studies

in Partial Fulfilment of the Requirements

for the Degree

Doctor of Philosophy

McMaster University

September 1971

DOCTOR OF PHILOSOPHY (1971)
(Electrical Engineering)

McMaster University
Hamilton, Ontario

TITLE: Theory, Design and Implementation of Time Optimal Digital Position Control

AUTHOR: Barna Szabados, Diplôme d'Ingén. (E.N.S.I. de Grenoble)
M.Eng. (McMaster University)

SUPERVISOR: Dr. N.K. Sinha

NUMBER OF PAGES: 156, ix

SCOPE AND CONTENTS:

The theoretical problem of the minimum time position control is investigated and leads to an original switching characteristic.

A digital bang-bang controller is built using the above control law, and a new digital tachometer is developed to improve angular velocity readings.

ABSTRACT

The following study is an attempt to design a minimum-time digital position controller.

The investigation of the theoretical problem of the minimum time position control leads to a survey of stepping motors, which seem to provide a natural solution to the problem. However the permanentic d.c. motor is shown to be more suitable. Approximate switching characteristics are derived from the mathematical models chosen.

Quantizing the shaft position, a digital controller is practically implemented and the experimental results confirm the theory.

To solve the trickiest problem of measuring the velocity of the shaft, a new concept of digital tachometer is derived and implemented. Providing a very high precision and resolution, the new tachometer proved itself much better than any other instrument available now, and its direct application to the controller simplifies the latter and improves it considerably.

REMERCIEMENTS

Ce travail a été effectué au Laboratoire d'Electrotechnique de McMaster University, à Hamilton, grâce à l'agrément de son Directeur Dr. S.S. Haykim.

Je suis heureux d'exprimer ici toute ma reconnaissance à mes co-directeurs de recherche, au Docteur N. Sinha et à Monsieur le Professeur Commandant C. diCenzo, qui ont su me prodiguer les conseils précieux de leur expérience. Qu'ils soient remerciés tout particulièrement de l'ambiance de bonne humeur et de franche liberté qui ont régnées dans ce Laboratoire. Je leur suis reconnaissant de la confiance qu'ils ont su m'accorder tout au long de ce travail.

J'adresse également ici mes remerciements au Docteur C.K. Campbell qui a bien voulu me prêter l'équipement de son laboratoire et principalement son groupe de calcul qui m'a servi au plus haut point.

Je voudrais aussi manifester ma gratitude au "National Research Council" qui a financé le projet, et au "McMaster University Research Board" qui a apporté une aide financière additionnelle très précieuse qui a permis de construire un modèle expérimental du tachomètre.

Enfin mes remerciements vont à tout le personnel enseignant du Département, et particulièrement au Dr. Kitai et à son équipe qui m'ont beaucoup aidé dans la partie digitale du projet.

Je voudrais mentionner aussi tous mes camarades et personnel du Laboratoire qui ont toujours manifesté une franche camaraderie et même amitié.

NOTATIONS USED

EM : electromagnetic

PM : permanentic (permanent magnet excitation field)

Ω : speed in rd/s

E : no-load voltage

U : armature voltage under load conditions

i : field excitation current

I : armature current

$\delta=E-U$: total voltage drop within the machine

ε : armature reaction

λ_m, λ_r : electromagnetic motor torque and resistive torque transferred on the rotor shaft

R : armature resistance (include inter-poles if that is the case)

L : armature equivalent inductance seen from the input of the machine

a,b : friction coefficients

J : moment of inertia

All results are given in the MKSA system of units.

TABLE OF CONTENTS

TABLE OF CONTENTS (cont'd) Page

TABLE OF CONTENTS (cont'd) Page

LIST OF GRAPHS AND FIGURES

LIST OF GRAPHS AND FIGURES (cont'd)

LIST OF GRAPHS AND FIGURES (cont'd)

CHAPTER 1

INTRODUCTION

1.1 Statement of the Time-Optimal Position Control Problem

The control of the angular position of a shaft is quite an old, yet important, problem and has been solved in many ways. The problem gets a little more involved if it is required that a given change in the angular position be obtained in minimum time.

If the angular displacement, angular velocity and armature current are chosen for state variable representation of an electrical motor having a constant excitation field, as often used in servomechanisms, the following definitions can be written.

$$\left.\begin{aligned} x_1(t) &= \theta(t) && \text{angular displacement} \\ x_2(t) &= \frac{d\theta}{dt} = \Omega(t) && \text{angular velocity} \\ x_3(t) &= I(t) && \text{armature current} \end{aligned}\right\} \qquad (1\text{-}1)$$

Any electrical motor can be described by two basic equations. The electrical equation expressed at the level of the armature voltage can be stated as

$$\boxed{\begin{matrix}\text{Armature} \\ \text{Voltage applied}\end{matrix}} = \boxed{\begin{matrix}\text{counter e.m.f.} \\ \text{generated}\end{matrix}} + \boxed{\begin{matrix}\text{Joule Volt.} \\ \text{drops}\end{matrix}} + \boxed{\begin{matrix}\text{Inductive} \\ \text{e.m.f.}\end{matrix}} \qquad (1\text{-}2)$$

From the basic conservation of energy, a mechanical equation relating the different torques developed on the shaft can be written as

Electrical Torque produced on the shaft	=	Frictional torque	+	Inertia Torque	+	Load Torque	(1-3)

These sets of equations permit one to describe the system and can also be used to determine the control law.

The optimum control to obtain minimum time will be achieved by varying the developed torque in a bang-bang manner, thus requiring step changes in the armature or field current (the other current being held constant in the conventional mode of operating of a d.c. servomotor).

In practice, such changes are ruled out due to the inevitable presence of inductance. Further complications are introduced due to non-linearities of inductance and resistance, and the effect of dead-zone caused by static friction.

Therefore, it may be said that a practical solution of the minimum-time control problem is still unavailable.

1.2 Some Problems in Implementation

The position control problem has been very widely used, and one can say that almost any control system has somewhere a minor-loop realizing positioning. The general implementation is realized by monitoring the angular velocity with analogue tachometers, and the angular position by a multiturn potentiometer giving an analogue voltage measuring the position. This voltage is compared to the desired position analogue voltage, hence generating an error function called "distance from the target", to be minimized and brought to zero.

This closed-loop control is very well known and its implementation

is versatile. Such factors as damping, inertia, overshoots etc., have to be considered, and a proper choice of gain and feedback can improve considerably the time-response. Unfortunately, the true minimum-time response cannot be achieved because the switching characteristics previously discussed are unknown.

1.3 Industrial Applications

The continuous analogue servomechanism is widely used and quite well known. Unfortunately, even for complete packaged servos, long, precise empirical adjustments have to be made, and the analogue signals are often very noisy and of relatively poor accuracy and resolution. Furthermore, the constant development of digital instrumentation, the use of direct computer drive, and the evolution of the discrete control system theory, along with cheap digital logic components lead to a desire of direct digital servomechanisms.

In many applications, for example, a machine tool, the dead-time when the machine cannot be used for effective production occurs during the changes of position. In another field, computer science, the speed of access to outside units, tapes or other recorders and printers is limited. Those peripherical units are very slow compared to computer speeds, and each of them is a position servo. Therefore, the minimum-time position problem is very much desired and multiplies considerably the possibilities of a computer. Moreover, if the control can be digital, no analogue interface is needed, the computer can control the servo directly.

Hence, in many applications the minimum time problem is encountered, often together with heavy loads, and the choice of direct digital control has become increasingly popular.

1.4 Outline of the Thesis

Chapter II gives a survey and analysis of steppers in control application. These devices seem to suit particularly the position control problem, and the minimum-time control is discussed on a specific example.

In Chapter III the permanentic d.c. motor is shown to be much more suitable for very fast responses and bang-bang control. The investigation of the minimum-time position problem, using exact mathematical models, leads to a set of practical switching characteristics, which, although resulting from an approximation, give very good practical solutions, and are general for any d.c. motor.

Chapter IV describes a general design method for determining a bang-bang position controller using the switching curves previously derived. A quantization of the switching curve leads to a direct digital control.

Chapter V presents experimental set ups and results, followed by discussions and criticisms of the design leading to the need of a digital instrument measuring the angular velocity.

Chapter VI surveys the existing digital methods to determine angular velocities and shows how inadequate these devices are for the minimum-time position problem.

Therefore, a new idea is proposed and an entirely new concept is

developed for measuring rotating shaft velocities. The principle of the instrument is developed.

Chapter VII presents the effective design and implementation of the "high precision digital tachometer" previously derived, together with experimental results and possible applications.

Finally, Chapter VIII shows how this new digital tachometer fits perfectly the minimum-time position control problem and that the performances expected are very close to the theoretical minimum-time, with a possible extension to on-line identification in the case of variable load parameters.

CHAPTER II

STEPPERS IN CONTROL APPLICATIONS

2.1 Historical Background

The idea of mechanically stepping in angles goes as far back as the clock escapement. However, the first known electrical step motors were used in the Royal Navy in the 1930's for a remote positioning system for transmitting shaft rotations. The step transmitter was a simple switch [A10, 12]. This system was adapted later by the U.S. Navy and used widely in World War II.

During that period rotary solenoids were used for steering torpedoes, using a serial pulse train. But at that time the conventional continuous closed-loop servosystem had many advantages; size, speed, accuracy as well as resolution. Moreover, digital devices and control logic for all-digital systems were not yet available. Hence, closed-loop continuous servos were predominant in the period of 1944-1957 [A12].

In 1957 only one machine tool application was reported using a stepping motor of larger size [A1], discussed further on.

From that time interest has been growing in stepping motors, to provide automatic drives compatible with computers and digitally stored programs [A12].

In 1960-1961, S.J. Bailey [A2,3,4,5,6] published a series of articles describing briefly the interest and applications of steppers. A few attempts have been made to present some oversimplified equations

and operations [A7,8,9,11,12].

One has to wait till 1965 to see Baty [A13] and mainly Fredriksen [A14] publishing a thorough study of performance and application of a stepping motor.

Then, in 1968-1969, more precise studies involving steppers have been brought to knowledge [A18,19,20,21,22,23,24,25]. The apparent simplicity, together with the evolution of the electronic switching devices boosted the growing interest in steppers.

2.2 Classification of Steppers

Depending on the criteria chosen, steppers can be classified in many ways. S.J. Bailey [A3] used 5 different criteria:

a) two basic types - phase pulsed synchronous and solenoid ratchet type

b) step starting and stopping methods

c) rotation (uni or bidirectional)

d) inputs and output acceptance

e) output torque.

A brief qualitative description follows and will enable the understanding of the basic operation of the two type of steppers.

2.2.1 Solenoid Ratchet Type [A3]

A simple stepping device with electromagnetically preloaded actuating springs is shown in Figure (2-1).

The critical elements are the dynamic ones: armature, armature

SOLENOID-RATCHET STEPPER

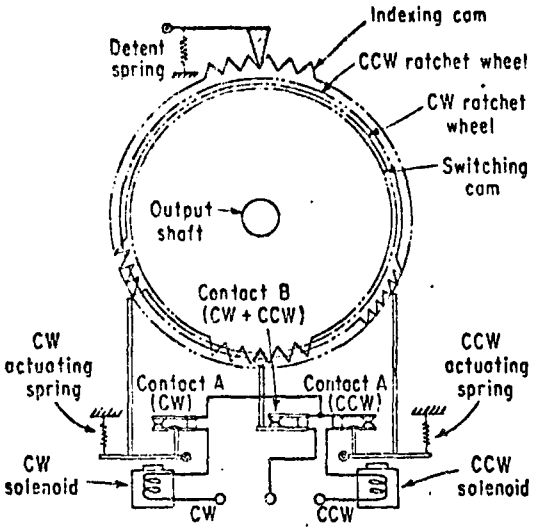

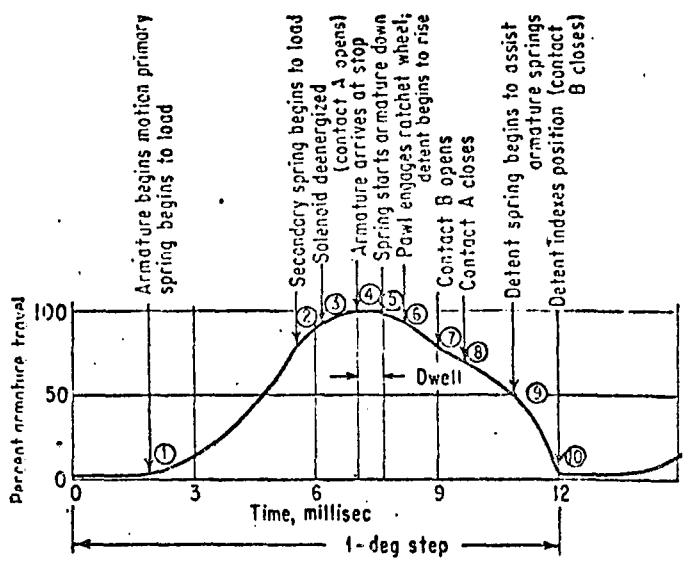

FIG 2-1: Simple stepping device, typical of the solenoid-ratchet type and B—its armature travel during a single step of its output shaft.

hinges, bearing, contacts, ratchet wheels, pawl and detent.

The mechanical detenting is chosen to provide accurate positive steps and prevent wandering. The detent spring at the top aids the armature spring action in the final stage of deceleration while preventing overshoot. Using an optimum solenoid force, armature motion is reduced to a minimum.

Armature hinge and bearings must be carefully designed for minimum friction. The actuating ratchet wheel enables a one-step travel if a current pulse appears, or a repetitive stepping while continuous current is applied.

This particular stepper described is actuated by a 28V - 1A pulse of 10-15 ms duration. As obviously seen, this stepper is very complicated and requires very precise mechanical adjustments. The mechanical movements generate very long mechanical time constants and hence only very low frequency pulses can drive this stepper.

2.2.2 Phase Pulsed Synchronous Type [A26]

Detenting and holding in the reference position is accomplished magnetically.

The Two-Phase Synchronous Motor

For simplification, Figure (2-2) shows two phases which produce fluxes in quadrature (for a multiple stepper the electrical angle is considered).

Each phase can be excited with positive or negative current. The vector flux resultant from a given excitation defines a magnetic axis

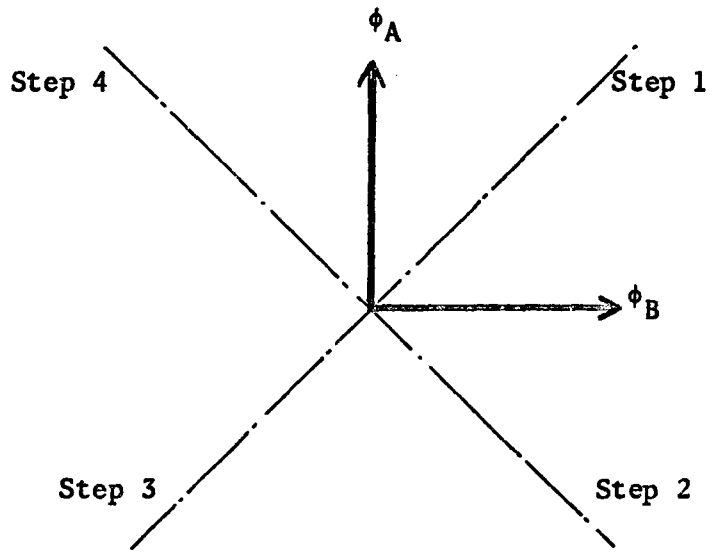

Control Law

CW

A	B	St
+	+	1
-	+	2
-	-	3
+	-	4

CCW

A	B	St
+	+	1
+	-	4
-	-	3
-	+	2

TABLE A

Fig. 2-2 Stepping Motor Principle

called "step".

A magnetic moment $\vec{m}$ placed in this field will tend to align itself with it according to Maxwell's minimum flux rule.

Table A of Figure (2-2) describes the excitation sequence which will produce stepping either clockwise (CW) or counter clockwise (CCW).

Usually a synchronous stepping motor has 2n poles on the stator (50 to 200 poles) and the rotor consists of 2n permanent magnet multipoles. One actuating pulse will cause the shaft to rotate an incremental angle of $\frac{1}{2n}$ of a turn.

The two-phase synchronous motor is the most widely used nowadays, and therefore it will be discussed further on in much greater detail.

2.3 Comparison of a Continuous Control System with Incremental Servos

Incremental servos offer many of the advantages of closed-loop systems and minimize some troublesome or critical design problems.

Figure (2-3) shows the basic control diagrams of the same control function using continuous and incremental instrumentation.

Synthesis of the conventional system involves careful choice of several matched components and ultimate empirical adjustments of gain and stabilization to an optimum compatible with expected load variations. Even a packaged servo requires final adjustments.

On the other hand, an incremental servo specified for a certain load, torque, input, response time, positioning error, etc., can be used with a minimum amount of further adjustments. On the block diagram shown, a one-to-one correspondence of output shaft position to

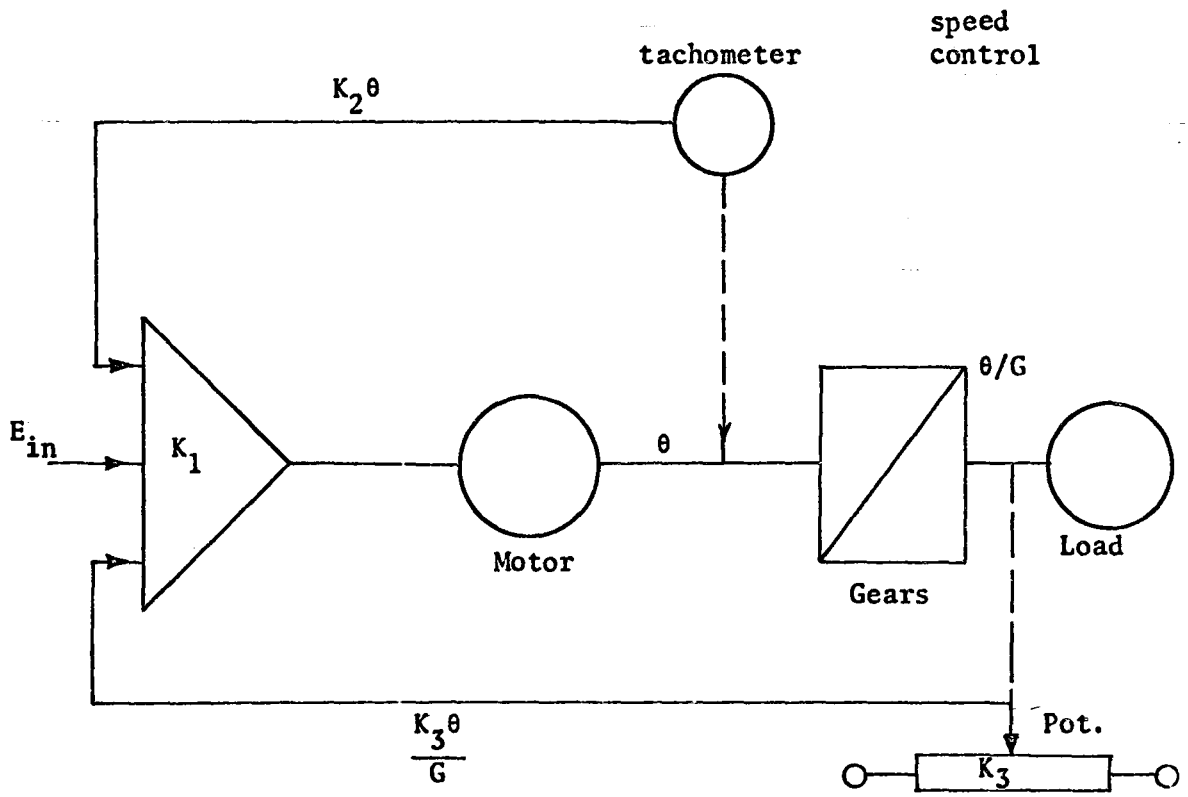

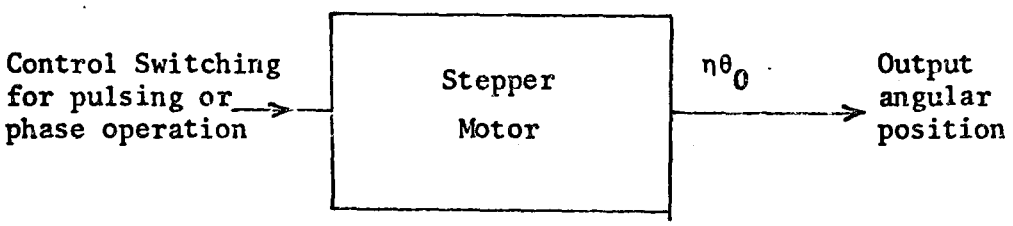

Fig. 2-3 Analogy of a continuous feedback control and an incremental stepper.

input signal results. Physically this resembles the feedback of a conventional positioning servo.

However, the stepping motor does not give a "true" position because it does not "measure" the position of its output shaft. If no system which keeps track of the past history of the stepping is incorporated (for example an up-down counter) the stepping motor responds only in a relative position displacement.

Figure (2-4) provides a concise comparison of the two velocity servo-types [A2].

The outstanding physical distinction is that whereas the velocity servo gets its linearity through high loop gain, the incremental servo derives its linearity from a carefully designed mechanical, or electrical detenting. The inherent stability of a stepper as compared with a stepless feedback device is perhaps the most important functional distinction. However, this same stability may become a problem under certain load conditions as discussed further on.

2.4 Versatility of Incremental Servos [A4]

A very brief survey shows here that conventional feedback control systems can be successfully replaced by a stepper in some applications.

- Stepping servo: usually a stepping motor replaces the block [amplifier-motor-tachometer and gear train] as shown on Figure (2-3).

Fig. 2-4 TABLE I—VELOCITY AND INCREMENTAL SERVOS COMPARED

CHARACTERISTICS	VELOCITY SERVO	INCREMENTAL SERVO
Nature of device	Displacement input, rate output	Pulse rate input, stepping rate output
Operational effect	Integration	Finite summation (may be analyzed as an integrator under certain conditio
Angle or distance of output member travel	Time integral of analog input	Exactly determined by number of input pulses
Inputs	Analog voltage—other inputs through D/A converter	Uniform pulse train or random positive or negative pulses—analog sign through A/D converter
Velocity feedback	Output member rate	Not required—may be used for self-stepping or hold gating
Loop gain-linearity	Set high for high linearity	Stepping linearity does not require feedback
Stability (as position servo)	With position feedback loop, depends on rate damping (non-dissipative), dissipative damping, and/or lead networks	Not ordinarily a problem when operated open-cycle as a position contr when operated closed-cycle, stability is a function of step-to-signal fr quency ratio
Error	With position feedback loop, depends on feedback transducer resolution and linearity, quadrature, noise, stability, etc.	Depends on accuracy of individual stepping mechanism within limits designed stepping rate
Resolution	Governed mainly by feedback transducer resolution assuming high loop gain	Depends on built-in step size
Response time	50 millisec, time to achieve maximum error correcting rate in typical instrument servo	10-30 millisec, time to complete one step (typical); total time depends error size
Frequency bands	Zero to high frequency response device	Relatively low frequency response device
Torque	Obtained through reduction gea. train	Usually available at output shaft of stepping device
Load variation	Develops driving torque through error feedback	Has no influence on motor drive under proper detent conditions
Digital programming	May be adapted with D/A input device and data encoder on output shaft	May be commanded directly by computer or tape pulse train
Two-mode operation (slewing or inching)	Readily adapted	Readily adapted—many steppers will slew as well as step
Quiescent power	Must be fully energized while awaiting command	Zero power drain while awaiting command
Life—reliability	Dependent on amplifier, motor tachometer, feedback potentiometer, and gear train	Dependent on pawl, ratchet, or other mechanical and electrical elements a single motor
Cost	Dependent on cost of amplifier, motor, tachometer, feedback transducer, and gear train	Dependent on cost of single torque unit, with or without control trigger

- Proportional control: can be suited for a self-balancing potentiometer.
- Pulse to analogue conversion: the stepper is actuated by a pulse train, and the shaft is connected to a multi-turn potentiometer giving the analogue conversion.
- Analogue to analogue conversion: the stepper acts as a filter to eliminate harmonics, noise, quadrature and phase shift (can be used for d.c. to a.c. or a.c. to d.c. conversion).
- Vector addition: both electrical and mechanical solutions are offered. This can lead to a function generator easily.
- Error signal storage: the stepper accepts saturation error signals, stores them, and resubmits them when critical servo features are vanished.
- Pulse summation: two steppers drive a differential multiturn potentiometer giving the analogue equivalent of the algebraic sum of the two pulse-trains.
- Remote stepper interlock: when the stepper has completed a full unit step, it signals the interlocking trigger to pulse the other stepper which signals back his completion of its step. This process gives a complete synchronization.
- Assynchronism detection: any differential voltage between two output pots causes one stepper to take an extra step, restoring synchronism (this could only be done digitally).

These functions, easily implemented could be used for control systems for pressure transducer calibration, improving response near null, altitude hold servo, railroad car sorting, digital differential altimeter, weighing station and many other applications [A2].

Without going into details here the performance range where stepping motors are used successfully can be illustrated in two examples [A5,12].

In the first one an instrument stepper has an accuracy (stepsize) of 3 minutes of arc and can step up to 100 pulses/sec. Hence, the maximum rotational speed is less than 1 rpm. The output torque is very low, ranging from 1 to 50 oz-inches.

At the other extreme, a second example consists of a "power" stepping motor, capable of driving a table on a milling machine. It could step at 350 steps/sec., giving a speed of 175 rpm. The stepsize is 3 deg of angle and the output torque culminates at 3000 lb-inches. However, the power does not exceed 1/2 HP. No stepping motor, with a reasonable price and resolution has been tried above 1 HP range in this literature survey, and hence it has been found that, although very versatile, the stepping motor has a limited use especially in power actuating systems.

2.5 Advantages and Limitations

Briefly, the main advantages of the incremental servo over conventional continuous systems could be discussed as follows [B14]:

- When properly applied, the stepping motor offers all the desirable features of a feedback system, without hunting or instability problems.
- Careful fabrication enables very small errors with relatively clear null threshold.
- Inherent low velocity without gear reduction, and possessing close speed control over a wide range.
- Low starting currents are used.
- Minimum wear and maintenance is required hence no mechanical contact is needed for electromagnetic steppers.
- Instant and quiet step response is obtained and if the input pulse is well chosen no skipping of steps occurs.
- Power consumption in quiescent periods can be reduced to zero.
- Use of an essentially digital system follows recent trends established in control systems.

However, some limitations prevent the stepping motor from being the universal solution for modern control systems. These are

- Low, to very low efficiency.
- Relative low torques and always small size motors only.
- Some types are sensitive to heat (torque can decrease by a factor of four!)
- A fundamental limit is on load inertia. Overshoot, increase of response time and limit of stepping rate are the main inconveniences.
- Stepping motors are essentially low frequency devices.

- If damping cannot be adjusted, and if a proper size motor is not available, a mismatch results in a rough, hammering drive, furthermore, these matchings are very much load sensitive.

2.6 Discussion of a Specific Application: A Bang-Bang Position Controller

2.6.1 Description of the Proposal

T.R. Fredriksen describes an interesting application of the closed-loop stepping motor [A18]. The article presents a near optimal time controller, which, with a scheme of discrete-state variable instrumentation, operates the stepping motor as a digital position servo.

In fact, as will be seen, only a near time-optimal servomechanism is designed based on a second-order transfer function model with a rather coarse staircase approximation to the switching curve.

A Bipolar winding two phase synchronous stepping motors is used. Hence, four stator windings A_1, A_2 - B_1, B_2 are energizable. Each winding has only two states, either completely energized or turned off. That means no inversion of current is necessary and only positive pulse drive is used, as the two windings of each phase produce opposing fluxes in the machine.

Table C of Figure (2-5) gives the correct driving sequences for the different modes to be applied, out of the 8 unique configurations.

Each input pulse causes the rotor to lock itself in one of the steady-state positions. As a result the motor shaft can be stepped in fixed increments.

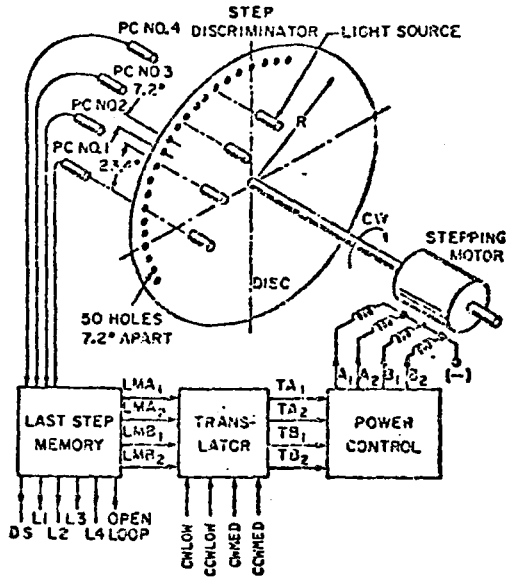

Fig. 2-5 Implementation of a bang-bang position controller using a stepper.

Control mode	Rotor Position				Control mode
2 phases	1	2	3	4	1 phase
CWLOW	B_1	A_2	B_2	A_1	CW
CCWLOW	A_1	B_1	A_2	B_2	STOP
CWMED	A_2	B_2	A_1	B_1	HISPEED
CCWMED	B_2	A_1	B_1	A_2	CCW
STOP	A_1B_1	A_2B_1	A_2B_2	A_1B_2	CWLOW
CW	A_2B_1	A_2B_2	A_1B_2	A_1B_1	CWMED
CCW	A_1B_2	A_1B_1	A_2B_1	A_2B_2	CCWLOW
MISPEED	A_2B_2	A_1B_2	A_1B_1	A_2B_1	CCWMED

Table C

The closed-loop stepping motor principle is based on the fact that if the type of the steady state position when the motor locked itself in at any given time is known, a complete set of unique motor actions can be sequenced. Those sequences are well defined and a control, based on the knowledge of the previous state can be designed.

The step discriminator is set up for a 1.8 deg. stepping motor and feeds pulses to the "last step memory", which applies a zero-order hold and converts the signal into a 2 bits code for logic. The translator operation is found from table C and gives the driving functions as:

STOP = CWLOW + CCWLOW

CW = CWLOW + CCWMED

CCW = CCWLOW + CCWMED

HISPEED = CWMED + CCWMED

Both forward and reverse torques are available by selecting and switching the proper inputs, hence, because of its digital nature, the plant is inherent to bang-bang control.

T.R. Fredriksen considers the case of a two dimensional controller only. Positional error (distance in steps from the target) and motor velocity are used as control state vectors.

The relative position is chosen here, that is to say counting the steps travelled from an initial position corresponding to the last position where the shaft has locked in.

Figure (2-5) describes the experimental plant using a Slo-Syn Model SS250 stepping motor, which moves a carriage through a lead

screw-drive. The specifications are 512 steps travelled, within 300 ms, correction of overshoots are permitted within 30 ms after being detected by the new position checker.

The basic concept and design are following the chart

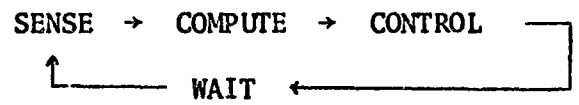

Sense: measuring the state of the system.

Compute: calculates the new control from past history, present state, and prevailing algorithm.

Control: setting plant parameters and control inputs.

Wait: delays due to sharing or processor sampling rates.

A three-step final trajectory approximation is chosen to build the controller, each region of the state space corresponds to a pre-determined control sequence. Some experimental verifications are reported by Fredriksen.

512 steps are reached as 200 ms acceleration time. The 2000 steps/sec corner is well noted as a "hash-spot" and 1000 steps/sec level is more distinct (10 ms flat where control oscillates). Then the deceleration brings the plant towards a low speed of 200 steps/sec. Finally, at the target step, the motor locks on the final steady state position with a certain amount of ringing.

Ignoring the ringing the final stage is reached in 298 ms, while the optimum case would be 279 ms.

2.6.2 Some Criticisms

Positive

(a) It is certainly an elegant way of solving the position control problem, with reliable instrumentation and almost no further adjustments of the controller once it is built, hence a checking-loop correcting any malfunction is included.

(b) Exclusively digital instrumentation, allowing very fast controller response is used.

(c) Self-locking in a final steady-state position is realized.

(d) The checking-loop corrects at low speed control the errors, hence, no hunting will occur.

(e) Bipolar windings allow a better commutation because no inversion of current is necessary to produce reverse flux, and further more only positive pulsing power control is needed.

Negative

(a) Very sensitive to load.

(b) Oversized stepping motor has to be used.

(c) The low efficiency of the inherent functional mode of the stepping motor is reduced by the control law which applies reduced torques by using only partly the windings. Only 1/2 of the copper is used at the best and 1/4 at the worst.

(d) The controller is only near-time optimal. Maximum accelerations and decelerations are not used at all for fear of losing synchronism. A compromise is really presented by Fredriksen.

(e) The system design is based on a pulse control of given frequency.

By varying the control law the same pulse frequency is split into different speed levels (low-medium-high). This concept gives good results for this specific application, but the more stringent the load is, the more the system is away from time-optimality. To obtain better performances, different pulse frequencies ought to be used, resulting in very expensive instrumentation for slight improvement only.

(f) The near minimum time controller is designed for a maximum of 512 steps. Any other destination diverges from the time-optimum concept.

(g) The switching staircase is an experimental curve and does not allow generalized applications.

As a summary, this position controller, although elegant in implementation is suitable only for the specific application and any other use requires a completely new analysis and probably new concepts. Fredriksen himself writes: "However, the controller can only set up a control sequence based on the state of the plant, and thus, the state variables must be selected and instrumented before any bang-bang control can be implemented".

The example of this controller shows that if a stepping motor is utilized in a minimum time controller, the design is empirical only, using an oversized power supply, and reaching really a "fast response" but so far from minimum-time performances that it should not even be called "near minimum-time".

2.7 Conclusion

Although the stepping motor appears very suitable for position control, it is not useful for the minimum-time problem. However, the study undertaken in this chapter was of great use because the bang-bang controller derived later is directly inspired from Fredriksen's model despite the fact that the stepper actuator has been replaced by a permanent magnet excitation direct-current servomotor called "permanentic".

CHAPTER III

MINIMUM TIME POSITION PROBLEM USING A PERMANENTIC D.C. MOTOR

3.1 Advantages of the Permanentic D.C. Servo Motor [B14]

The principle of the d.c. electric motor has been known for almost 150 years, from the origin of the electrical engineering science, therefore, designing and manufacturing does not present any problem. The only weakness lies in the use of a mechanical commutator bar on the rotor and the existance of brushes. However, the present designs are near optimum.

A permanentic d.c. motor can be called a very efficient mechanical energy converter. The excitation flux is provided by permanent magnets of high quality, and the existing materials like Alnico IV for example, allow a very good stabilization of the magnetic circuit (either open-circuit or short-circuit, whichever is needed). The B-H curves of those alloys are of rectangular shape and allow a lot of energy to be stored. The shaping of the poles help the brush commutation and also lower the leakage factor.

The efficiency of the copper windings in a d.c. machine depends on the number of slots and the number of conductors per slot. Nowadays a near optimum is reached in the design of windings.

These design considerations lead to permanentic d.c. motors of 10 HP, on the other hand no synchronous stepping motor has been produced on an economical and reliable basis over 3/4 HP.

The torque characteristics of a d.c. motor are interesting. In a good approximation the torque produced in a permanentic d.c. motor is proportional to the armature current [B12,13], thus a smooth acceleration and deceleration response results. The steady state speed is smooth, provided rotor inertia is not too low.

In most cases no oscillations occur because the damping coefficient is chosen to make the system slightly overdamped. With a rigourously constant step voltage, maximum acceleration is produced very simply. A load variation on the shaft affects only the steady-state speed. All these features seem to adapt perfectly to the bang-bang control procedure.

A single power drive source, able to provide sufficient peak current for starting can be used. By construction a permanentic d.c. motor can withstand step voltage starting without any additional series resistors added to the armature circuit limiting the starting current. This feature is predominant and makes the permanentic d.c. motor preferable to any other motor in control loops where starting strains are often required.

As a result the permanentic motor is more suitable for medium power control, and particularly for controls requiring high accelerations and torques. Its relative sturdiness makes it attractive for such applications.

3.2 Mathematical Representation of the Permanentic Motor

In a previous work [B10] very precise mathematical models for d.c. motors have been derived.

A recent publication [B11] summarized the methods of measuring the main parameters of a d.c. machine in a dynamic behaviour, and in further publications [B12,13] the mathematical models obtained for d.c. motors are analyzed and compared with experimental results.

The following work has been based on those mathematical models and represents an application for their use.

The general results are summarized in the next equations and provide a precisemodel for the permanentic servo motor.

Differential equations describing the system are

$$\left.\begin{aligned} U_m(t) &= K\Omega(t) + R(I) \times I + L(I)\frac{dI}{dt} - \varepsilon(I,i) \\ KI &= a\Omega(t) + b + J\frac{d\Omega}{dt} + \lambda_r(t) \end{aligned}\right\} \qquad (3\text{-}1)$$

In general R and L are functions of the armature current as presented in [B10,11].

If the second-order mathematical approximation is used (3-1) becomes

$$\left.\begin{aligned} U(t) &= K\Omega + RI + L\frac{dI}{dt} \\ KI &= a\Omega + b + J\frac{d\Omega}{dt} \end{aligned}\right\} \qquad (3\text{-}2)$$

where K, R, L, a, b, J are constants for a given load.

It has to be noted that equation (3-2) is valid only for $|I| > b/K$ if $\Omega=0$, and the armature current I must exceed b/K in order to overcome the static friction torque b.

3.3 Investigation of the Minimum Time Problem

The three state variables chosen, being the angular displacement $\theta(t)$, the angular velocity $\Omega(t)$ and the armature current $I(t)$ as defined by equation (1-1), the equations (3-2) can be rewritten in matrix notation as

$$\dot{\underline{x}} = \begin{bmatrix} 0 & 1 & 0 \\ 0 & -\frac{a}{J} & \frac{K}{J} \\ 0 & -\frac{K}{L} & -\frac{R}{L} \end{bmatrix} \underline{x} + -\begin{bmatrix} 0 \\ \frac{b}{J} \\ \frac{U}{L} \end{bmatrix} \tag{3-3}$$

It is required to find the control law $U^*(t)$ which will transfer the state from

$$\underline{x}(0) = \begin{bmatrix} 0 \\ 0 \\ \frac{b}{K} \end{bmatrix} \tag{3-4}$$

to the final state

$$\underline{x}(t_f) = \begin{bmatrix} \theta_f \\ 0 \\ \text{unspecified} \end{bmatrix} \tag{3-5}$$

in minimum time, subject to the constraint

$$|U(t)| < U_0 \tag{3-6}$$

which may be regarded as the constraint introduced by a constant voltage power supply.

The minimum-time problem may be considered as the minimization of the integral cost function

$$\phi = \int_0^{t_f} dt \quad . \tag{3-7}$$

If Pontryagin's Minimum Principle is used to determine the optimal control law [C4], the Hamiltonian for the system is obtained as

$$H(t) = 1 + \lambda_1 x_2 + \frac{\lambda_2}{J}[Kx_3 - ax_2 - b] + \frac{\lambda_3}{L}[U - Rx_3 - Kx_2) \tag{3-8}$$

where λ_1, λ_2, λ_3 are the adjoint or co-state variables which are the solutions of the following differential equations [C4]:

$$\dot{\underline{\lambda}} = \begin{bmatrix} 0 & 0 & 0 \\ -1 & \frac{a}{J} & \frac{K}{L} \\ 0 & -\frac{K}{J} & \frac{R}{L} \end{bmatrix} \underline{\lambda} \tag{3-9}$$

According to Pontryagin's Minimum Principle the optimal control law is obtained by adjusting U(t) to minimize H. It follows from (3-7) that this optimal law is given by

$$U^* = -U_0 \, \mathrm{sgn}(\lambda_3) \quad . \tag{3-10}$$

Thus, as expected intuitively, a bang-bang control law is obtained. To determine the switching instants, however, $\lambda_3(t)$ must be calculated. The solution of the differential equations (3-9) is quite involved since the initial conditions of λ_i's are not known, they must be such that the final conditions on the x_i's must be satisfied.

Further complication is introduced by the fact that the final time t_f is not known, and must be obtained from the equation

$$H(t_f) = 0 \qquad (3\text{-}11)$$

Moreover, when U_0 is replaced by $-U_0$, the machine starts working as a generator rather than a motor, which changes even the basic equations (3-4) and tangles up the problem further.

Considering these difficulties, it is seen that this method should be abandonned. It should just be considered for demonstrating theoretically the bang-bang nature of the control law for minimum-time response.

3.4 Study of the Acceleration Curve

3.4.1 Non-linear Modelling

The acceleration curve is the part of the trajectory obtained when a positive step-voltage, U_0, is applied to the PM motor. Initially starting from zero, the current rises in near-exponential manner, typical of an R-L circuit. When the value i=b/K is reached, acceleration is applied to the rotor as described by equations (3-1).

The "stalling" condition has a duration of t_s given by the solution of the differential equation derived from (3-1) as

$$\left.\begin{aligned} U_0 &= R(I) \times I + L(I) \frac{dI}{dt} \\ \Omega(t) &= 0 \end{aligned}\right\} \qquad (3\text{-}12)$$

This nonlinear differential equation can be integrated using the 4th order Runge-Kutta numerical integration method [C2] with Gill's modification [C3].

3.4.2 Second-order Linear Modelling

The piecewise linear modelling is chosen here. The loading torque $\lambda_r(t)$ is set as a linear function of speed, and the no-load resistance is taken as a constant for R and the no-load armature inductance is chosen as a constant for L. The load torque, therefore, can be included in the terms a and b of the friction coefficients of equation (3-2) which are valid only for $|I| > b/K$ when $\Omega=0$.

The "stalling" condition gives immediately from t=0 to t_s

$$\left.\begin{aligned} t_s &= \frac{L}{R}\,\ell n\,\frac{U_0 K}{U_0 K - Rb} \\ I(t_s) &= b/K \end{aligned}\right\} \qquad (3\text{-}13)$$

The usual gross linear approach is chosen here to solve (3-2). If s is the symbol used for the Laplace Transform variable, equations (3-2) are transformed into

$$\left.\begin{aligned} \Omega(s) \times K + I(s)[R + Ls] &= L\,I_0 + U(s) \\ \Omega(s) \times (a + Js) - K\,I(s) &= J\,\Omega_0 - \frac{b}{s} \end{aligned}\right\} \qquad (3\text{-}14)$$

The determinant of the system is

$$DET = JLs^2 + s(RJ + aL) + aR + K^2 \qquad (3\text{-}15)$$

and the poles are found to be

$$s_i = \frac{-(RJ + aL) \pm \sqrt{(RJ + aL)^2 - 4JL(aR + K^2)}}{2JL} \qquad (3\text{-}16)$$

If the motor starts at $t=t_s$, when $\Omega_0=0$ and $I_0=b/K$ transforming to the variable $t'=t-t_s$, the solution of (3-14) is found

$$\Omega(s) = \Omega_f \left[\frac{1}{s} + \frac{-s + 2A}{(s+A)^2 + w} \right] \tag{3-17}$$

$$I(s) = \frac{I_f}{s} + \frac{-I_f s + \beta}{(s+A)^2 + w} \tag{3-18}$$

where

steady state speed $\Omega_f = \dfrac{UK - bR}{aR + K^2}$ (3-19-1)

s.s. current $I_f = \dfrac{bK + aU}{aR + K^2}$ (3-19-2)

$$A = \frac{1}{2}\left[\frac{R}{L} + \frac{a}{J}\right] \tag{3-19-3}$$

$$W = \frac{aR + K^2}{JL} - A^2 \tag{3-19-4}$$

$$\beta = \left(\frac{ab}{JK} + \frac{U}{L}\right) - 2A\, I_f \tag{3-19-5}$$

In most cases over damping is chosen in the design parameters of a PM motor, and hence $W < 0$.

Equations (3-17) and (3-18) have inverse Laplace transforms written as

$$\left.\begin{aligned} \Omega(t') &= \Omega_f \left[1 + \frac{s_2}{s_1 - s_2} e^{s_1 t'} + \frac{s_1}{s_2 - s_1} e^{s_2 t'} \right] \\ I(t') &= I_f + \frac{\beta - s_1 I_f}{s_1 - s_2} e^{s_1 t'} - \frac{\beta - s_2 I_f}{s_1 - s_2} e^{s_2 t'} \end{aligned}\right\} \tag{3-20}$$

with s_1 and s_2 defined by (3-17) and rewritten also as

$$\left.\begin{aligned} s_1 &= -A + \sqrt{-W} \\ s_2 &= -A - \sqrt{-W} \end{aligned}\right\} \tag{3-19-6}$$

The speed and current characteristics during the acceleration are shown in Figure (3-1) and (3-2) comparing the solutions in the time domain of the ideal solution and the piecewise linear solution derived above. As seen on Figure (3-2), the current characteristics are very much different for the accurate model describing the system with at least a precision of 1% and the linear one. In the case of the speed characteristic Figure (3-1) shows quite a difference in the transient part, and unfortunately the bang-bang problem is involved precisely with the transient part. At a first glance it seems that for a general study one cannot use any simplified model.

However, the minimum-time problem deals with a trajectory represented in phase plane speed versus angular displacement.

It has to be noted that with the piecewise linear model the phase plane trajectory during the acceleration depends only on three auxilliary coefficients

$$\sigma = |s_1|$$

$$\mu = |s_2|$$

and Ω_f as defined by (3-19-1).

From equations (3-20) using the new notation, the phase plane trajectory is defined by the two parametric equations

$$\left.\begin{aligned} \Omega(t') &= \Omega_f \left(1 - \frac{\mu}{\mu-\sigma} e^{-\sigma t'}\right) + \frac{\sigma}{\mu-\sigma} e^{-\mu t'} \\ \theta(t') &= \Omega_f \; t' + \frac{\sigma+\mu}{\sigma\mu} + \frac{\mu}{\sigma(\mu-\sigma)} e^{-\sigma t'} - \frac{\sigma}{\mu(\mu-\sigma)} e^{-\mu t'} \end{aligned}\right\} \qquad (3\text{-}21)$$

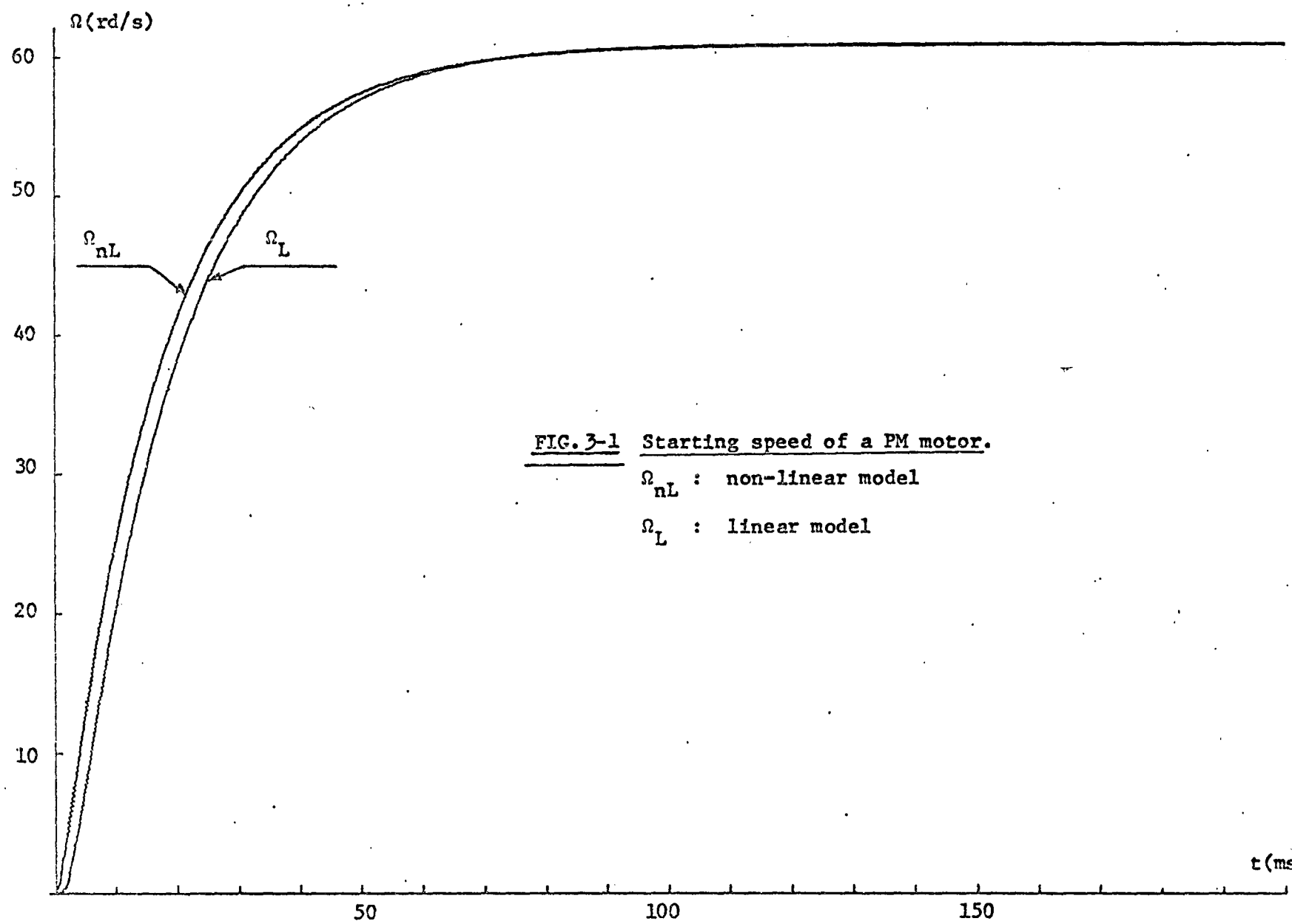

FIG. 3-1 Starting speed of a PM motor.

Ω_{nL} : non-linear model

Ω_L : linear model

FIG. 3-2 Starting current in a PM motor.

I_{nL} : non-linear model

I_L : linear model

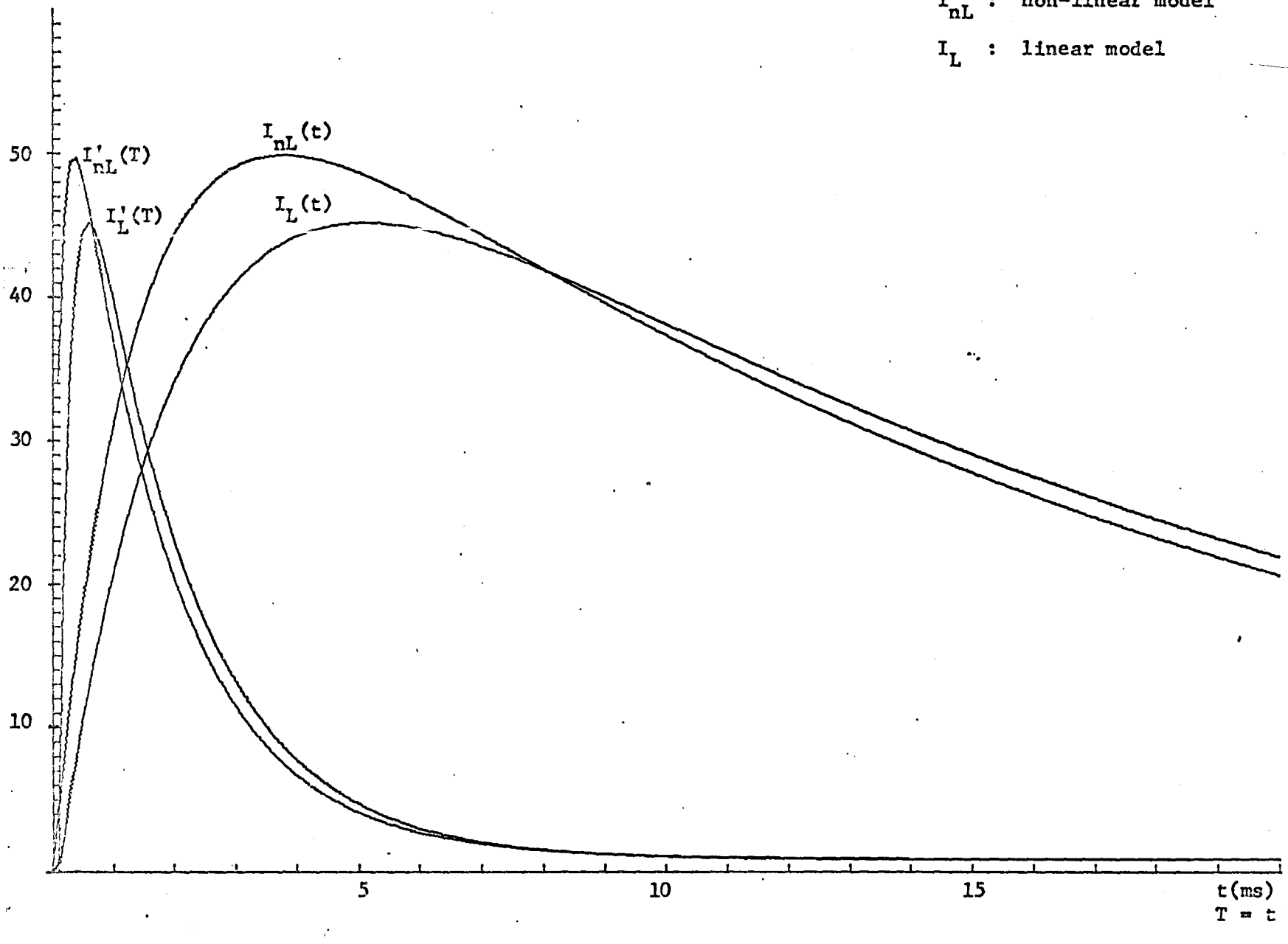

Figure (3-3) compares the exact model trajectory and the linear approximation solution given by (3-21). It can be seen that this would be a fairly good representation to work on provided one crosschecks the results from time to time to be sure that further errors do not drive approximate solutions too far from the exact one.

One should point out that an on-line parameter estimation during acceleration can give the auxilliary parameters σ, μ, Ω_f without measuring separately the load parameters a, b, J.

3.5 Study of the Deceleration Curve with Electrical Braking

In the preliminary study of the bang-bang nature of the problem, equations (3-11) were assumed to be representative of the system. Unfortunately, when reverse voltage is applied to the armature, the rotor has been accelerated and the machine stops behaving as a motor, but rather as a generator.

Figure (3-4) depicts the system when reverse voltage braking is applied.

The rotor has stored a kinetic energy which is a function of the speed at which switching is performed. Therefore, the machine becomes a generator delivering an e.m.f. function of speed which adds its effect to the armature voltage.

The current has to change sense and produces an antagonist torque realizing a heavy electrical braking.

The differential equations governing the system are written as

$$\left.\begin{aligned} -U &= K\Omega - RI - L\frac{dI}{dt} \\ -KI &= a\Omega + b + J\frac{d\Omega}{dt} \end{aligned}\right\} \qquad (3\text{-}22)$$

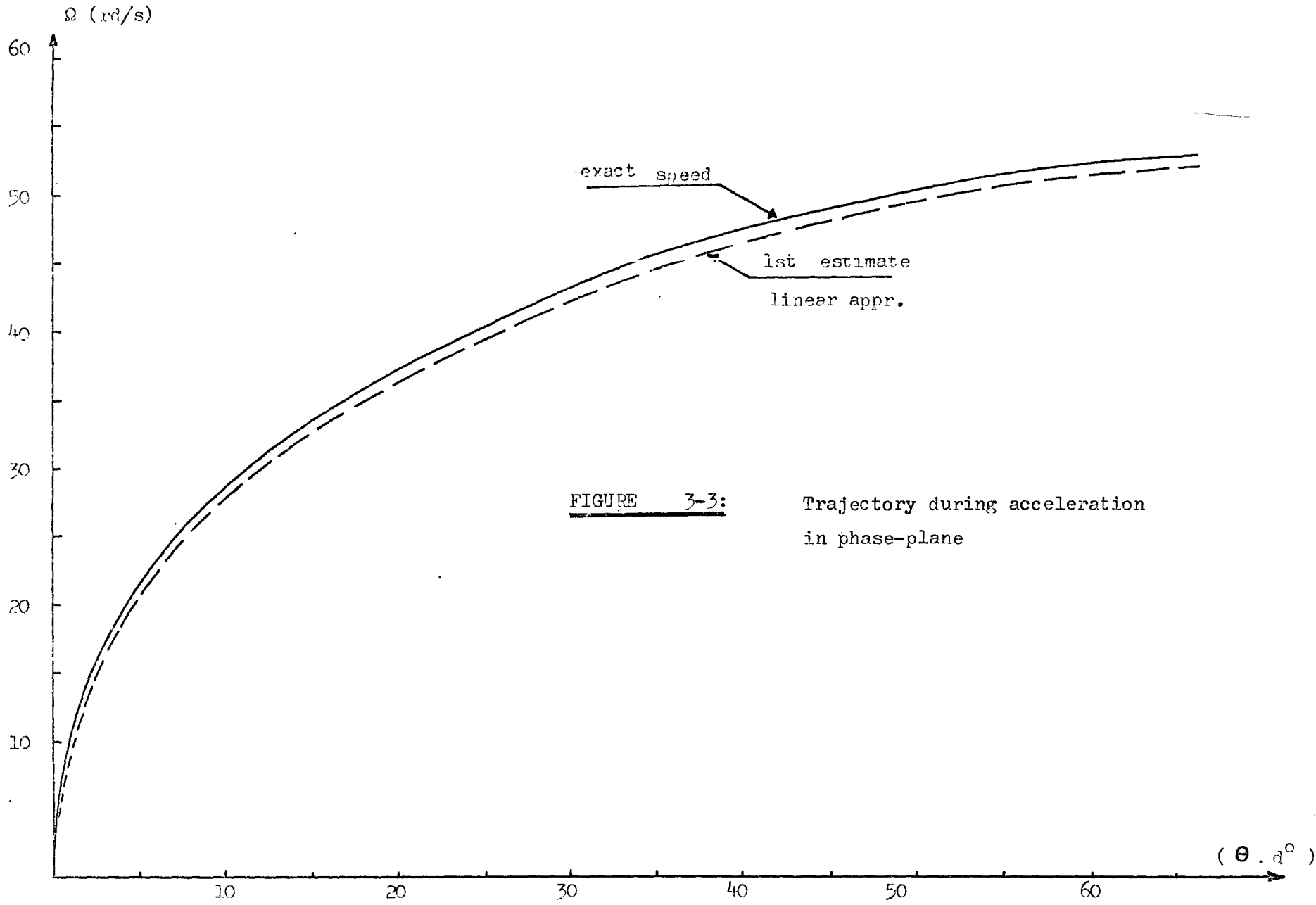

FIGURE 3-3: Trajectory during acceleration in phase-plane

FIG. 3-4 : PERMANENTIC DC MOTOR BECOMING GENERATOR

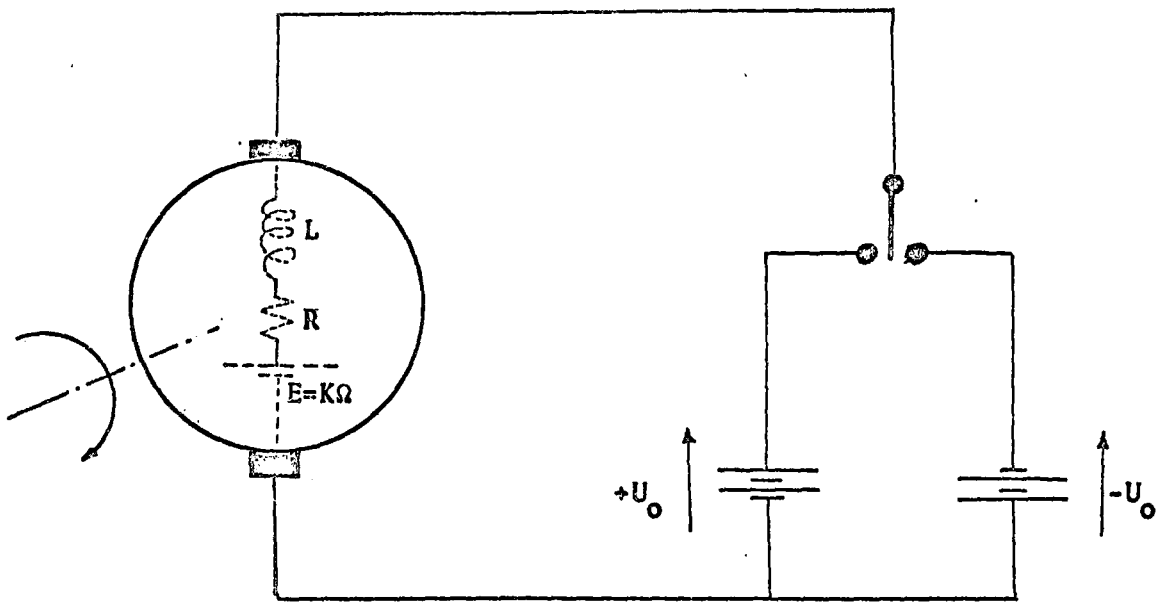

It can be noted that if one calls I = -I (bearing in mind that physically the current has changed sense) equations (3-21) are identical to (3-13) provided K is changed into -K. This notational trick helps when using the equations either in numerical analysis or physical analogue simulation, since the same subroutines or same patchings can be used.

With the above remark, equation (3-18) is still valid for the braking condition, provided K is negative now.

Suppose the switching occurs at $\Omega=\Omega_{sw}$ when $t=t_{sw}$. During the open circuit the current has to decay to zero value and change sense. The assumption of quasi instantaneous decaying is made, and at $t=t_{sw}$, with a change of variable $t''=t-t_{sw}$, the initial conditions are

$$\Omega_0 = \Omega_{sw}$$
$$I_0 = 0$$

Using these values in equation (3-18) the inverse Laplace transform leads to the braking trajectory

$$\left.\begin{aligned} \Omega_{br}(t'') &= A_2 + B_2 e^{s_1 t''} + C_2 e^{s_2 t''} \\ \theta_{br}(t'') &= A_2 t'' + \frac{B_2}{s_1} e^{s_1 t''} + \frac{C_2}{s_2} e^{s_2 t''} \end{aligned}\right\} \qquad (3\text{-}23)$$

where

$$A_2 = \frac{-KU_0 - bR}{aR + K^2} \qquad (3\text{-}24\text{-}1)$$

$$B_2 = \frac{-\Omega_{sw}\left(s_2 + \frac{a}{J}\right) - \frac{b}{J} + s_2 A_2}{(s_1 - s_2)} \qquad (3\text{-}24\text{-}2)$$

$$C_2 = \frac{-\Omega_{sw}(s_1 + \frac{a}{J}) - \frac{b}{J} + s_1 A_2}{(s_2 - s_1)} \qquad (3\text{-}24\text{-}3)$$

and s_1 and s_2 are defined in (3-19-6).

Some braking characteristics have been reproduced in Figure (3-5), switching from different speeds. The same remarks apply, as for the acceleration curve. Although the exact curves differ from those obtained from the linear model, the phase plane trajectories are sufficiently close for all practical purposes.

It has to be noted that when the speed reaches zero, the armature current must be brought to zero (or to a value less than b/K), so that the rotor will stay in that position, because there is no kinetic energy stored and no external driving torque to overcome the static friction.

3.6 Practical Switching Characteristics

In the previous sections, it is assumed that the switching instant t_{sw} is known, in order to reach a prescribed destination. This involves solving for $\text{sgn}(\lambda_3)$ as stated in equation (3-10). Unfortunately, as pointed out in a previous section, this computation is fairly tedious and time-consuming. Moreover, for every given final destination, the switching time must be re-calculated.

Evidently, it would be much more helpful if the switching time could be related explicitly to the specified target point. One could have tried calculating the trajectory backwards in time, from the target, but this cannot be done since the final value of one of the true state

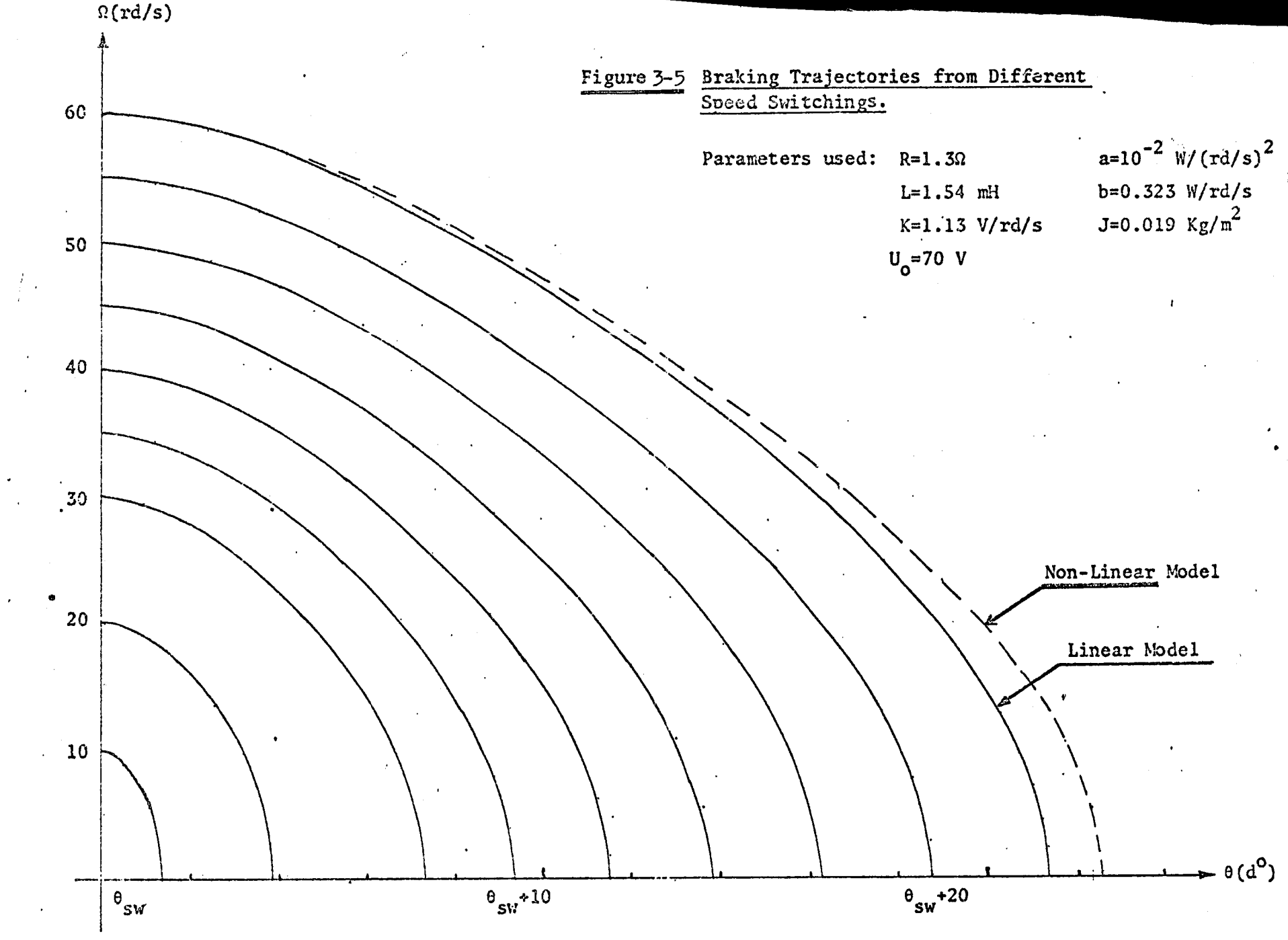

Figure 3-5 Braking Trajectories from Different Speed Switchings.

Parameters used: R=1.3Ω $a=10^{-2}$ W/(rd/s)^2
L=1.54 mH b=0.323 W/rd/s
K=1.13 V/rd/s J=0.019 Kg/m^2
U_o=70 V

variables is unspecified. An approximate method for the determination of the switching time will now be derived.

It can be seen from equation (3-24-1) that the coefficient A_2 depends only on the basic parameters, and B_2 and C_2 are linear functions of Ω_{sw}.

In a first approximation the term $e^{s_2 t''}$ may be neglected in equations (3-23) since $|s_2| >> |s_1|$ in a well designed machine.

From the first equation of (3-23) one can immediately show that the approximate time needed to stop from a speed Ω_{sw} is given by

$$\hat{T} = \frac{1}{s_1} \ell n \left(\frac{-A_2}{B_2(\Omega_{sw})}\right) \tag{3-25}$$

Second Approximation

The error in speed, if the estimate $\hat{T}$ is used instead of the true braking time T, will be

$$\Delta\Omega = \Omega_{br}(T) - \Omega_{br}(\hat{T}) = C_2 e^{s_2 \hat{T}} \tag{3-26}$$

Hence, from (3-25)

$$\Delta\Omega = C_2 \left(\frac{-A_2}{B_2}\right)^{s_2/s_1} \tag{3-27}$$

Combining this equation with

$$\left(\frac{d\Omega}{dt}\right)_{\hat{T}} \simeq s_1 A_2$$

and $\Delta\Omega \simeq d\Omega$

$\Delta t \simeq dt$

the second approximation leads to a corrective factor

$$\Delta\hat{T} = \frac{C_2}{s_1 A_2} \left(\frac{-A_2}{B_2}\right)^{s_2/s_1} \tag{3-28}$$

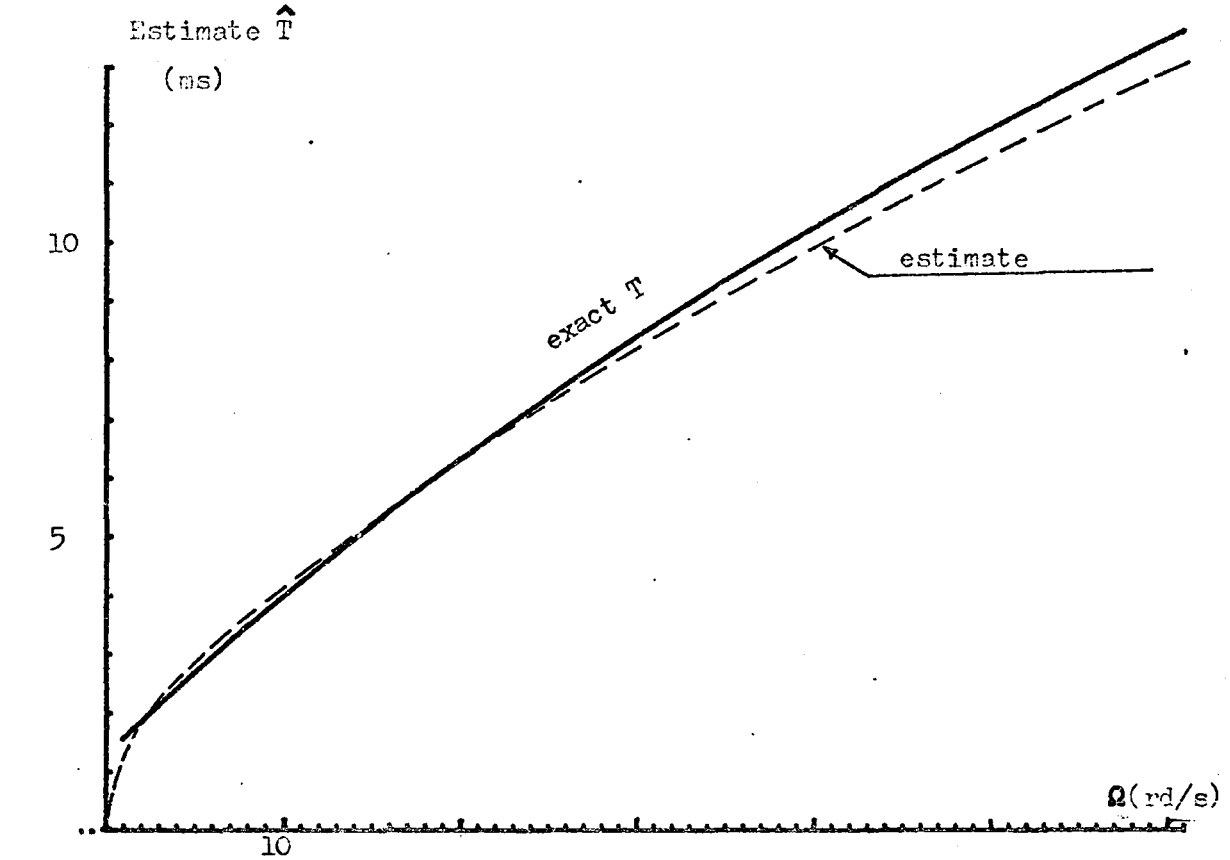

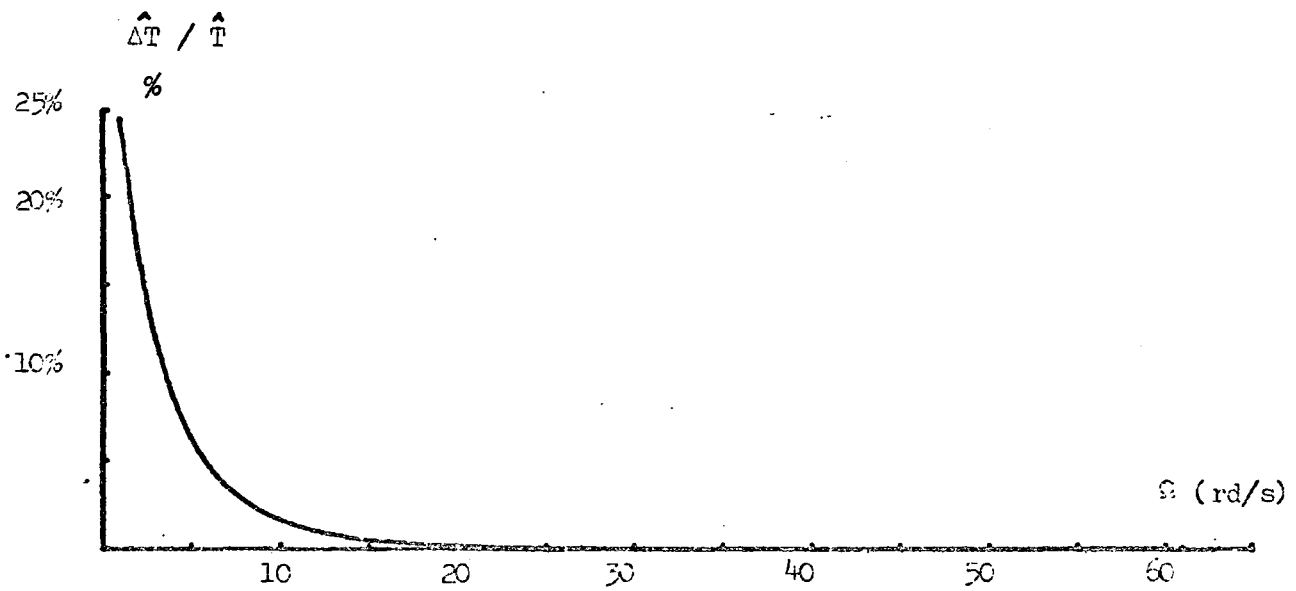

FIGURE 3-6 Linear estimate for reverse voltage braking time

Figure (3-6) shows a comparison for a given load between T, the first estimate $\hat{T}$ and the corrective factor expressed as $\frac{\Delta\hat{T}}{\hat{T}}$. One can see immediately that the error $\frac{\Delta\hat{T}}{\hat{T}}$ becomes very rapidly small and it would be useless to complicate the equations by adding the corrective factor.

Therefore, the first approximate $\hat{T}$ is used, and substituted into the second equation of (3-23) one obtains immediately

$$\vartheta_{brake} = \frac{-1}{s_1} A_2 \ell_n\left(\frac{B_2}{-A_2}\right) + A_2 + B_2 \qquad (3\text{-}29)$$

The auxilliary variable ϕ as a linear function of Ω_{sw} is introduced as

$$\phi = \frac{B_2}{-A_2} \qquad (3\text{-}30)$$

and leads to a simplified notation of (3-29) as

$$\vartheta_{brake} = -\frac{A_2}{s_1}(\ell_n\phi + 1 - \phi) \qquad (3\text{-}31)$$

In Figure (3-7), a comparison is made between the real predictor curve obtained from the original equations and the approximate prediction given by equation (3-31).

It can be seen that with the exception of very low speeds, which are out of our range of interest anyway, the approximate curve is fairly accurate over a wide range.

The phase plane trajectory expressed by equation (3-31) will be called the "switching predictor" curve, and used widely for finding the minimum-time control law.

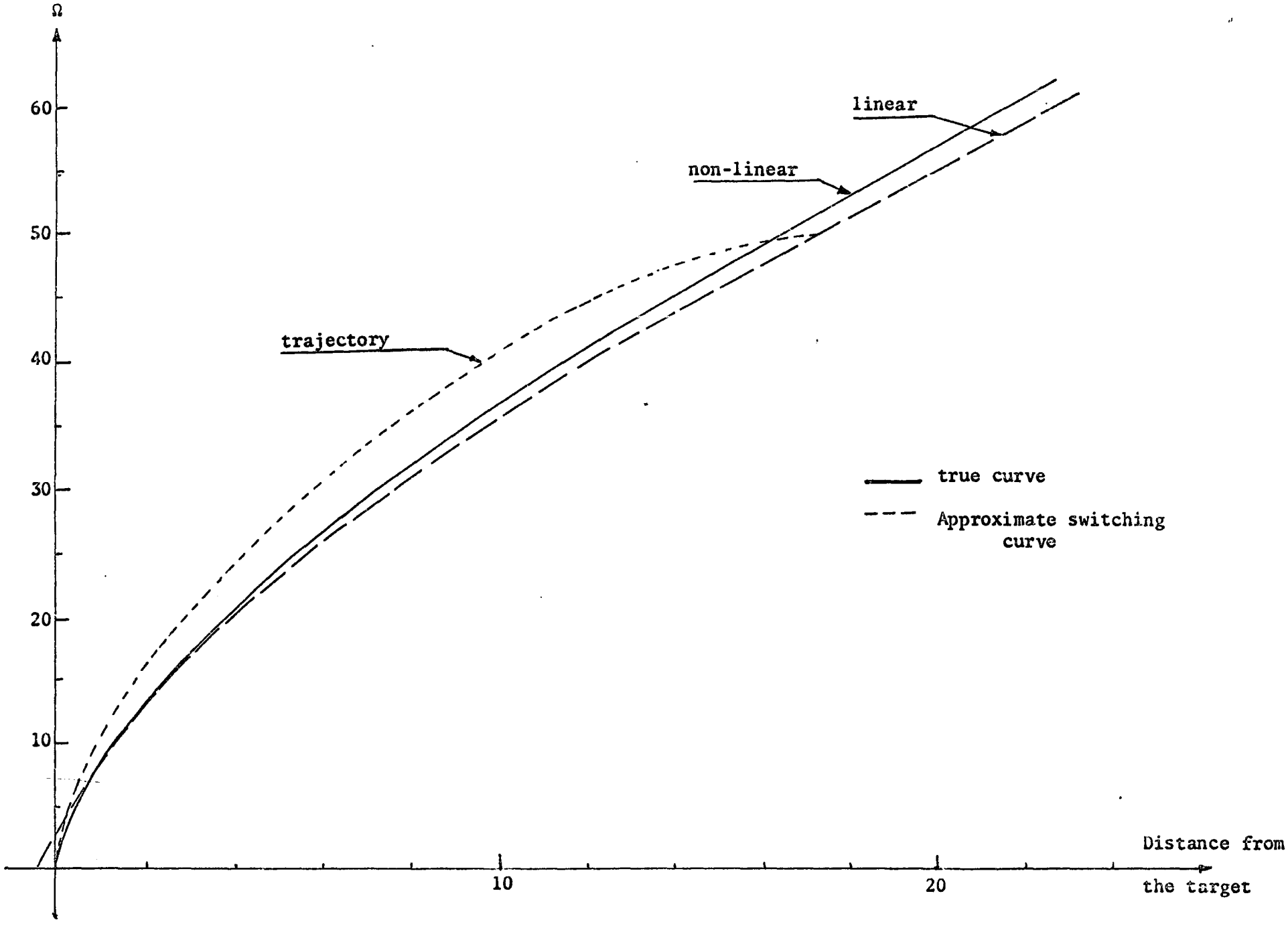

Fig. 3-7 SWITCHING PREDICTOR

Conclusion

In this chapter the permanentic d.c. servo-motor has been shown to be very suitable for the bang-bang control. The theoretical approach by solving difficult equations has been avoided and the derivation of a switching predictor curve which determines the switching instant related to the target point was a big step in solving the minimum-time position problem.

CHAPTER IV

PERMANENTIC MOTOR AS A STEPPER;
IMPLEMENTATION OF THE MINIMUM-TIME POSITION CONTROLLER

The investigation of the exact mathematical model of the d.c. permanentic motor has brought out the low time constants allowing step voltage inputs to the armature. The current handled, although high, is admissible in the windings for transients [B10] without any additional series resistors.

Hence, the bang-bang control mode is possible and allows very high accelerations and decelerations producing very high torques at any speed.

The following examples are taken for a permanentic d.c. motor [1 HP / 90 Vdc / 9.5 A / 650 rpm], and the conclusions discussed can be applied to devices ranging up to a couple of HP.

4.1 Principle of the Bang-Bang Controller

The effective sequence to realize the minimum-time position control is given by the flow chart.

ON → SWITCH → OFF

ON: apply $+U_0$ to the armature

SWITCH: reverse the voltage to $-U_0$

OFF: remove the voltage source, and bring the current below a value i_0

Figure (4-1) shows two typical phase plane trajectories using the above scheme.

FIGURE 4-1

Phase Plane Trajectories

for ON-SWITCH-OFF order

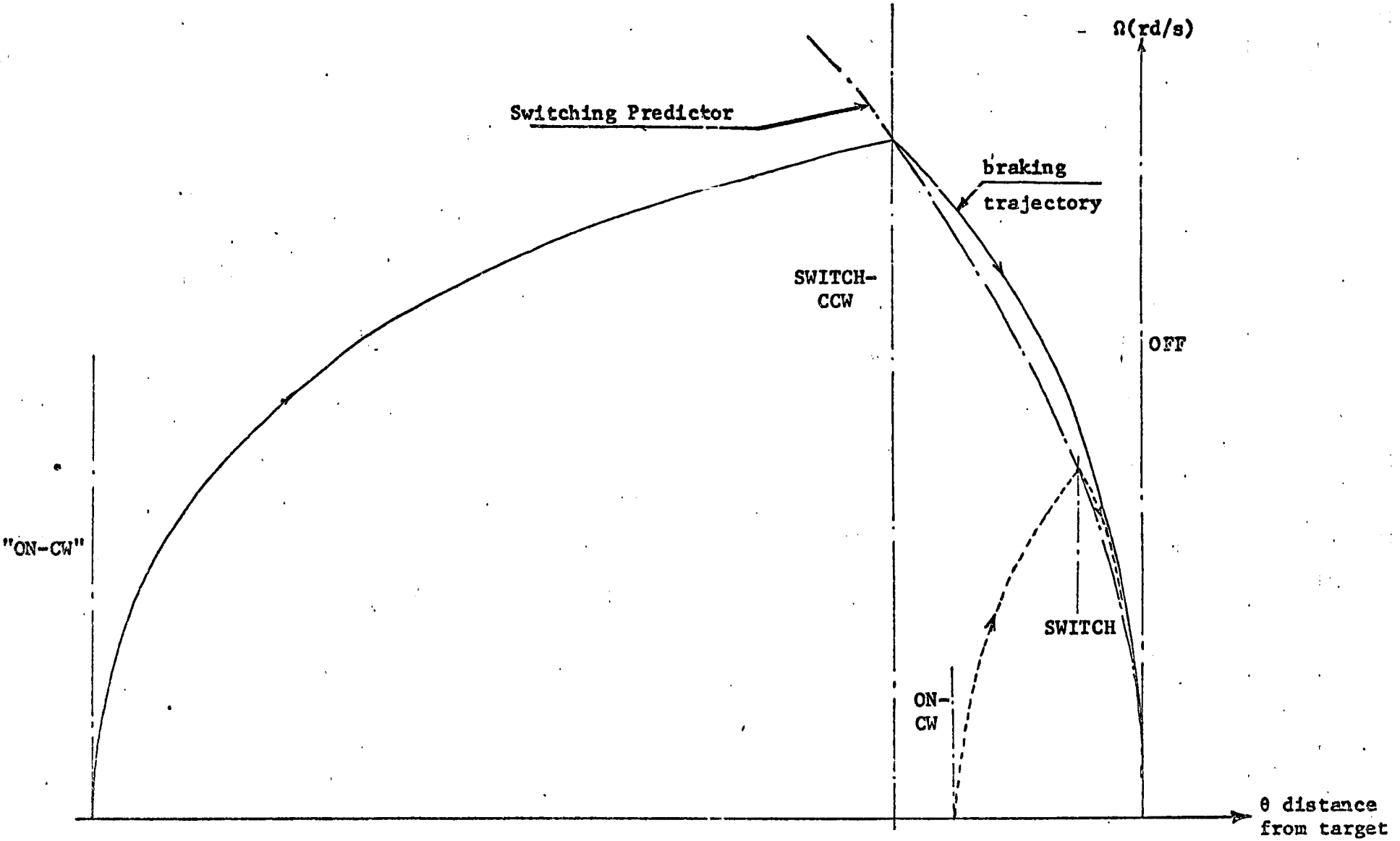

If the switching curve defined in Chapter III could be stored, say in a diode function generator (DFG), an analogue voltage produced by a tachometer and an analogue voltage given by a multiturn potentiometer indicating the position could be used to determine the switching decision. The principle of an analogue controller is depicted in Figure (4-2). Basically, the distance from the target (dft) is measured and fed into the DFG, giving the speed level Ω_{sw} (switching speed). The comparator will give the switching order from $+U_0$ to $-U_0$ if the actual speed becomes greater than or equal to Ω_{sw}.

Further on, as the speed reaches the narrow band of the dead zone (due to mechanical friction) the order to remove the source and short-circuit the armature is given.

A high speed of resolution is required for the controller. Moreover, very precise analogue noise-free voltages must be used, because a slight error in the switching point will drive the shaft away from the target. The main limitations are in this case due to the analogue transducers and the associated filtering problems. However, depending on the accuracy in the positioning wanted, this system can be very useful in certain applications where very high torque and fast responses are necessary.

4.2 Quantization of the Switching Curve

The expansion of computerized digital control has directed the research towards stepping motors, where direct digital implementation is easier.

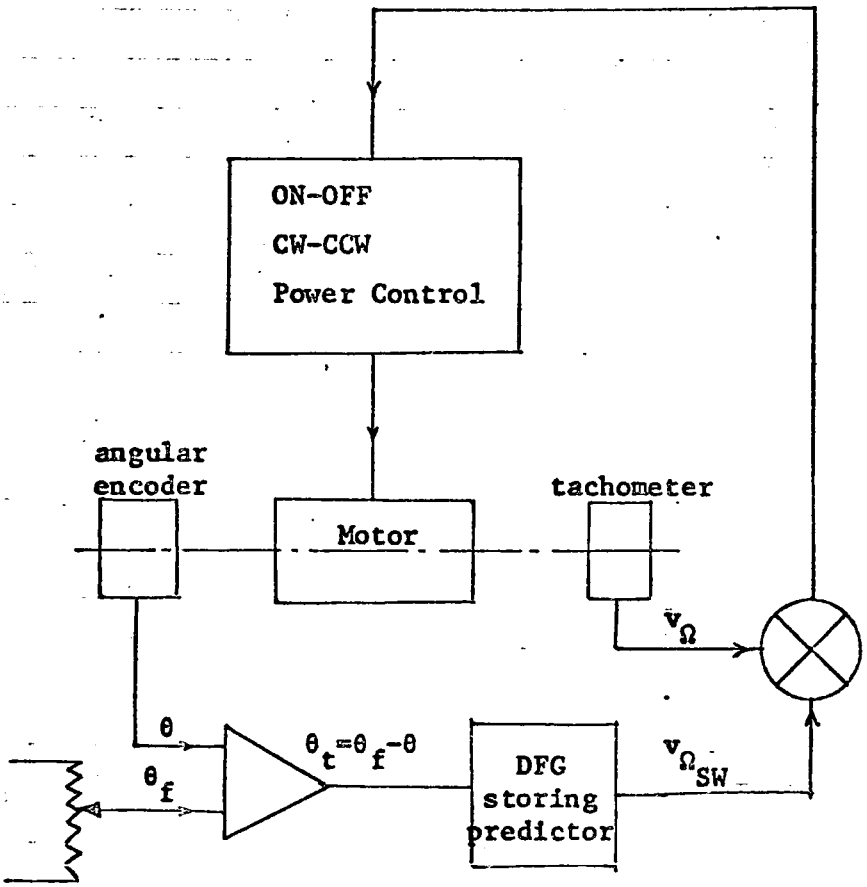

FIGURE 4-6: Control Logic Unit

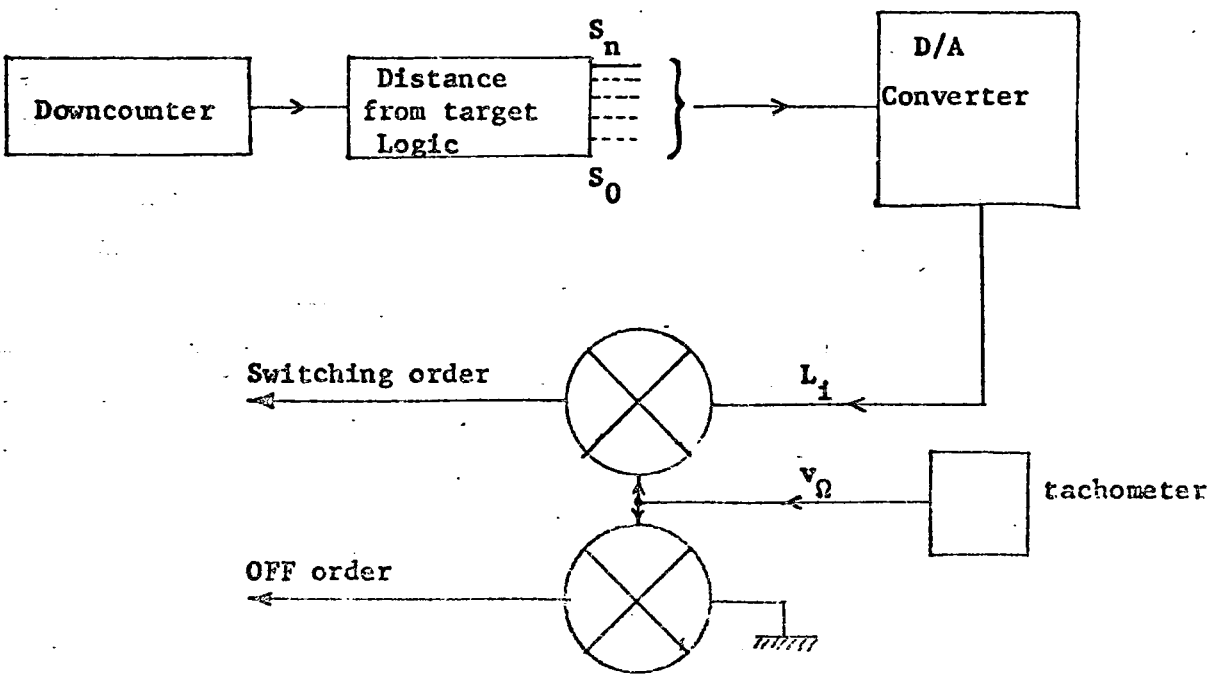

Suppose the angular displacement on the shaft can be quantized, say with a system of slotted disc and photo sensors. A step is defined as a position of the shaft between two quantization positions. Figure (4-3) gives the representation compared to the true stepper mode. The multistep mode is shown on the same Figure and the advantage of a stepping motor can be seen as a self-locking device, while the advantage of a d.c. motor lies in the smooth operation and true minimum-time response.

Suppose the angular displacement quantization positions are called "steps". Using the "switching curve predictor" given by Equation (3-31), Figure (4-4) shows how the steps S_i define by intersection with the predictor, corresponding speed levels, L_i, called switching levels.

4.3 Control Law

The phase plane is now partitionned in a complete set of regions defined as

$$\text{REG } ij = \{R_i \ , \ S_j\} \tag{4-1}$$

It can be seen easily that each region is characterized by the following statement

$$\text{REG } ij = \{\text{braking in less than } i+1 \text{ steps and more than } i \text{ steps}\} \tag{4-2}$$

The control law becomes straightforward. The distance from the target, as a quantized number, generates the corresponding levels L_i. In each region REG ij a comparison with the actual speed will give the switching decision according to Equation (4-2).

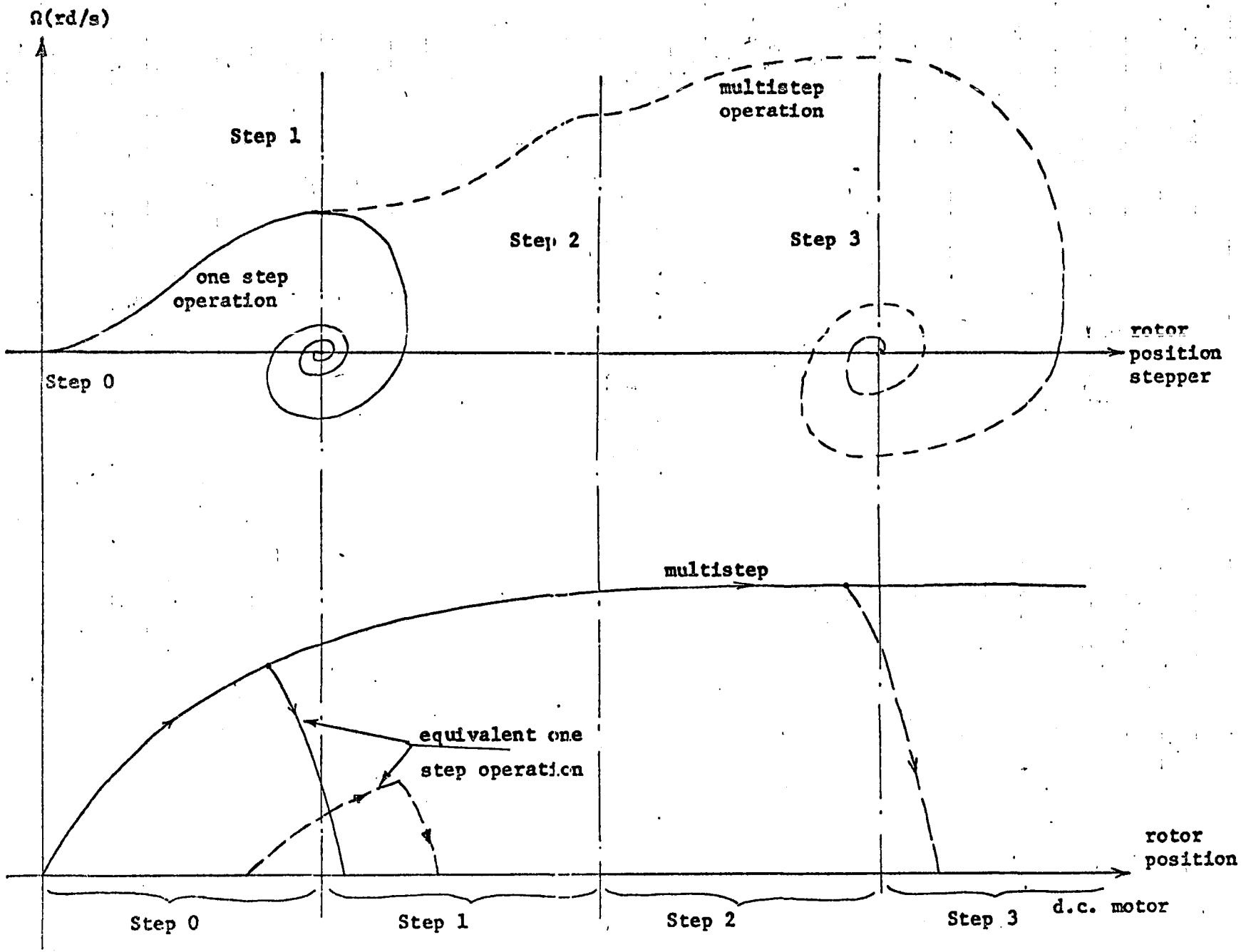

FIGURE 4-3 : Analogy of Stepping Operation for a True Stepper and a d.c. Motor

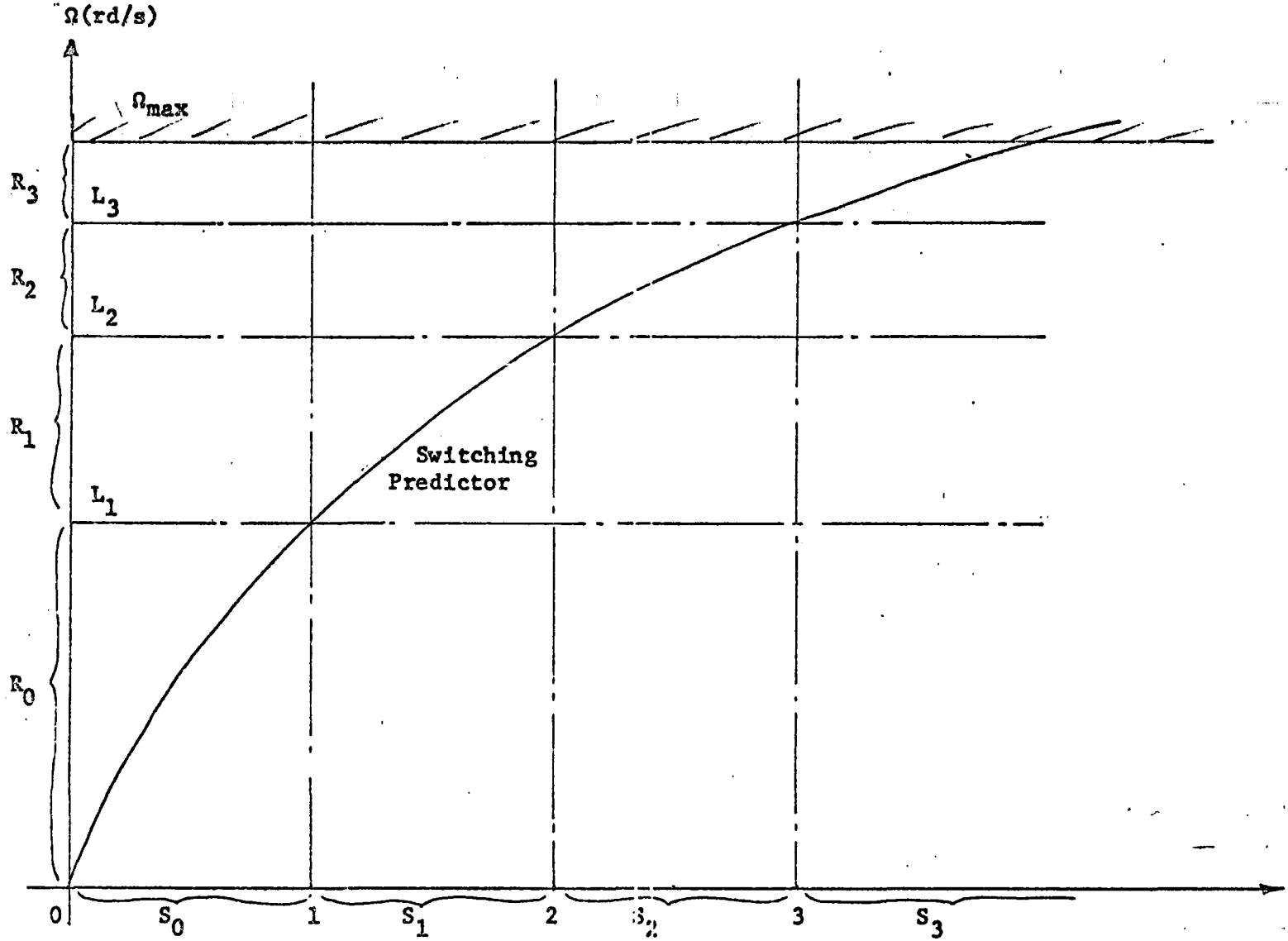

FIGURE 4-4 : Control Regions in Phase Plane

4.4 Practical Implementation of the Bang-Bang Controller (BBC)

The scheme of Figure (4-5) is chosen for the digital implementation. The angular encoder is constituted by a slotted disc. A light source activates a photo-diode which provides, through a pulser circuit described in Appendix A sharp edged pulses indicating the passage from one step position to the next one. As this measures only a relative positionning the pulses are fed into a counter to keep track of the effective angular position.

In the position control problem one is interested in the distance from the target which should be brought to zero. Therefore, this is automatically realized by using a presettable downcounter.

An analogue tachometer fed into a low-pass filter will provide the speed information required by the control law.

The information on speed and position is fed into the BBC control logic unit which will have the decision ability.

Figure (4-6) shows a scheme for general implementation of the control logic unit.

The distance from the target generates the digital levels S_i which are transformed into analogue levels L_i to be compared to v_Ω, analogue speed level delivered through the low-pass filter by the tachometer.

This scheme seemed preferable to the one using an A/D stage from the tachometer and then comparing the digital levels to S_i. The implementation would appear to be much more costly.

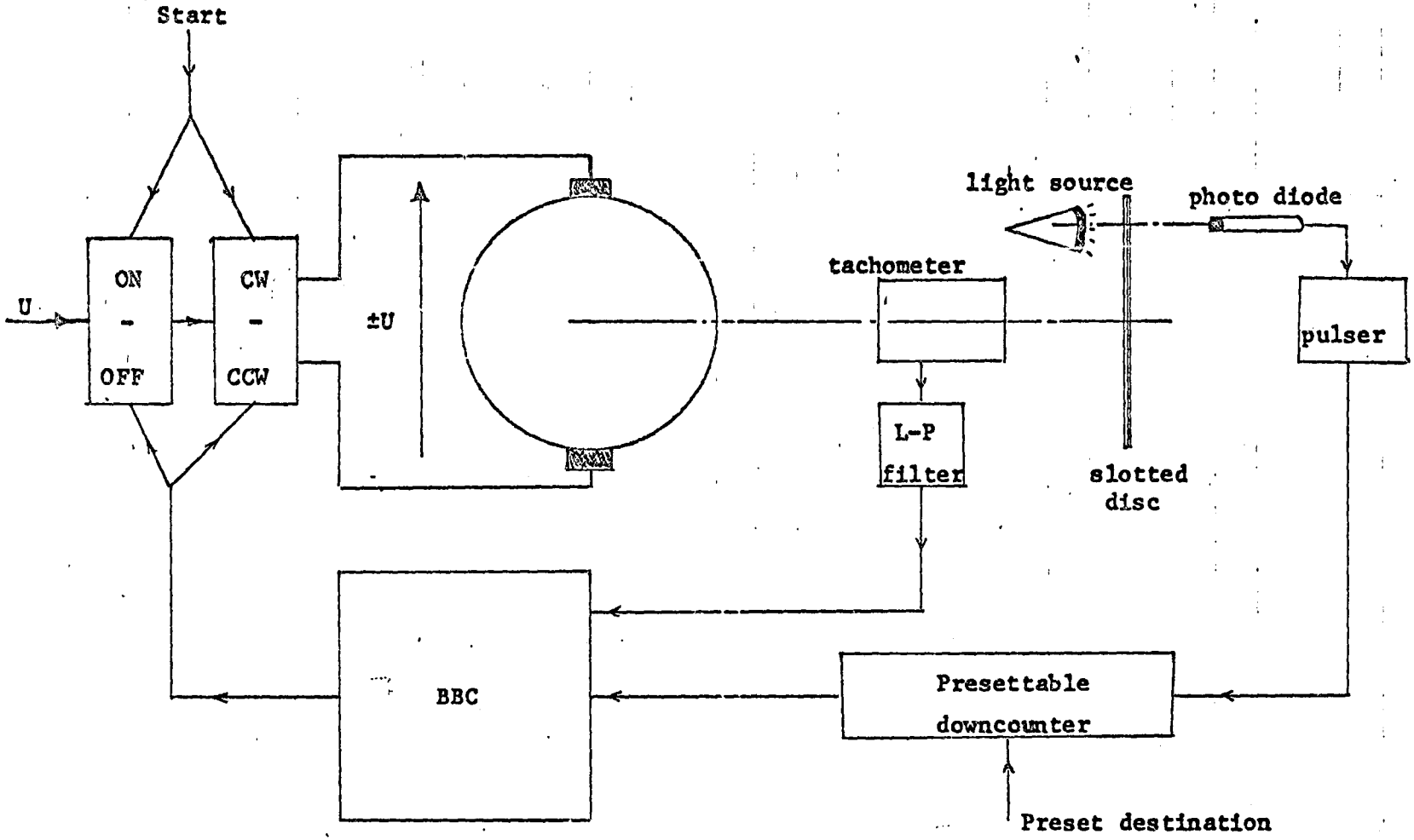

FIGURE 4-5: General Block Diagram of the Position Control

4.4.1 Level Selector

4.4.1a "Distance from the Target" Logic

Suppose, for a specific application, N levels are needed as defined by Figure (4-4).

The presettable counter should be of synchronous kind otherwise false switching could occur at the undetermined transition stages.

The highest level L_N should be generated when the d.f.t. is equal or more than N steps; if Q_i's are the binary outputs of the K bits synchronous counter, the high level S_N should be written in boolean algebra as

$$S_N = \sum_{N}^{K} Q_i \qquad (4\text{-}3)$$

Hence S_N = "1" when d.f.t. $\geq$ N.

For the N-1 other levels generation, a simple decimal decoder is used. The subscript of the level corresponds to the actual d.f.t. in decimal count. Hence

S_j = d.f.t. in decimal for $1<j<N-1$

4.4.1b D/A Level Converter

A simple D/A converter is designed here which converts a digital information into a voltage level.

Figure (4-7) shows the converter, and in the table of values given for the specific example built (5 levels adjustable separately).

Each output from the digital logic (IC) being at a 4V logic level, must be buffered. The use of a field effect transistor has been chosen for its natural ability of isolating the output from the base input.

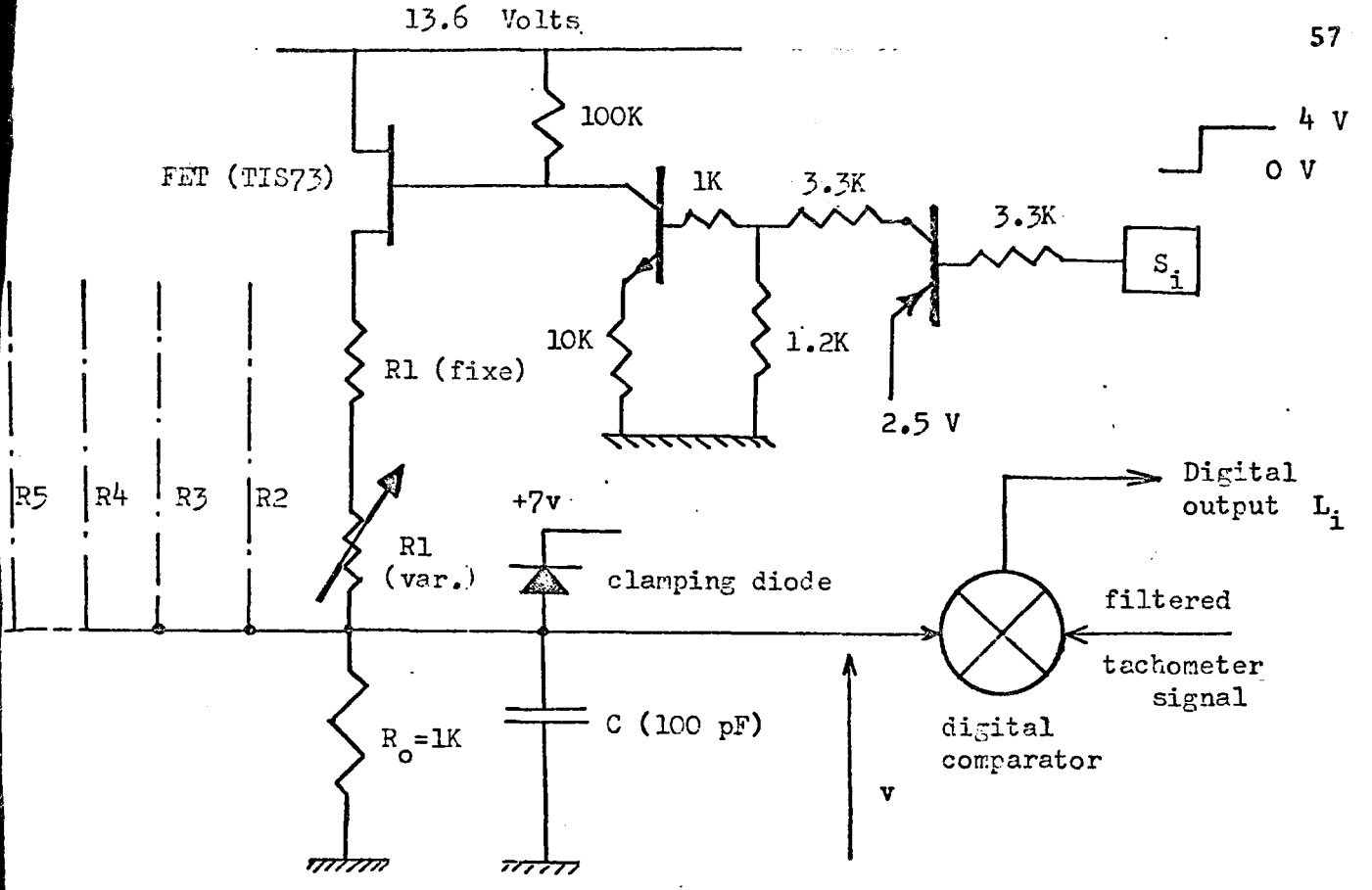

FIGURE 4-7: D/A converter (5 identical stages)

R_o=1K	FET drain-source resistance: 750 Ω				
	fixe	coarse	fine	v min	v max
R1	4.7 K	10 K	.5 K	.8 V	2.2 V
R2	3.3 K	7.3 K	.2 K	1.1 V	2.8 V
R3	2 K	2.5 K	.3 K	2.4 V	3.6 V
R4	1 K	1.5 K	.5 K	2.8 V	5.0 v
R5	.5 K	1 K	.2 K	4.0 V	5.9 V

Typical Resistor Values for a 5 level B.B.C.

As the digital comparator used cannot accept a higher voltage than 7V d.c. an output clamping diode is used.

One should notice that the output S_i is equivalent to an exclusive "or" gate output, therefore, only one FET can be on at a time, the others blocked present almost infinite resistance, hence equivalent to the open circuit.

It has to be noticed here that in the case of the d.f.t. being zero, none of the S_i's are in the stage "1" therefore, the reference voltage generated will be automatically zero since every FET is blocked. This is particularly suitable for the region REG11 where braking should occur at once whatever the speed is.

Before using the controller, one has to set the precalculated levels. Because of noise parameters and input impedance (not well defined) of the comparator, a coarse and a fine adjustment is possible for each level.

For convenience a 0.1 volt scale is chosen for a 1 rd/s speed. Since the speed never exceeds 61 rd/s the comparator is working in its full range of sensitivity.

One should notice at this point the simplicity of the converter, and the fact that the output voltage levels L_i's can be set separately and independently of the others, by simply presetting d.f.t. equal to i. The choice of FET switching is compatible with the high frequency switching needed.

4.4.2 ON-SWITCH-OFF Digital Signal Generation

On Figure (4-6) the command signal generation is shown as being straightforward. Unfortunately practical difficulties are encountered. These difficulties are caused by the indefinite state of the comparator when the speed is zero, hence at start.

This problem is solved by building a sequential logic using two comparators realizing the same features as a Schmidt-Trigger device. Although complicated because of memory requirements, this system is cheaper than a commercial Schmidt-Trigger for the same performance.

Figure (4-8a) gives a schematic of the ON-OFF control together with the switching order.

On a typical cycle, as depicted on Figure (4-1), a start pulse sets the memory "CONTROL" only if the comparator C_2 shows the motor shaft to be at standstill. The memory "AUXIL" is disabled to any unwanted clock pulse from C_2.

The motor starts and the switching pulse is generated by the comparator C_1 associated with the gate "ORDER" as defined by the conditions

$$\{(dft \leq N) \quad \text{and} \quad v_\Omega \geq L_i\} \tag{4-4}$$

The switch state is held in memory enabling the memory AUXIL to accept a clock pulse from the comparator C_2 when the speed drops to zero.

The signal SW is pulsed, resetting the memory CONTROL to OFF, and after a time delay τ resets to ON. This procedure will be discussed later in connection with the power control.

Figure (4-8-b) shows the selection of the sense of rotation at start, which will define the sign of the initial voltage applied.

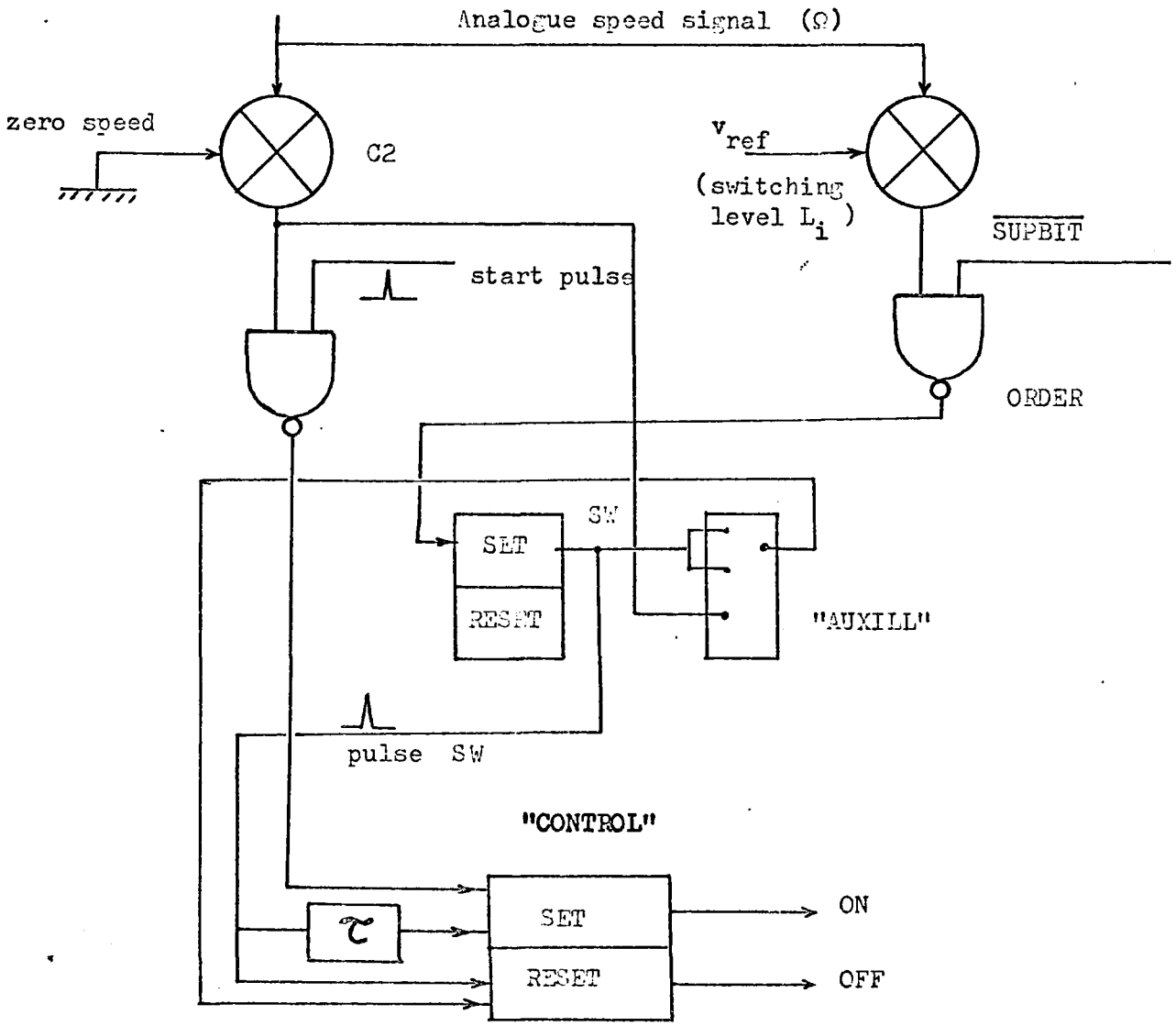

FIGURE 4-8-a: ON-OFF control orders

(Note: if Ω > ref , C_i has an output "HI")

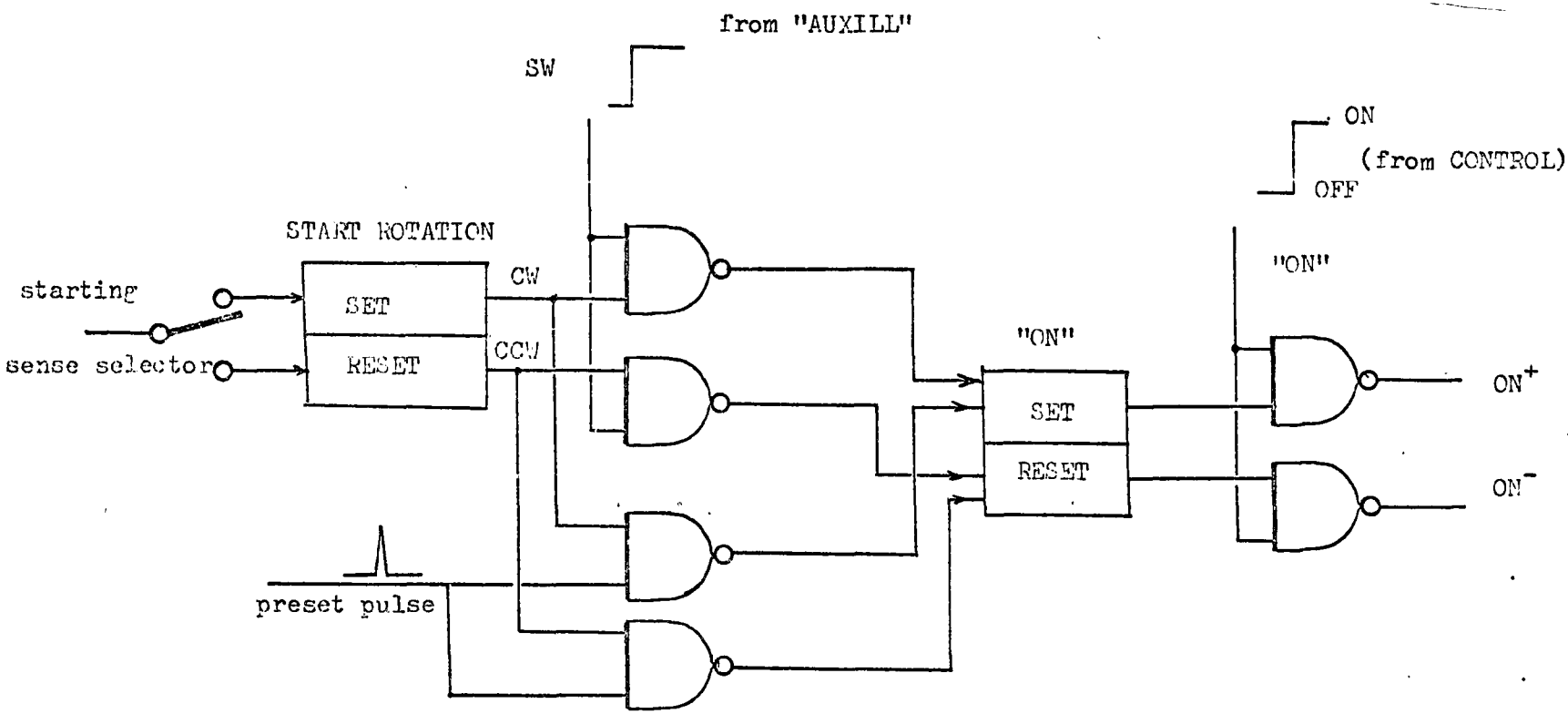

FIGURE 4-8-b: ROTATION SELECTOR

4.4.3 Power Source

For convenience the constant voltage has been chosen to be 70V dc. A single power supply is desired. Therefore ON-OFF operation should be combined with voltage inversion, which is a very difficult practical problem when high currents and fast switching are involved.

Figure (4-9) proposes a practical scheme realizing the desired control.

Power Silicon Controlled rectifiers (SCR) are used as shown by the quoted specifications.

V_{block} 600 V ; Forward current: 25A

$\frac{dV}{dt}$ = 10 V/μs $\frac{dI}{dt}$ = 20 A/μs

turn off: 75 μs trigger voltage 3 V

Basically the following table gives the sequence of firing the SCR's to perform the correct control function.

	1	2	3	4	5	6	7
ON-CW		ON	ON	ON		ON	
OFF	ON						
ON-CCW		ON	ON		ON		ON

The ON function is performed by firing SCR 2 and SCR 3, with the appropriate two others to obtain the desired sense of rotation. The capacitor C is being charged through SCR 2. This one will turn off when the current drops below the holding current. Unfortunately, the decaying

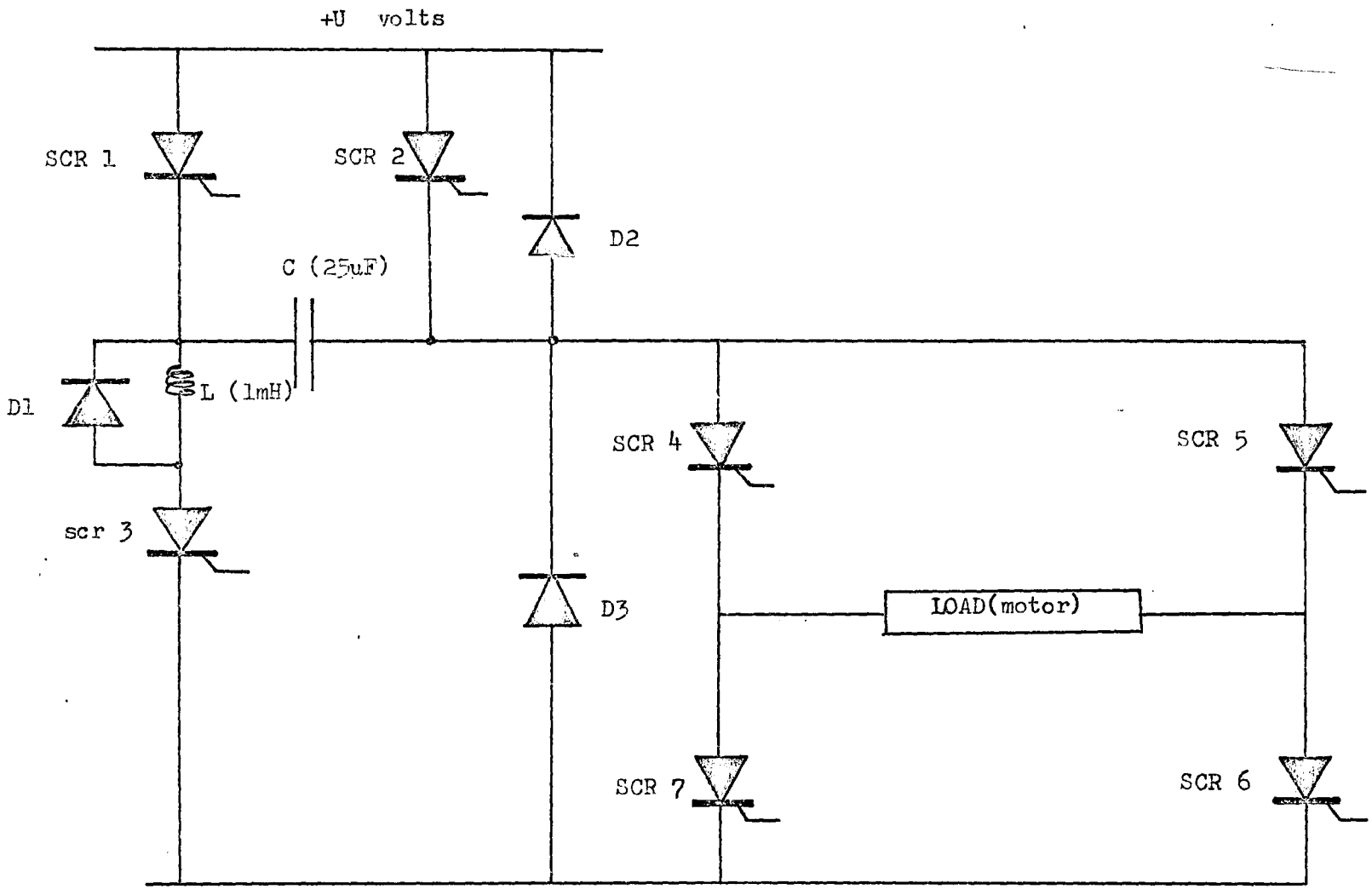

FIGURE 4-9 : Power Switching

exponential shape of charging current is inappropriate for fast switching. Hence an inductance L has been introduced in series with the capacitor and SCR 2, and provides a high frequency oscillatory charging current. Hence the SCR will cut off at the first passage by zero of the current.

A larger capacitor is needed, but the switching time is very satisfactory as will be seen from the experimental results.

The circuit is turned OFF by firing SCR 1. The voltage across the capacitor C is suddenly applied, with reverse polarization to SCR 3, forcing it to turn off. As no path exists, the other SCR's will turn off by starvation.

Protective diodes absorbe the unnecessary voltage peaks and provide a return path when SCR's are cut off.

The boolean functions are defined as follows

$$ON = (1) \cdot (2) \cdot ((4) \cdot (6) + (5) \cdot (7))$$

$$OFF = (1) \cdot \overline{(2)}$$

4.5 Analogue Computer Simulation - First Tests

4.5.1 Analogue Simulation

Because of the extremely fast operations required in practice, together with current handling capacity reaching 100 A, it has been desirable to test the controller by analogue simulation first.

Two TR20 analogue computers have been slaved to simulate the motor. In order to be able to record the theoretical curves, it was decided to scale down the real time.

One could patch the exact equations of the motor using equations (3-1). Unfortunately the use of two function generators and multipliers are necessary. The inaccuracy of the multipliers around zero voltage would introduce a much higher error than the result obtained by semilinearizing the equations. Hence L(I) has been set to its most probable value in transient conditions, when high currents are used, say the saturated value. One function generator gives the function R(I) armature resistance. The scaling of the variables has been performed as indicated:

$$t_1 = \tau t \qquad I_1 = \alpha I \qquad \Omega_1 = \beta\Omega \qquad \theta_1 = \gamma\theta \tag{4-5}$$

The symbols with subscripts represent voltage outputs defined by the relations (4-5). If μ represents ± 1 depending on whether the machine is running as a motor or a generator, the analogue equations to be patched are:

$$\left.\begin{aligned} \frac{dI_1}{dt_1} &= \left(\frac{\alpha}{\tau L}\mu\right) U(t_1) - \left(\frac{\alpha K}{\tau_\beta L}\right)\Omega_1 - \frac{R\left(\frac{1}{\alpha} I_1\right) I_1}{L\tau} \\ \frac{d\Omega_1}{dt_1} &= \left(\frac{\beta K}{\tau\alpha J}\right) I_1 - \left(\frac{a}{J\tau}\right)\Omega_1 - \left(\frac{\beta}{\tau J}\right)[b + \lambda_r(t_1)] \\ \frac{d\theta_1}{dt_1} &= \frac{\gamma}{\tau\beta}\,\Omega_1 \end{aligned}\right\} \tag{4-6}$$

By setting

$$\tau = 10^3; \qquad \alpha = 10^{-2}; \qquad \beta = 10^{-2}; \qquad \gamma = 1.02$$

the real time is multiplied by 1,000 and 1 Amp. or 1 rd/s will be represented by 1 Volt analogue voltage output. The schematic of the patching is shown on Figure (4-10).

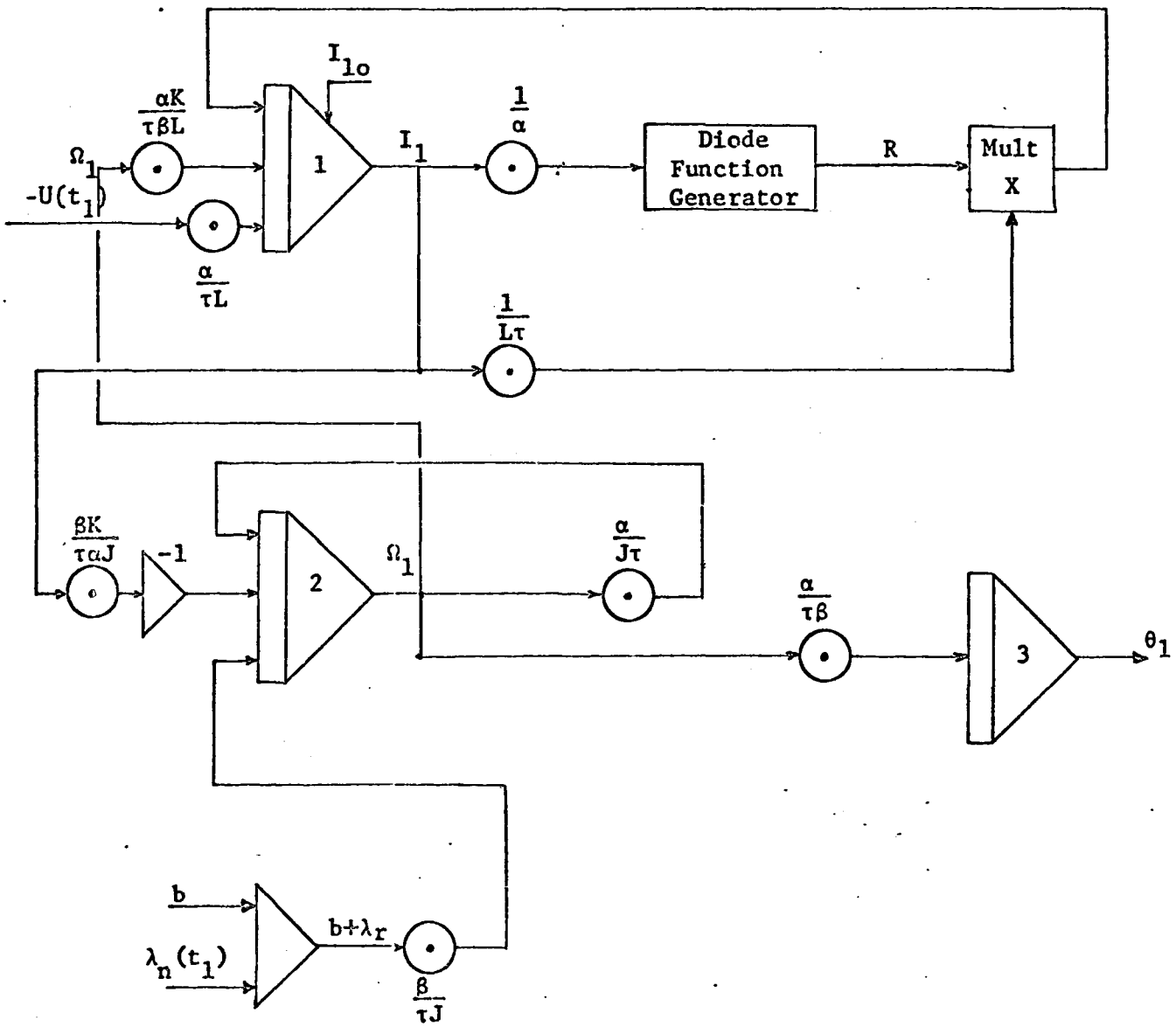

FIGURE 4-10 :

Schematic patching of a d.c. motor equation on an analogue computer.

4.5.2 Quantization of an Analogue Signal

In order to use the digitalized version of the BBC, one needs to provide quantized step pulses. A quantizer system is built, which will transform the analogue voltage simulating the position of the shaft, into pulses representing "steps".

Two comparators associated with a bistable multivibrator will realize a Schmidt-Trigger operation. The output of the bistable controls two FET transistors, the sources of which are connected to the analogue voltage representing the speed, and its negative value. The drains are connected to the input of the integrator. As only one FET is passing current at a time the integrator will perform

$$\theta = \int_0^t \Omega \, dt = \int_0^{t_1} + \Omega_1 \, dt + \int_{t_1}^t (-\Omega_1) dt \qquad (4\text{-}7)$$

Figure (4-11) shows the implementation of the step converter as well as the characteristic curves obtained. One can see the recycling properties of the system.

The FET switching seemed to be very adequate - no leaking is found when blocked - and the impedance isolation provided by the base controlled mode is very useful.

4.5.3 Practical Simulation Results

At this low speed, with noise-free signals provided by analogue simulation, the BBC is connected to an artificial switching relay system. The sequence of operations for one cycle is shown on Figure (4-12).

FIGURE 4-11 : Step converter for continuous analogue signal

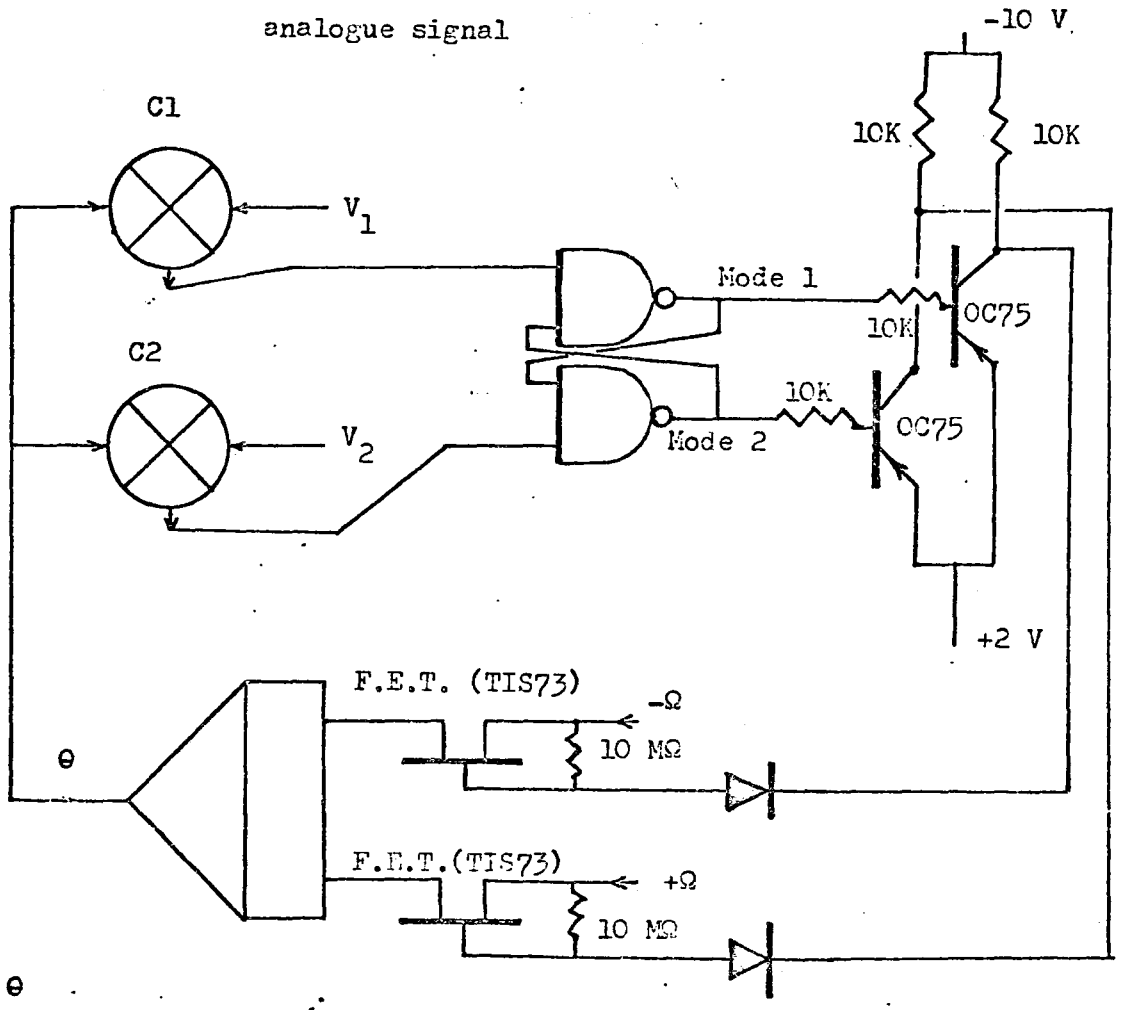

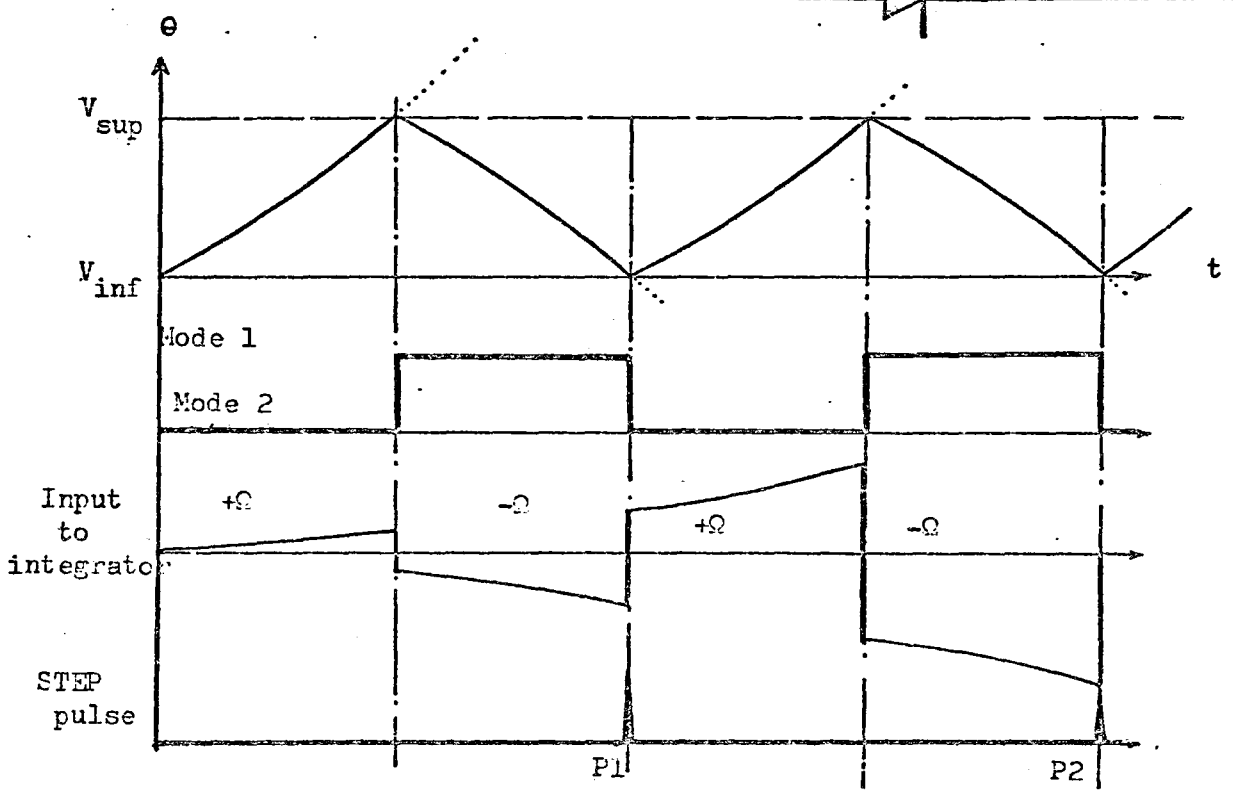

FIGURE 4-12 : Analogue simulation of a complete cycle,
Auxilliary relays and sequences of operations

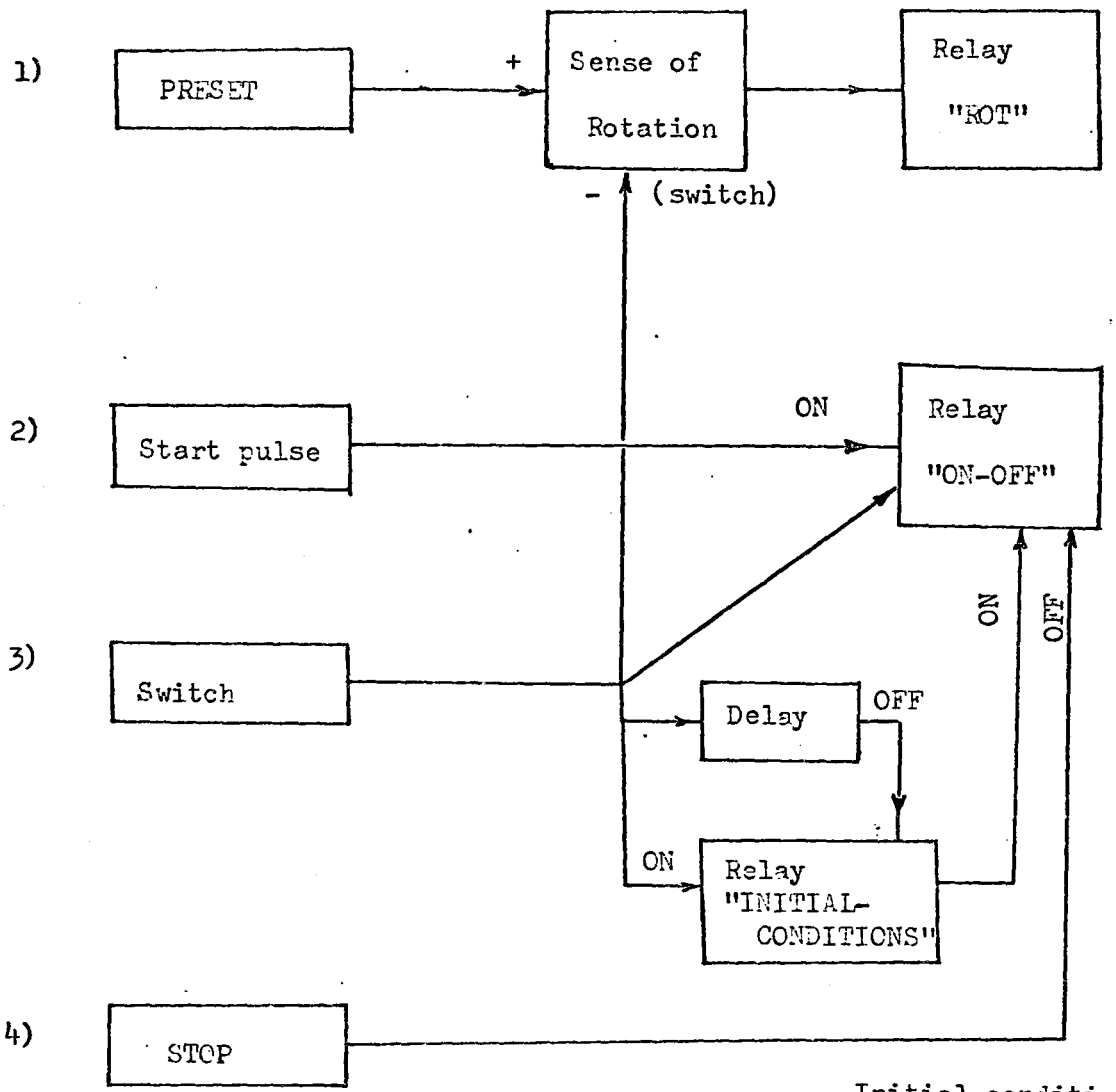

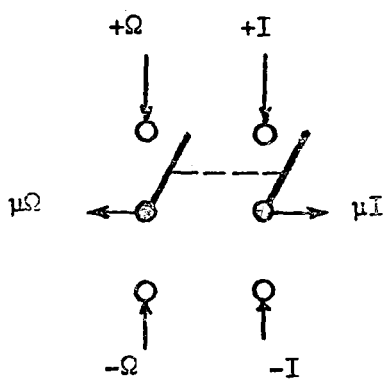

RELAY "ROT"

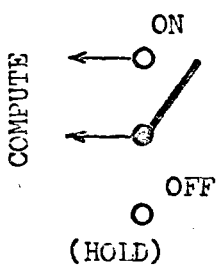

RELAY "ON-OFF"

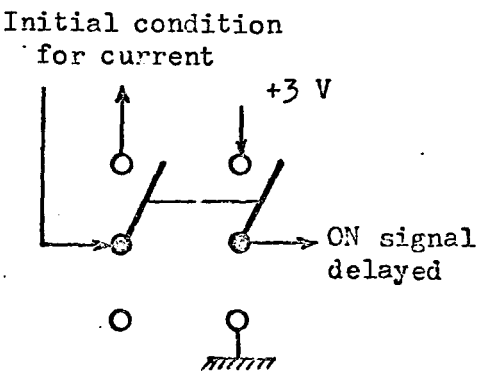

RELAY "INITIAL-CONDITIONS"

The final curves of Figure (4-13), representing a phase plane plot of a set of trajectories, were found repetitive and show that the controller drives effectively the system in the theoretical minimum-time to the desired target.

However, the addition of a noise to the analogue voltage monitoring the speed, has led to poor performances, since overshoots or early brakings were generated.

It was necessary to try to improve the design at that stage, since noise is unavoidable in practical systems.

4.6 Improved Version of the BBC

Slight load variations and mainly noisy signals are unavoidable and are shown to cause errors in the final destination. Fortunately, the tests on analogue computers seemed to show that a maximum of one step error could occur with noise parameters of 10% rms added to the analogue voltage representing the speed. Hence, the new idea was to introduce a checking loop in the BBC design.

Basically, the counter is used in both UP-DOWN possibilities, which enables one to measure the deviation from the target.

From the final destination preset on the counter, this one will count down as previously, but as the state d.f.t.=0 is reached, the counter is switched in the up-counting mode and the information UP count is stored in memory.

Suppose now that an overshoot happens when the motor stops the content of the counter shows the next d.f.t.. A new "start pulse" can

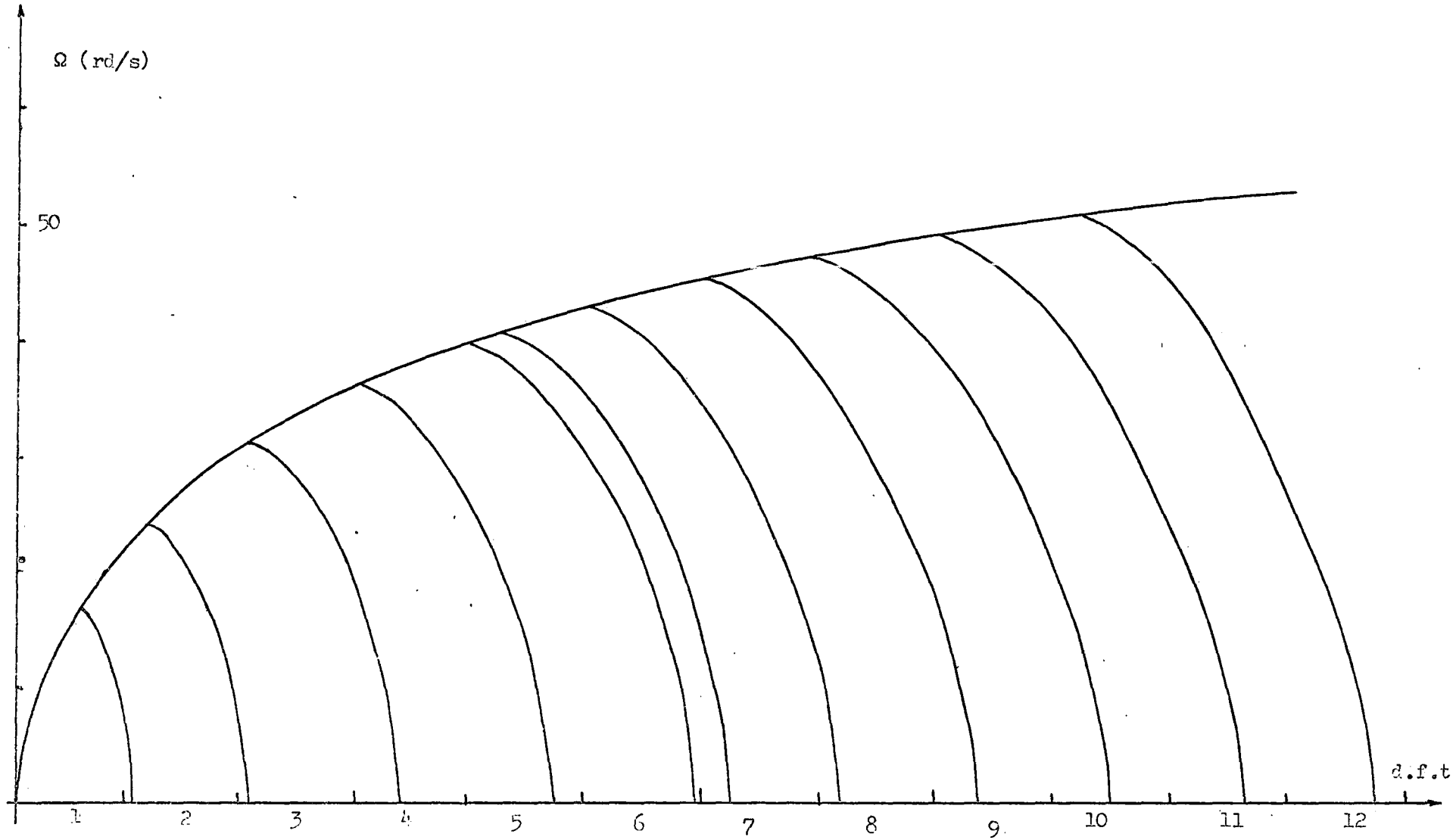

FIGURE 4-13: ANALOGUE SIMULATION; Phase plane trajectories obtained by presetting destinations from 1-12 steps

be generated, which will drive the system to this new target following the usual cycle, but now starting in the opposite direction as previously shown.

If an early stop is realized, the d.f.t. is again in the contents of the counter, and a new start pulse without changing the sense of rotation will drive the system to its new destination.

As seen previously, if the d.f.t. is zero, the corresponding level L_0 is zero as well, and no start can happen. Therefore the only modification required will be to store the information UP-count as the zero state is encountered, which will decide on the new sense of rotation to start with.

The new sequence of operation becomes

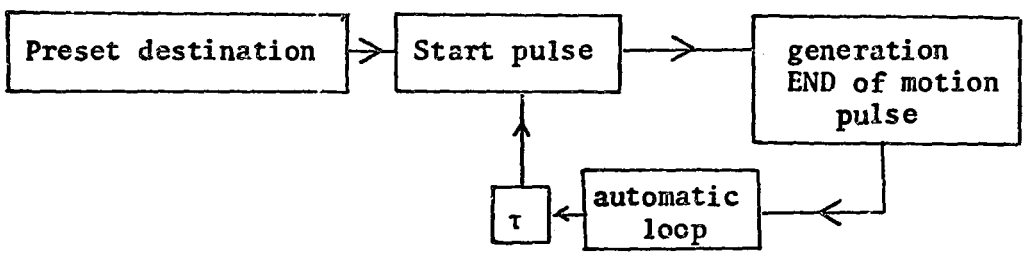

4.7 Digital Computer Simulation: General Design Program

Once the set of parameters have been measured for a given P.M. motor coupled to a given load, the switching predictor is calculated.

Suppose the step size is given (example one desires a certain angular resolution), then the maximum number N of control levels L_i needed are calculated as

$$N = Int\left(\frac{\theta_{brake}(\Omega_{max})}{Stepsize}\right) \quad . \tag{4-8}$$

Otherwise if the bang-bang controller has to be limited at a fixed number of levels, say N', the minimum stepsize is constrained by

$$(\text{Stepsize})_{min} = \frac{\theta_{brake}(\Omega_{max})}{N'} \qquad (4\text{-}9)$$

Usually one sets this value to the upper nearest simple angular division for hardware purposes.

This general program will receive first the machine and load parameters, and the information on stepsize or maximum number of levels is processed to finally print out the set of control levels and their value; this information being enough to build the BBC.

To check the design, random destinations, given as the number of steps to travel, are tested using the precise mathematical model. A possibility of adding a given random tachometer noise is introduced by making

$$\Omega = \Omega_{true} \times (1 + 0.01\eta) \qquad (4\text{-}10)$$

where η is the percentage of rms noise wanted.

The general block diagrams of Figure (4-14) illustrate the overall program.

Results

A set of very stringent conditions were studied to see whether or not the design is matched. With r.m.s. additive noise factors up to 10%, the probability of missing the target by more than one step is practically negligible.

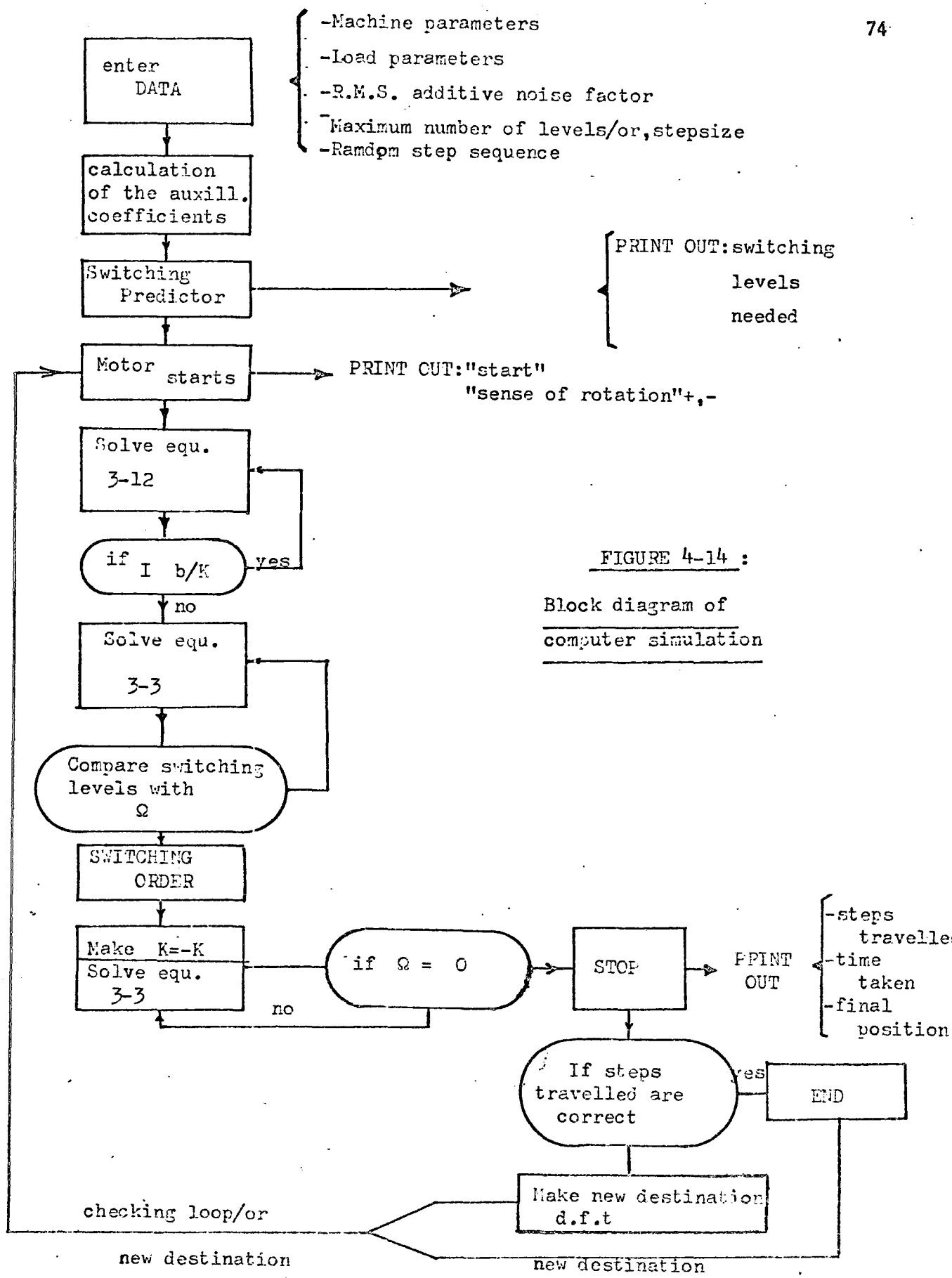

FIGURE 4-14 :

Block diagram of computer simulation

Hence, if needed, the checking-loop is used and the cost of the correction is always less than one full step travel, which represents a maximum of 20 ms. This performance seems to be far better than any other continuous feedback loop system performance.

An interesting fact was that no hunting occured even with 10% noise parameters. Besides, a very simple control of the power is used, ON-OFF, and no power amplifier is needed.

These considerations seemed to justify the approach which is obviously empirical, although based on a theoretical derivation of switching predictors.

CHAPTER V

EXPERIMENTAL RESULTS - DISCUSSIONS

Practical difficulties encountered through design and experimentation will now be discussed.

5.1 Power Switching

Because of the very high speed of switching involved, one has to use Silicon Controlled Rectifiers (SCR) for the power stage.

If two opposite voltages $\pm U_0$ are available at the source the switching would be simplified, unfortunately it would be advisable to use a simple voltage source which has to be inverted.

The basic circuit and its general functions have been described in the previous Chapter. Here, only a discussion based on experiment will be given.

5.1.1 Triggering

The high current SCR's used need quite a certain amount of power to be injected into the gates. The logic level outputs of the IC components used in the BBC require a buffer stage associated with a pulse transformer.

Figure (5-1) shows a typical circuit used successfully to trigger several SCR's at a time from a digital switching order.

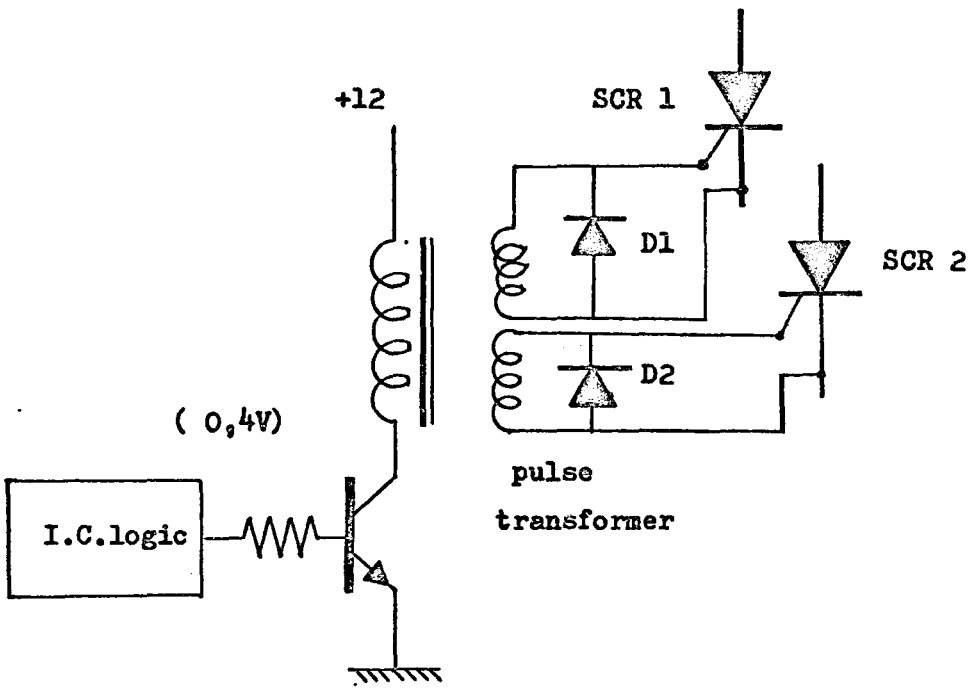

FIGURE 5-1 : SCR triggering circuit

-4 Volts logic is buffered and the pulse is shaped by the pulse transformer

-Isolation of the gate circuits are realized for simultaneous triggering

One should notice the use of bypassing diodes which prevent oscillatory signals into the gate which may cause misfiring of the SCR.

5-1-2 Practical Experience

The general configuration of the power SCR's was shown on Figure (4-9). The choice of a 25 μF power capacitor and a 1 mH inductance seemed to meet the purpose.

When SCR's 2 and 3 are fired the capacitor is charged by a high frequency oscillatory current. At the first passage by zero of the current, SCR 2 is cut off. Experimentally it has been found that .4 ms is a safe time to allow before attempting to turn the system off.

The capacitor C is charged sufficiently to provide enough energy to turn SCR 3 off. The switching off time when SCR 1 is fired can be considered less than .2 ms at maximum current handling.

Normally, the operation ON-CW followed by an OFF order, and immediately (.3 ms later) a generation of an ON-CCW order will realize the electrical braking.

The theoretical analysis assumes instantaneous switching, while the reality is very complex. Unfortunately no equations can describe accurately enough the switching capabilities of the circuit, too many unknown parameters and assumptions have to be stated. However, in practice, as the experimental characteristics prove it, a maximum of 1.5 ms random transients for switching are found and then followed by the predicted current within good experimental accuracy.

A particularly interesting feature has been found, although accidentally.

If the current to be switched drops below 17 A, the OFF order is unnecessary. Suppose SCR 4 and 6 are "on" for CW rotation. By firing simply SCR 5 and 7, without turning the system off previously, the current in the load is found to be switched as desired within .1 ms.

Although the firing of SCR's 5 and 7 show theoretically a straight short-circuit across the power supply the switching occurs. Further experimental investigations, such as replacing the load by a purely resistive load, have led to the conclusion that the unexplained switching is realized because of the inductive load which reacts with the natural capacitance of the SCR circuit.

When SCR's 5 and 7 are fired very high current transients of very complicated shape are generated, and if the amplitude of those oscillations is large enough, it causes SCR 6 and 4 to block automatically. Experimentally it has been found that below 17 A of load current the system switches over.

The experiment leading to this result has been simply to control the firing of SCR's 4 and 6, and 5 and 7 by a flip-flop while the motor was rotating. The clock frequency controlling the flip-flop is gradually decreased till a complete short-circuit across the load opens the protective high speed breaker.

A reliable switching is realized if the period of switching is above 25 ms, which, according to the theoretical curves corresponds to switchings for destinations superior to 4 steps usually.

Unfortunately, in the stringent cases where a few steps are desired, the switching must be slowed down by applying the off order first.

This weakness of the circuit is certainly subject to criticisms, but this is an engineering problem, and one had to solve it the best way possible, with a circuit presenting simplicity and reliability. Therefore, a compromise must be accepted.

5.2 Tachometer

It has been mentioned that a tachogenerator has been used in the first part of the consideration of the BBC.

The main problem arisen, and already pointed out, was the noise associated with an analogue tachometer.

Brushless tachometers are excluded automatically because of their inability to follow the high transients expected in starting and decelerating of the electric motor.

Therefore, a tachogenerator is chosen which provides a very good transient response provided the output is connected to a very high impedance circuit in order to unload the tachometer as much as possible.

Unfortunately, the tachogenerator, because of the presence of brushes, is delivering a voltage which is mixed with a very complex noise factor.

Part of the noise is definitely random, and this part could be easily taken care of by averaging methods. However, the main components of the noise factor come from the brush commutation, and the first harmonics of this noise depend on the actual speed of the shaft, and the number of commutator bars. Therefore, a filter is necessary before comparing the output signal with a noise free level L_i.

Unfortunately, the noise ratio, from peak to peak is sometimes 50 to 70% of the true average value, which is obviously inacceptable in our case.

A low-pass filter has to be built, which would cut off the high frequency parasites. But, as pointed out above, the first harmonics of the noise depend on the speed of the shaft and it so happens that those harmonics are of the same order as the basic harmonics of the speed characteristics. This means that if accurate filtering is used, most of the information is lost and the transient characteristic obtained is just as far from reality as the noisy signal.

Even notch-filtering with adjustable pass band and cut-off frequency would be of great difficulty to use. First one would take out of the signal a basic set of harmonics which deteriorate the information. Then a very complex filter tuned to the commutator bar frequency is very expensive, and its time response is questionable for the range of high accelerations this work is dealing with.

A medium, which is very far from "happy" was chosen for filtering, trying to suppress only the high frequencies above the main harmonics of the effective signal, and the noise parameter had to be accepted. The introduction of the checking loop takes care of missed targets.

5.3 Practical Difficulties

Other minor difficulties arisen during the testing were found. Although they could be avoided easily with more elaborate instrumentation, they added their effect to the experimental "failure" of the project.

Unfortunately, the odd 70 V power supply needed for the motor was a great mistake at the start, because it was not powerful enough to provide great currents as precalculated in the theory. But, as the motor was already on the premises, the lack of funds to buy another more suitable motor or another power supply did not leave any choice. The project had to be conducted with the existing apparatus.

5.4 Criticism of the Design

As in any engineering problem, the project can be questioned on several points. A few major points are discussed below as they appeared in the design and experimentation.

5.4.1 Weaknesses

The main weakness seems to lie in the use of the tachogenerator. In theoretical simulation as well as in practice the main part of the error came from the noisy signal.

One of the consequences of the use of a tachogenerator is obviously the deterioration of the information. In such heavy transients the slightest error in the speed information is leading to a missed target. On the other hand, the use of a D/A stage is compulsory, and this stage reveals itself as heat sensitive, which adds to the imperfection of the switching order detection.

However, the switching moment not very well detected did not seem to have as much consequence as the false detection of zero speed. As a consequence, an early stop signal while electrical braking is

applied, results in a "running down" condition, which just drives the shaft far away from the target.

On the other hand, a late stop signal leads to the shaft accelerating in the opposite direction, and then the open-circuit leads to another "running down" condition where, no braking being applied, the shaft is driven again away from the target.

Fortunately, the tachogenerator speed being low around zero speed, the noise is less important and zero detection becomes more accurate than switching level detection.

One can partially overcome this difficulty by including in the system a "short-circuit" condition across the armature when "stop" signal is applied. This would result in less deviation from the target when early or late stop signals are generated.

Another idea would be to add on the shaft an electric clutch system which is energized when STOP signal arrives, and therefore increases artificially the friction parameters of the load without changing the inertia. Hence, a much higher current would be required to overcome the friction and the kinetic energy stored in the shaft would be dissipated much faster.

In special cases, by analogy with incremental steppers, where mechanical locking devices are used, such a locking ring could overcome by its friction, the errors in the positionning, and even correct it, although more slowly, by locking it in the present step.

In very elaborate systems where self locking and fast accelerations and high torques are desired, the bang-bang controller together with the

d.c. permanentic motor could provide the torque characteristics, and on the same shaft, a much smaller stepping motor could be used only when the target is reached to add its locking property. The power required by the stepping motor would be only a pull-in torque, high enough to compensate for the false parasitic torque generated by inaccurate switching and stop orders to the main driver.

5.4.2 Advantages: Applications

The tremendous acceleration rates and braking capabilities, together with the simplicity of the design and implementation, make this project valid for certain applications.

If the positioning at the final position is not that important, but emphasis is on the rectangular speed characteristic desired, then the method presented is fully valid.

For example, a tape drive for computers does not require very precise stopping. For instance, one could wait a few inches before marking or reading off the tape. Likewise one could only apply the switching and braking order after the marking "END" (or end of reading) is met. The important thing in this process is to reach a high speed almost as a step output, and to stop as fast as possible, while constant tape drive is provided during the writing or reading off of the tape.

Nowadays computers are limited by the peripheral input-output systems, and any improvement in an input-output stage like tape or disc register would increase considerably the speed of the total process.

In another domain, like automatic tooling the digital bang-bang controller could be used as a "rough" displacement of the tool in minimum-time, and a "slower" accurate positioning could be performed by a stepper through a lead-screw positioning, for example.

The total cycle would still be much less in time than the use of oversized stepping motors alone, since the stepping motor would be used only in the "one step" operation where the pull-in torque is the highest. Therefore, the efficiency of the group would be very high, besides, the stepping motor could be used as position transducer while it is not energized for actuator purposes.

Conclusion

Although imperfect, the actual BBC associated with the d.c. motor gives relatively good results. It definitely provides maximum acceleration and maximum deceleration, and therefore, provided the target is reached, responds as closely as possible to the theoretical minimum-time.

However, the main problem is caused by the speed sensing and, as a consequence, the D/A stage in the bang-bang controller.

A fully digitalized system would be appreciated, provided the speed is given directly in digital form, with the requirements of the theoretical performance, that is, high resolution, high rate of information, noise free signals and possibility of zero speed detection.

Therefore, the above conclusion has led to the development, design and implementation of a special high precision, high resolution digital tachometer described in the following chapters.

CHAPTER VI

DIGITAL MEASUREMENT OF SPEED PRINCIPLE

As seen in the previous chapter, the main limitation in applying the digital bang-bang controller is the impossibility of obtaining a good information for speed transients.

Hence, the project has led to an investigation of the digital measurement for determining speed. The existing principles will be analyzed and proven inefficient, and a new approach will be proposed, meeting the requirements for minimum-time control.

6.1 Survey of Existing Methods

Many methods are available for measuring velocities of rotating shafts. The bulk of these are based on analogue principles, but a few adopt hybrid digital-analogue techniques, leading to wholly digital procedures as well.

The simplest and most direct method is the use of tachogenerators, either a common d.c. commutator machine or a homopolar generator. Another kind of tachometer is obtained by rectifying pulses produced by magnetic or optical transducers delivering pulses of a frequency proportional to speed. The latter is one of the hybrid systems used.

However, in any case, filtering must be applied. If a commutator machine is used, it is necessary to filter out the cummutator ripple and the brush noise. Some ingenious methods have been proposed [C10],

like a narrow band filter which is kept tuned automatically to the frequency of the commutator ripple. But, as pointed out previously, in high transients the commutator ripple is within the frequency range of the output information, and the filtering will alter the analogue output.

In the case of a pulse rectification, again the filter has to remove the a.c. component. This method could only be used for very slowly varying speeds hence, the filter must have a very low cut off frequency.

The same remark can be applied to brushless motors, hence a rectifying condenser will disable higher frequency components.

In all these cases, a degradation of the response information has to be accepted.

Wholly digital methods are proposed for measuring angular acceleration and speed [5-6]

Optical or magnetic transducers exist nowadays, and they provide a very large number of uniformly spaced pulses per revolution. Basically, the principles used for obtaining angular velocities have been to measure an angular displacement during a given time, by counting these uniformly spaced pulses. Hence, the angular velocity is obtained by a count, n, equivalent to integrating over a given interval of time.

The resolution of such a system is directly proportional to the number of quantizations per revolution, N_m, hence very sophisticated transducers have to be used.

On the other hand, the error in a measurement depends on $\frac{1}{n}$, hence n should be as high as possible. As the quantization number is limited by the transducer, the interval of sampling time should be increased for higher precision. To be able to reach 1% precision on a count, a minimum of 10 ms and usually 100 ms sampling intervals are used.

However, it is easy to see that the average value of the speed over 100 ms, as it is obtained, can be of little value if transient speeds are to be considered. Figure (6-1) shows a typical starting curve and the effective measurements provided by a common digital tachometer. Suppose in the case of our BBC, the starting transient has a duration of 50 ms, obviously 100 ms, even 10 ms sampling interval cannot be considered at all.

Furthermore, low speeds are unmeasurable since n, being too small, the error in the measurement is higher than the resolution of the system.

These principles can only be used for steady state speeds or slow transients, at relatively high speeds. Some applications can be found in speed regulations like tape drivers, or use of up-down counting speed regulations as proposed in [11]. But it seems that for fast transients they can be of no use in control systems.

A new type of low-noise tachogenerator has been proposed by Stephenson [12], which seems to be more applicable. His device claims the following advantages: (i) "a pulse repetition rate not being zero at zero speed", (ii) "the ratio of maximum to minimum repetition rate over the operating range can be adjusted to a suitable value", and

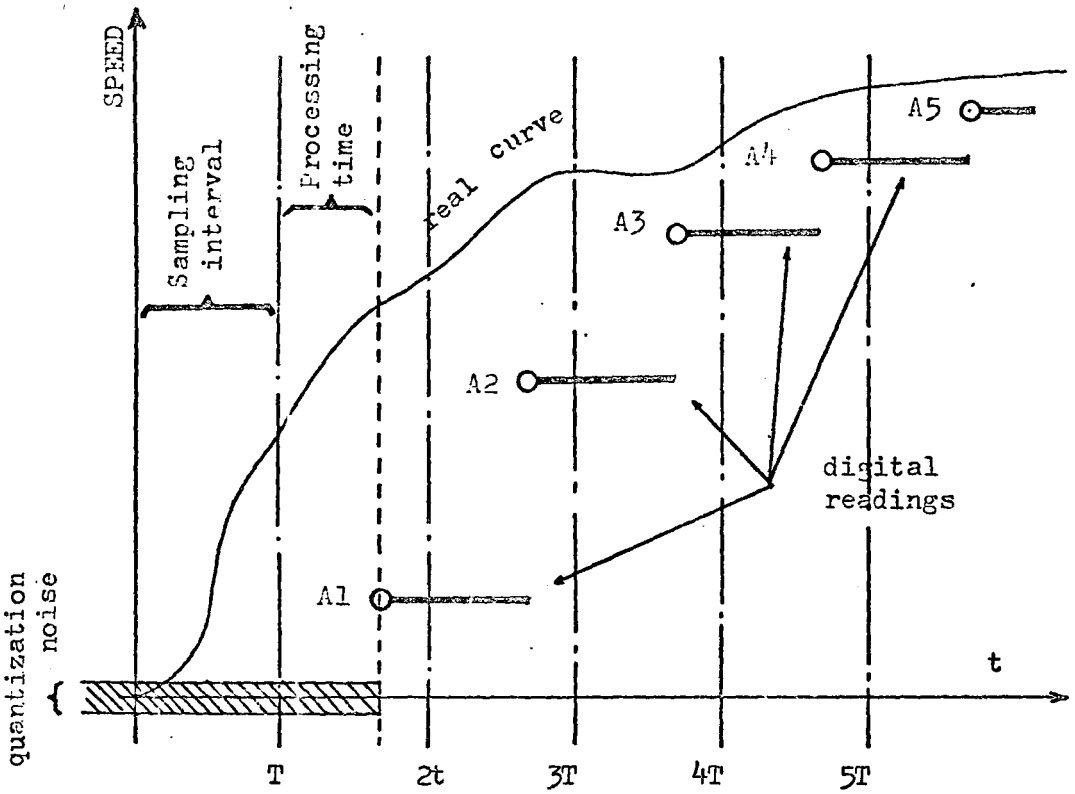

FIGURE 6-1 : Starting curve recorded with existing digital tachometer

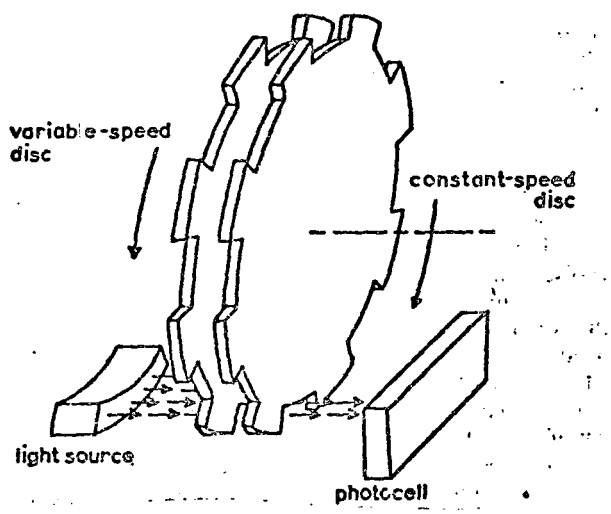

FIGURE 6-2 : Constant biasing speed added

(iii) "the minimum repetition rate can be kept constant, say 100 times higher than the highest frequency of the required passband and hence can be easily removed!"

The principle of this device is shown on Figure (6-2). Two slotted discs rotate in opposite directions. One disc has a constant speed and the other rotates with the shaft the speed of which is to be measured. If a light beam, greater than one slit pitch, is picked up by a photosensor, all slit coincidences are detected at whatever angular position they occur (within one slit pitch). Hence, the frequency of the pulse train detected is proportional to the speed of the variable speed disc and the constant speed disc. One can picture the realization as the zero speed has been raised to a minimum frequency repetition rate which can be relatively high, say 10 kHz. The suppression of the different noises are easier now since the measured frequency spectrum has been shifted towards high frequency range. Basically, the pulses generated are shaped in a square-wave and then averaged (i.e. filtering) using a non-distorting filter but which removes as much noise as possible. The zero speed is backed-off, and the resulting signal can be filtered again.

One can see that this tachogenerator, although complicated, meets some of the requirements, as the zero speed detection and much better noise filtering.

6.2 General Principle of the New Instrument

The division by time has been carefully avoided in the existing instruments. The new one, however, is based on division by time, performed effectively by a digital processor.

A schematic diagram of the proposed instrument is shown on Figure (6-3).

It relies on the two new ideas. The first consists of measuring the relative speed between the rotating shaft to be studied, and another rotating in the reverse direction at a strictly constant speed, called "biasing speed".

The transducer discussed later provides a pulse train called "Rotator pulses".

The second principle is to measure the time t between two Rotator pulses, so that the relative speed is proportional to $\frac{1}{t}$.

Suppose f_o is the reference speed, f_m the speed to be measured (both in rps) then, the Rotator pulse rate f should be:

$$f = f_m + f_o \tag{6-1}$$

and related to the time between two pulses measured:

$$f = \frac{k}{t} \tag{6-2}$$

where k is a constant depending on the transducer. Hence, from (6-1) and (6-2), the desired speed is

$$f_m = \frac{k}{t} - f_o \tag{6-3}$$

The knowledge of t and f_o will lead directly to the result expected.

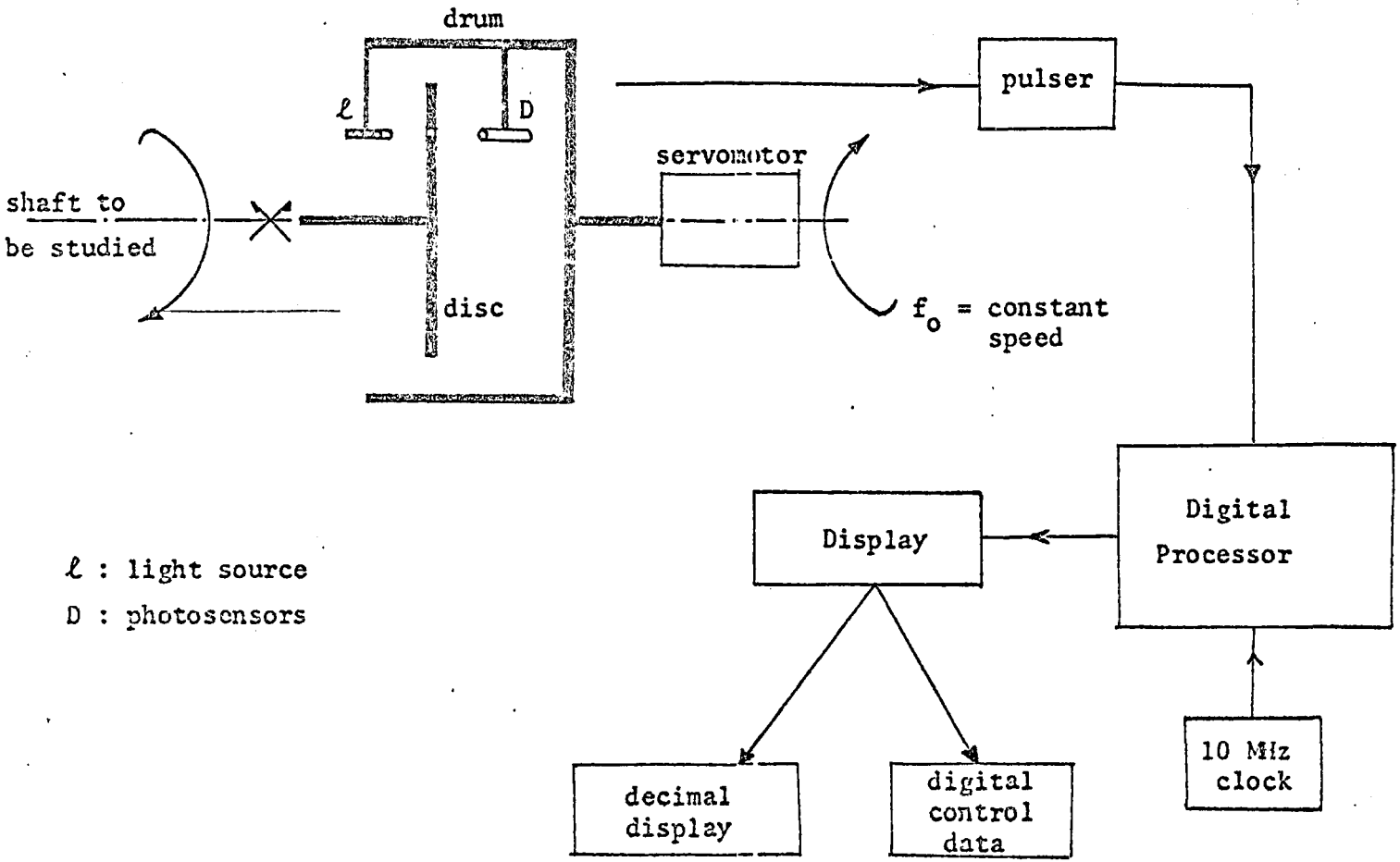

FIGURE6-3 : General System Implementation

6.3 Optical Transducer

A low inertia and frictionless disc, with N_m evenly spaced slots (or any other suitable means of obtaining contrasts) engraved, is tightly coupled to the shaft to be studied. It has to be noted here that resolution and precision will not depend on N_m, hence N_m can be small.

An auxilliary drum, having D pick-up sensors in parallel (photo-sensors for optical contrast) is coupled to an auxilliary motor rotating at a constant speed in the opposite direction. The drum should have a relatively high inertia to maintain a strictly constant instantaneous speed. The signals picked up by the sensors are fed into a pulse shaping circuit as described in Appendix A, and constitute the Rotator pulse train.

6.4 Treatment of the Result - Practical Algorithm

Suppose now that equation (6-3) is scaled so that only integral numbers are used, and capital letters represent the integers corresponding to each symbol already defined. Equation (6-3) is then transformed to

$$F_m T + F_o T = K \qquad (6\text{-}4)$$

If F_o is an exact power of 2, say $F_o = 2^N$, the general algorithm can be followed on Figure (6-4).

Once T has been obtained, its binary coded number shifted by N digits to the left represents the multiplication

$$F_o \times T = T \times 2^N$$

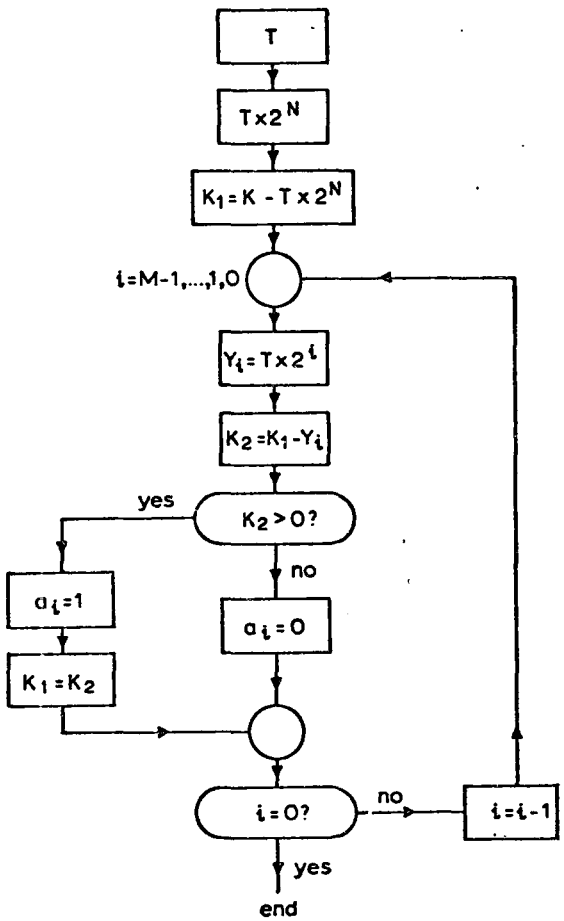

FIGURE 6-4 : *Block diagram for basic algorithm*

As K is a known constant, a binary parallel adder performs

$$K_1 = K - F_o T \tag{6-5}$$

K_1 is substituted into equation (6-4) and leads to

$$F_m \times T = K_1 \tag{6-6}$$

In binary coded form, F_m is written as

$$F_m = \sum_{i=0}^{M-1} a_i 2^i \qquad \text{with} \begin{cases} i=0,1,\ldots,M-1 \\ a_i=1 \text{ or } 0 \end{cases} \tag{6-7}$$

The binary division is performed by searching for the coefficients a_i by a succession of shift and add operations.

If (M-1) is the highest power of 2 which will ever be encountered, T shifted by M-1 digits to the left represents $T \times 2^{M-1}$. Hence, if $K_1 < T \times 2^{M-1}$ the M-1th power of 2 is not contained and one should store $a_{M-1}=0$.

If $K_1 > T \times 2^{M-1}$ the power of 2 is contained in F_m and one should retain $A_{M-1}=1$ and perform $K_1 - T \times 2^{M-1}$ and substitute this new value for K_1.

One digit shift to the right will lead to the M-2 stage and so on until all the a_i's are determined.

6.5 Special Purpose Instrument - The Digital Processor

6.5.1 Scaling the Numbers

The active part of the instrument is the digital processor which will effectively perform the division by time, although theoretically, this is no problem. In fact, an engineering problem is raised. One should accept a compromise between resolution and precision, and register sizes.

The practical instrument built was not designed in view of optimizing it, but to obtain a reasonable hardware with adequate performance. The example treated shows however the approach with empirical engineering feeling.

A careful choice of f_o and units used for speed measurement will be important factors in the reduction of register sizes.

Suppose N_m is chosen to be 100 (which does not present any manufacturing problem), D equal to one. The constant k of the transducer becomes $\frac{1}{100}$. If F_o is chosen to be 2^{10},

$$f_o = 16.2 \text{ rps} = 975 \text{ rpm} .$$

The maximum time measured will be when $f_m = 0$, hence

$$t_{max} = \frac{1}{f_o} = 616 \times 10^{-6} \text{ sec.}$$

If a 10 MHz clock is used for time basis, the count for T will be

$$T_{max} = 6160$$

which is represented with 13 binary digits.

Suppose a four decimal display is desired for f_m, F_{max} must be

$$F_{max} = 11{,}023$$

hence

$$K = \text{int}(2\pi \times 10^6)$$

which is represented by 23 binary digits.

With these numbers, a resolution of 0.1 rd/s can be obtained, since the result in decimal display will be ten times the speed expressed in rd/s.

However, the final result is expected to be less than $\frac{10K_o}{T_{max}}$ otherwise the error due to sampling will be higher than the resolution

capability, hence

$$(F_m)_{max} < 10^4 .$$

A 13 binary digits number provides $(F_m)_{max} = 8191$ leading to a display of approximately

$$(f_m)_{max} = 130 \text{ rps} = 7800 \text{ rpm}.$$

6.5.2 The Central Processor

Figure (6-5) describes the processor used for the above-mentioned data.

As subtraction is required, the 2's complement technique is used here. The 23 bits K register contains the right hand side of equation (6-4) or (6-6) and is connected to the B input of the parallel 23 bits binary adder. The term $2^i \times T$ is contained in the main 25 bits shift register. The 23 lower bits inverted are connected to the A inputs of the adder, while the "carry in" is at high state.

If the 2 bits of "overflow" register are empty and the "carry out" is in state "1", the number found on the adder as a result of (B-A) is positive and a gate converts the information into "SIGN" = "1".

Hence, a straightforward sequential logic follows for compilation of the result.

The 10 MHz clock feeds the upcounter I continuously. When the rotator pulse arrives, cycle 1 starts.

Cycle 1: The content of the counter is transferred into the register T and the 10 digits on the right, as well as OVERFLOW are cleared.

- The counter resets to zero and is enabled to sample the next

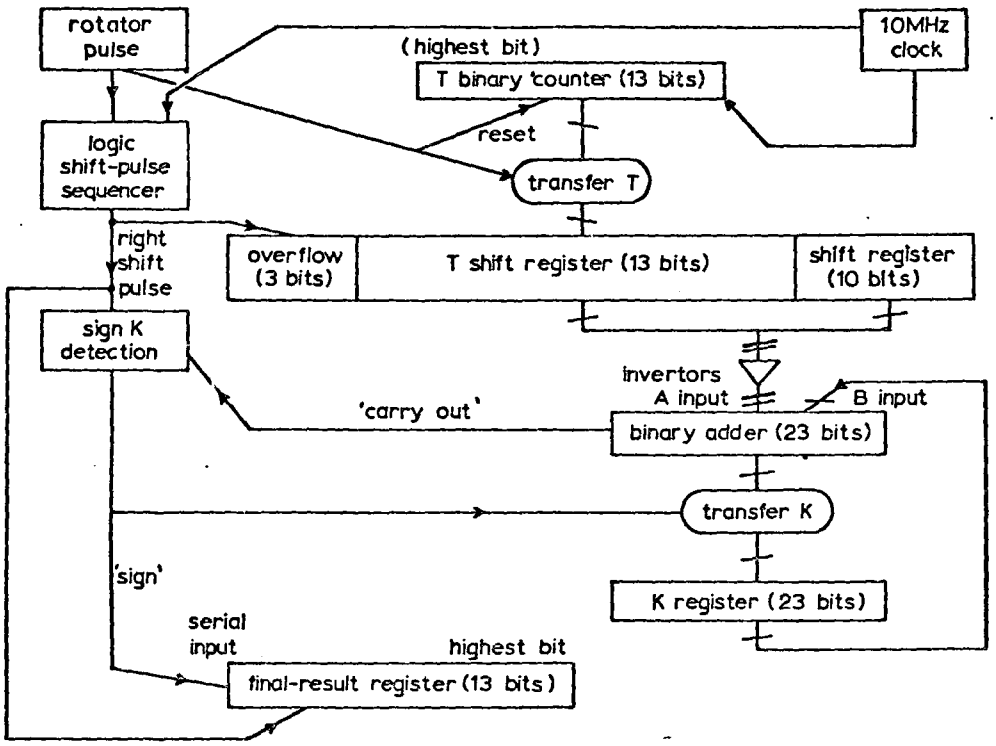

FIG 6-5 : *Block diagram of processor*

interval while the result is processed.

- K register is preset to $(2\pi \times 10^6)$.

Cycle 2: After a delay time allowing the adder to terminate its ripple through, the value of the output is transferred into the K register.

- 23 shift pulses follow, bringing back the number T into the position represented by $T \times 2^{13}$.

Cycle 3: After appropriate delay time, if SIGN is found to be "1", the result on the adder is transferred into the K register at the next shift pulse while SIGN is entered into the serial input of the final shift register FSH.

- If SIGN = "0" is detected, the transfer into the K register is inhibited and "0" is stored into FSH.

- After 13 similar operations all the a_i's are stored in FSH, the end of processing is reached and the processor resets to a waiting position, ready for the next compilation.

6.6 Modifications

It has been found quite difficult to adjust the biasing speed exactly at the given 975 rpm with the accuracy desired. Therefore, the design has been slightly modified to permit the presetting of the biasing speed automatically with the precision of the tachometer.

A synchronous motor is used, rotating at any speed lying within 900 and 1800 rpm. The high rotor inertia and the precision of the synchronized drive assures constant speed. As f_m=0 one uses the

tachometer to measure the speed of f_o. This is done by inhibiting the first transfer as described in cycle 2. Therefore, the result in FSH gives the speed f_o and is transferred to an auxilliary 11 bit shift register.

Now cycle 2 will be modified. The first 11 pulses in cycle 2 will transfer the content of the adder to the K register only if the corresponding bit of the auxilliary shift register is in the state "1", as

$$F_o = \sum_{i=0}^{N-1} \alpha_i 2^i \qquad \left\{ \text{with } \alpha_i = \text{"0" or "1"} . \right\}$$

The operation realized is really to subtract from the initial K the value

$$T \times \left(\sum_{0}^{N-1} \alpha_i 2^i \right)$$

instead of only $2^{N-1} \times T$.

Besides, instead of resetting the counter to zero, it is advisable to reset it to 2 and disable the first two clock pulses. This is realized in order to prevent coincidence with rotator pulse and ripple through of the asynchronous counter used, which would lead to meaningless results.

Subjectively some main features of the tachometer should be pointed out at this stage.

- The clock precision and the constancy of the biasing speed are the only limitations for accuracy of results.

- The precision and resolution does not depend on N_m, hence a cheap rotator can be available.

- Since the biasing speed is applied, a zero speed on the disc shaft is detected with a reasonably high rate of information without quantization noise, as seen $t_{max} \simeq 0.6$ ms, hence $B_{min} \simeq 1600$ samples/sec at zero speed.

- The resolution is 0.1 rd/s which is one of the best reached by any existing models.

- The rate of information increases from $f_m=0$ and reaches 16,000 samples/sec at maximum speed without deteriorating the resolution.

- The sampling time is very short, within 0.61 ms, hence the average speed defined can be considered as instantaneous for all physical systems.

In the next chapter a more detailed hardware implementation is presented, and will allow a deeper analysis of performances. But already at this stage it appears to be a device meeting all the requirements of control systems for fast transients.

CHAPTER VII

THE HIGH PRECISION-RESOLUTION DIGITAL TACHOMETER

As pointed out in the previous Chapter the scaling of the numbers of equation (6-3) has a great influence on the design of the tachometer. This Chapter will present an effective hardware realizing the desired function. However, it is not meant to be an optimum design, and some improvements can certainly be made towards directions pointed out during the proposal.

7.1 The Rotator

Figure (7-1) shows the exact representation of the Rotator. The slotted disc is rotating on a bearing guided shaft. Therefore, friction and inertia are as low as possible which would not disturb the initial coupled shaft to be studied.

The rotating drum is aligned exactly with the shaft of the disc and its inertia is rather high. One light beam and pick up sensor (photodiode) are placed on the drum so that the rotating disc can interrupt the light beam. Two slip rings plus a ground ring provide the power to the lamp as well as the pick up sensor's output. This output is fed into a Schmidt trigger as proposed by Appendix A.

The disc has 100 contrasts per revolution, and the drum is rotated by a 1000 rpm synchronous motor. If one finds the normal 60 Hz not stable enough, a simple oscillator controlled by a stable clock could be built to energize the synchronous motor.

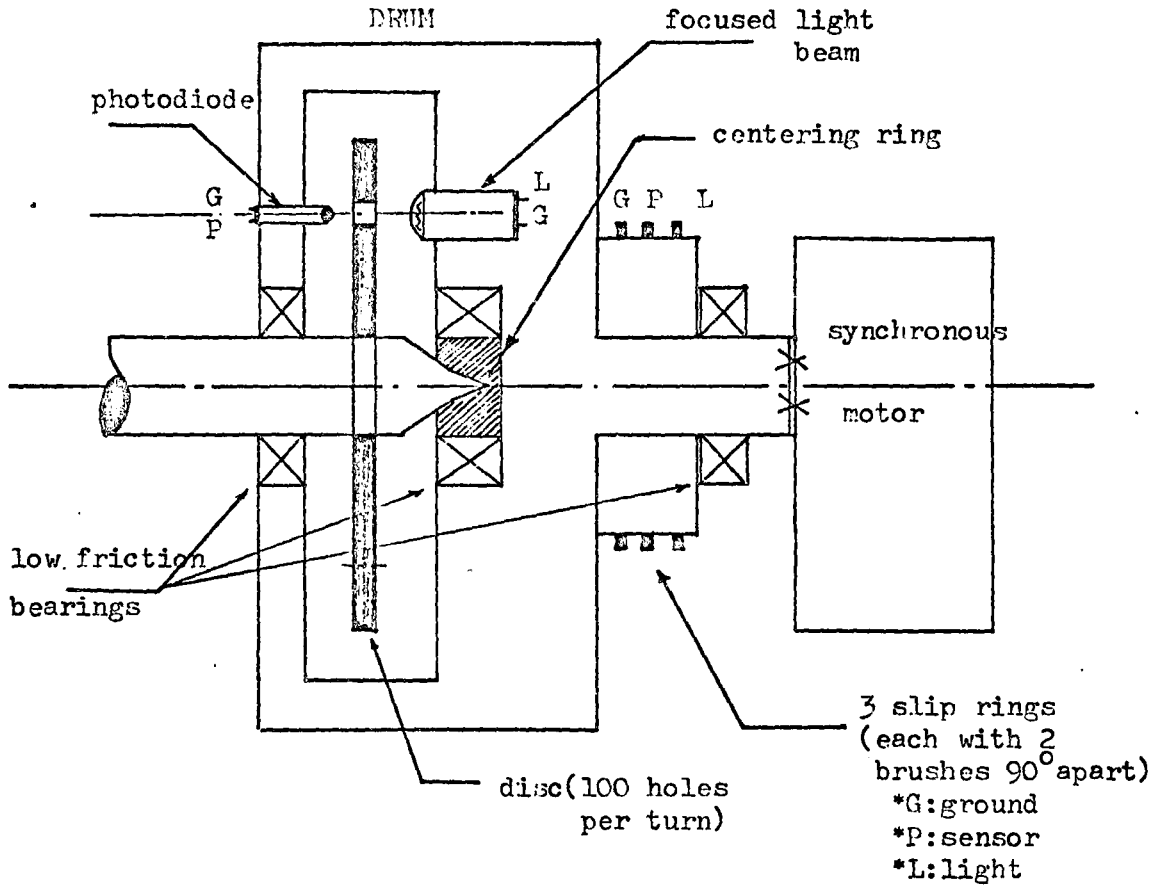

FIGURE 7-1: THE ROTATOR TRANSDUCER

7.2 Register Sizes

7.2.1

A 13 digit binary asynchronous counter is constantly fed by a 10 MHz clock. Hence the maximum time interval to be processed must be less than $T_{max} = 8191$. This corresponds to a minimum relative speed of $f_o = 12.2$ rps = 735 rpm. Hence, with the synchronous motor rotating at 1000 rpm, there should never be an overflow. The effective maximum time count should be for $f_m=0$

$$\{T_{max}/f_m=0\} = 6,000 \quad \text{then} \quad t_{max} = 0.6 \text{ ms} .$$

If the result can be processed during two sampling intervals, the minimum sampling rate will be at zero speed detection:

$$B_{min} = 1660 \text{ samples/sec} .$$

7.2.2

The final register FSH, having 13 bits, it results that the maximum speed to be detected can be $f_m = 130$ rps (7800 rpm). At this speed the sampling time will be minimum and $t_{min} = 68$ μs leading to a sampling rate of

$$B_{max} = 14,700 \text{ samples/sec} .$$

7.2.3

As seen previously from the algorithm, the maximum operational shift register size will be 25 digits. The parallel adder as well as the K register needs only 23 bits.

7.2.4

If one decides to preset the speed, the average value for 1000 rpm will be read as F_o = 1048. Hence an 11 bit number can store this information in the shift register'STORE".

7.3 Cycle Generator

Figure (7-2) shows the effective implementation realized for the cycle generator. If the modified algorithm is used, where F_o is any number, the following cycles have to be generated:

Cycle 1: (i.e., section 6.5.2)

Cycle 2: 11 shift pulses have to shift the number T through the register YSH, realizing T x 2^j, with (j=1,11), while the shift register STORE is pulsed as well. The serial output of STORE combined with the transfer pulse should enable or disable the transfer into K register.

Cycle 3: As register store has been cycled through, the shifting is inhibited. Twelve supplementary shift pulses should bring T back to the position T x 2^{13}, without allowing any transfers into K.

Cycle 4: 13 shift pulses, followed by transfer pulses allowed only when SIGN = "1" search for the powers of 2 which are entered into PSH shift register.

End of Process: A general clear will reset the processor to a waiting position, and an "END" pulse is generated, which can be used for a read out.

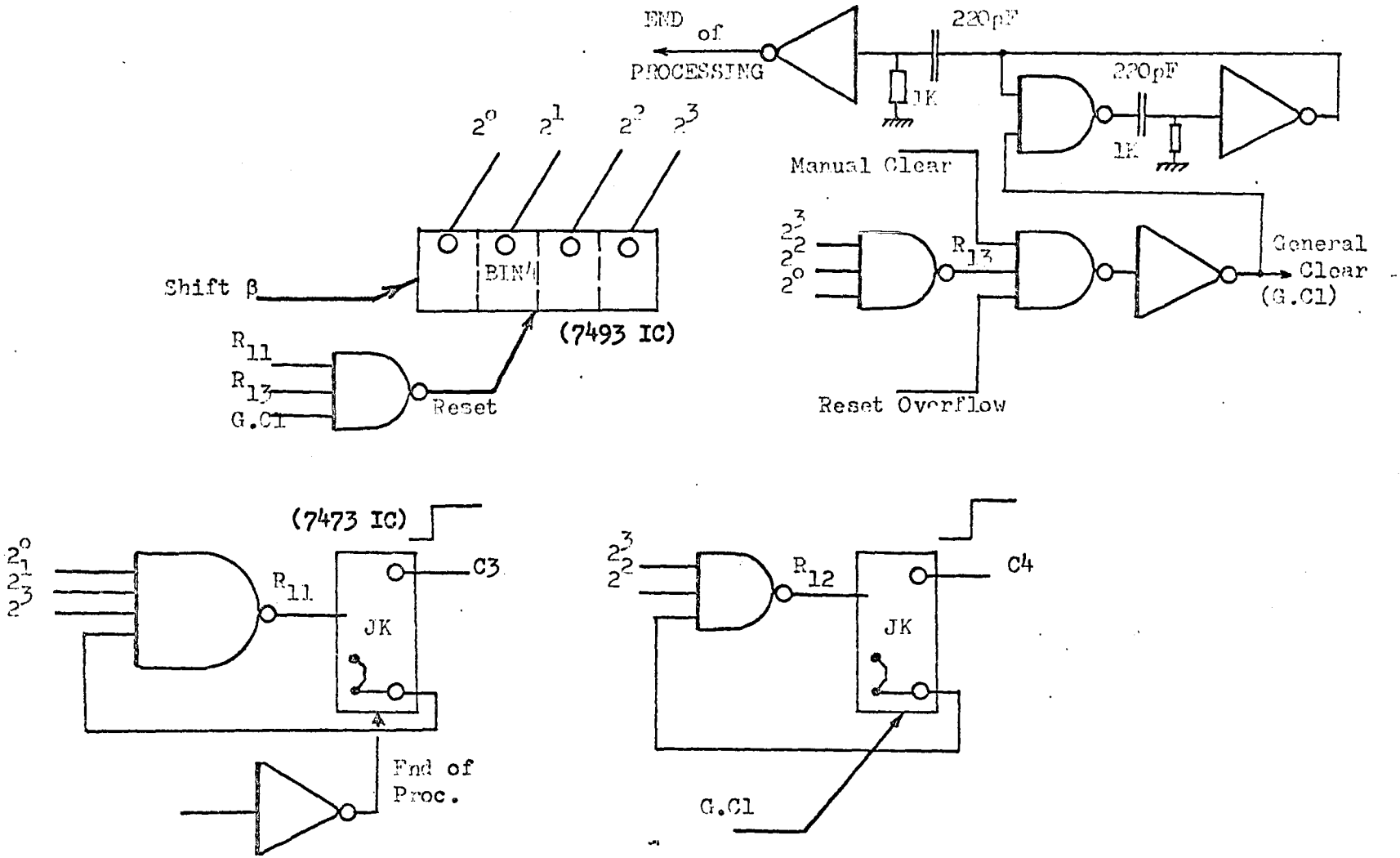

FIGURE 7-2 : CYCLE GENERATOR

A simple 4 bit binary up-counter is used in association with flip-flops storing the present cycle information.

7.4 Shift Pulse and Transfer Pulse Generation

Figure (7-3) shows an implementation realized for generating shift and transfer pulses.

The apparent complication of the circuit has been dictated by the safe time delays chosen for reliable commutations and ripple through of the different IC components. These time delays can be fortunately decreased, if "carry-look-ahead" components are used to speed up the parallel adder's performance. Nevertheless, in this design, one has tried to obtain a safe and reliable functioning first, even if top computational speed is not reached.

Basically, the 10 MHz clock is feeding a counter which counts up to 6 and resets. The diagram on Figure (7-3) shows how the delay times of 400 ns for adder ripple through are respected. Besides, some constraints of the K register are met. One has to maintain at least 100 ns for the input of the K register after having clocked the transfer.

On the other hand, for the start of processing one allows a safe time for the I counter to ripple through before transferring the information into TSH register and clearing the counter. Therefore, the sampling count is inhibited for 3 counts and obviously the counter reset to 3.

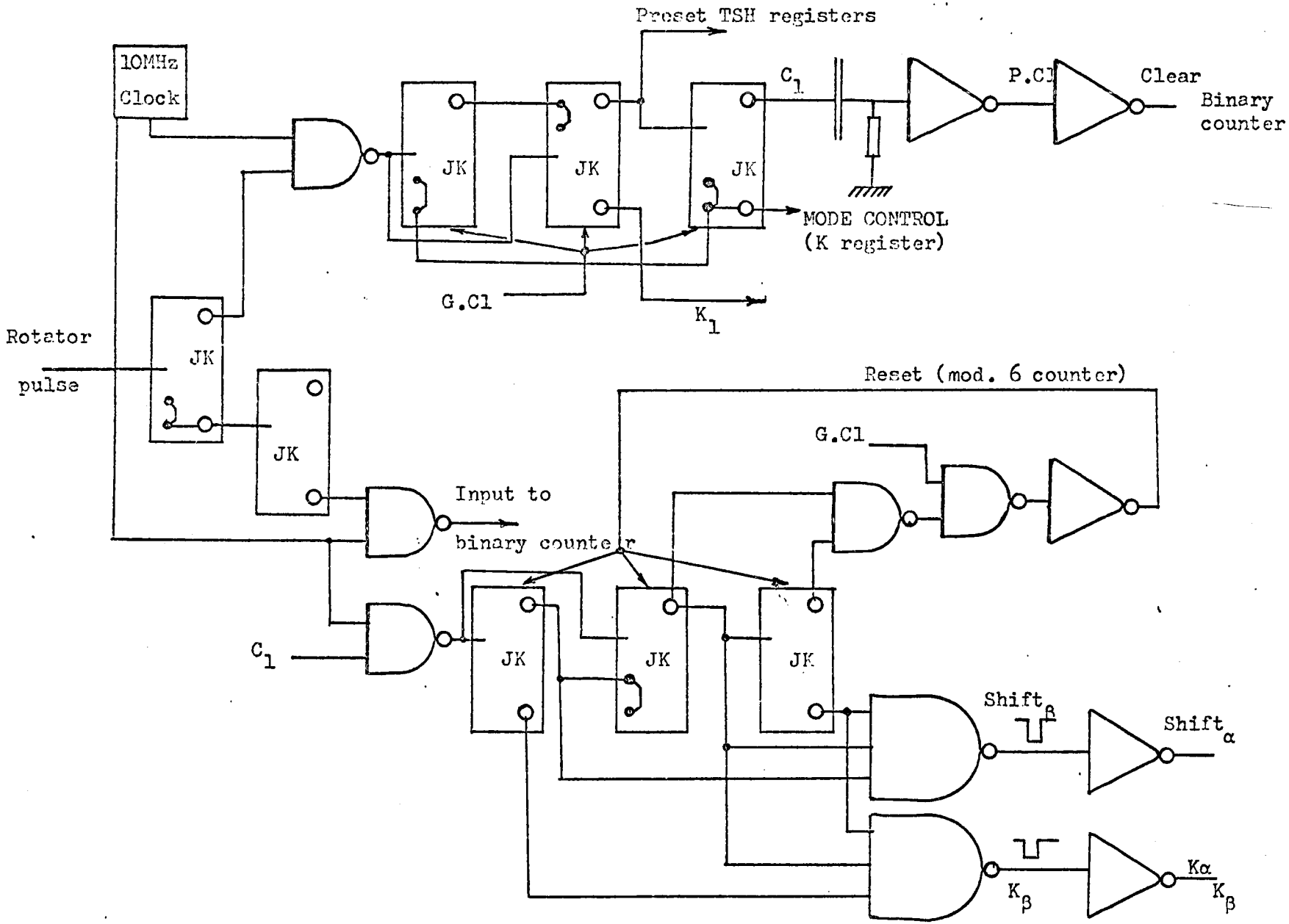

FIGURE 7-3: Shift and transfer pulse (K) generation

- Preset and clear ,of registers and counters

7.5 SIGN Detection - STORE - FSH Registers

As discussed previously, the SIGN generator is a simple gate detecting the register "overflow" to be clear and the carry out of the adder to be in stage "1".

Figure (7-4) shows how this has been implemented, together with the final storage process in FSH, and the auxilliary STORE register.

It has to be noted here that if STORE is empty (presetting f_o) the transfer pulse is inhibited during the 11 pulses of cycle 2, hence, no transfer occurs to the K register and the searches of the power of 2 begin with the initial value of K.

At this stage one can calculate the total processing time. As a Rotator pulse arrives the system starts the processing at the next clock pulse. 300 ns are required for transferring safely the content of the counter T into TSH, clearing the counter and presetting register K. Then 36 shift pulses follow as shown on the pattern of Figure (7-3). Each shift pulse is repeated after 600 ns. The total processing time will be

$$\tau = 300 + 36 \times 600 = 21{,}900 \text{ ns} \simeq 22 \text{ µs} .$$

This processing time does not involve the read out, but the result is available 22 µs after the rotator pulse has stopped the sampling. This time, although 1/3 of the minimum sampling interval, and therefore very good, could be brought down towards 16 µs if faster adders, with look-ahead carry-out components are used. But for this project the actual performance seems to be well enough.

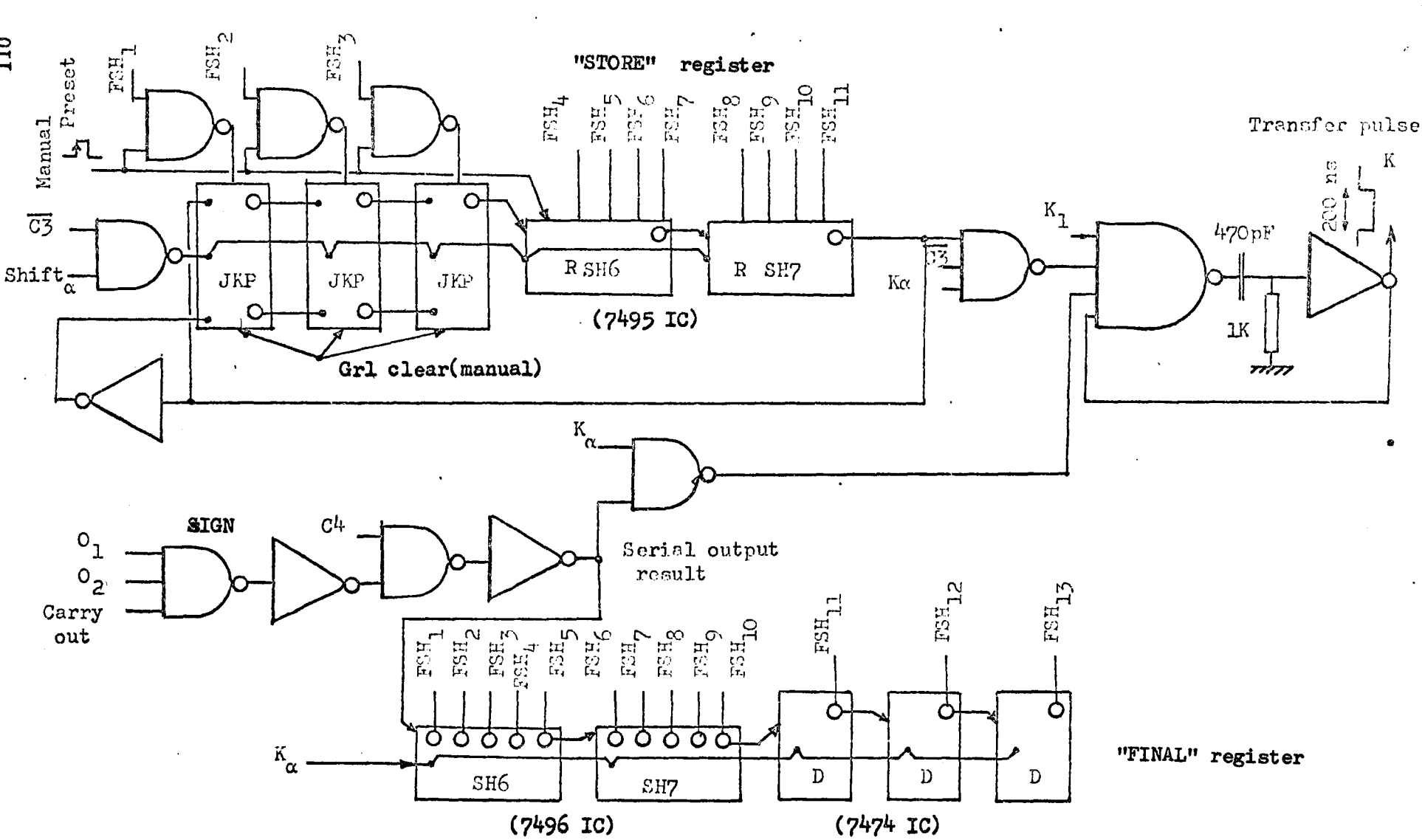

FIGURE 7-4: SIGN, FINAL REGISTER , STORE REGISTER
Implementation with standard IC.components

7.6 General Registers and Adders

Figure (7-5) shows the implementation of the different registers and adders discussed in section 7-2. It is a straightforward parallel subtraction, shift and transfer procedure.

7.7 Decimal Read Out

Although at such high rates of information, decimal read out would be unnecessary, a decimal display can be included, provided one takes readings at a reasonable frequency, separable by the human eye. For example, 10 readings per second seem to be the maximum that a human eye can perceive. Hence, decoding the binary read out can take 100 ms if needed. A simple binary count down and decimal up-counter will decode the result easily.

Figure (7-6) shows a simple implementation of the read-out.

Suppose a maximum of 130 rps has to be decoded, hence a count of 8191 has to be performed with the 10 MHz clock. The decoding will last a maximum of 0.82 ms.

7.8 Error Analysis

The error on counting up to n will be expressed as

$$e = \frac{1}{n}$$

Therefore, the maximum error due to counting will be reached when n is small, hence

$$e_{max} = \frac{1}{680} \simeq 0.15\%$$

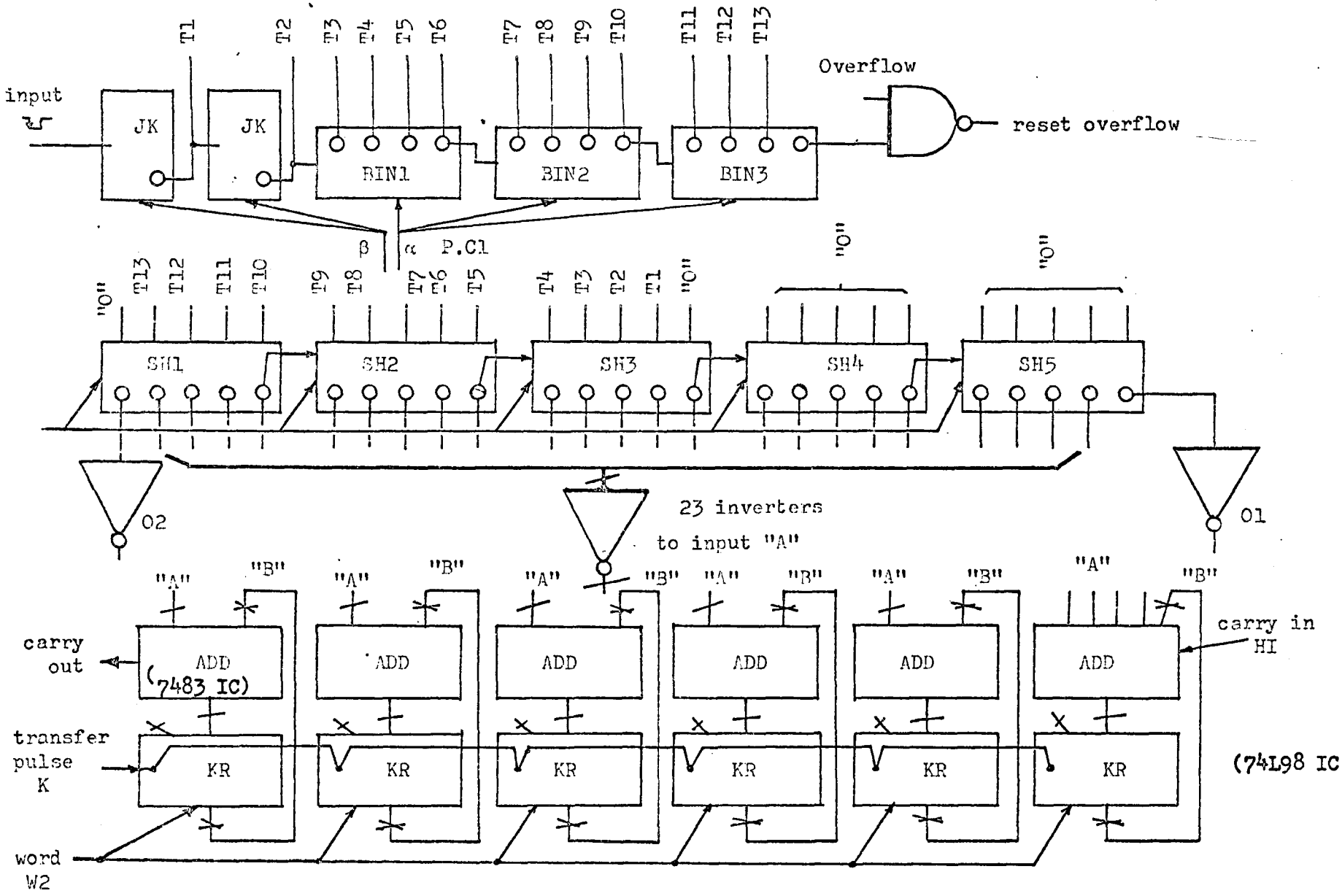

FIGURE 7-5: Binary counter for time / tsh shift register/ parallel binary adder/K register- -General implementation-

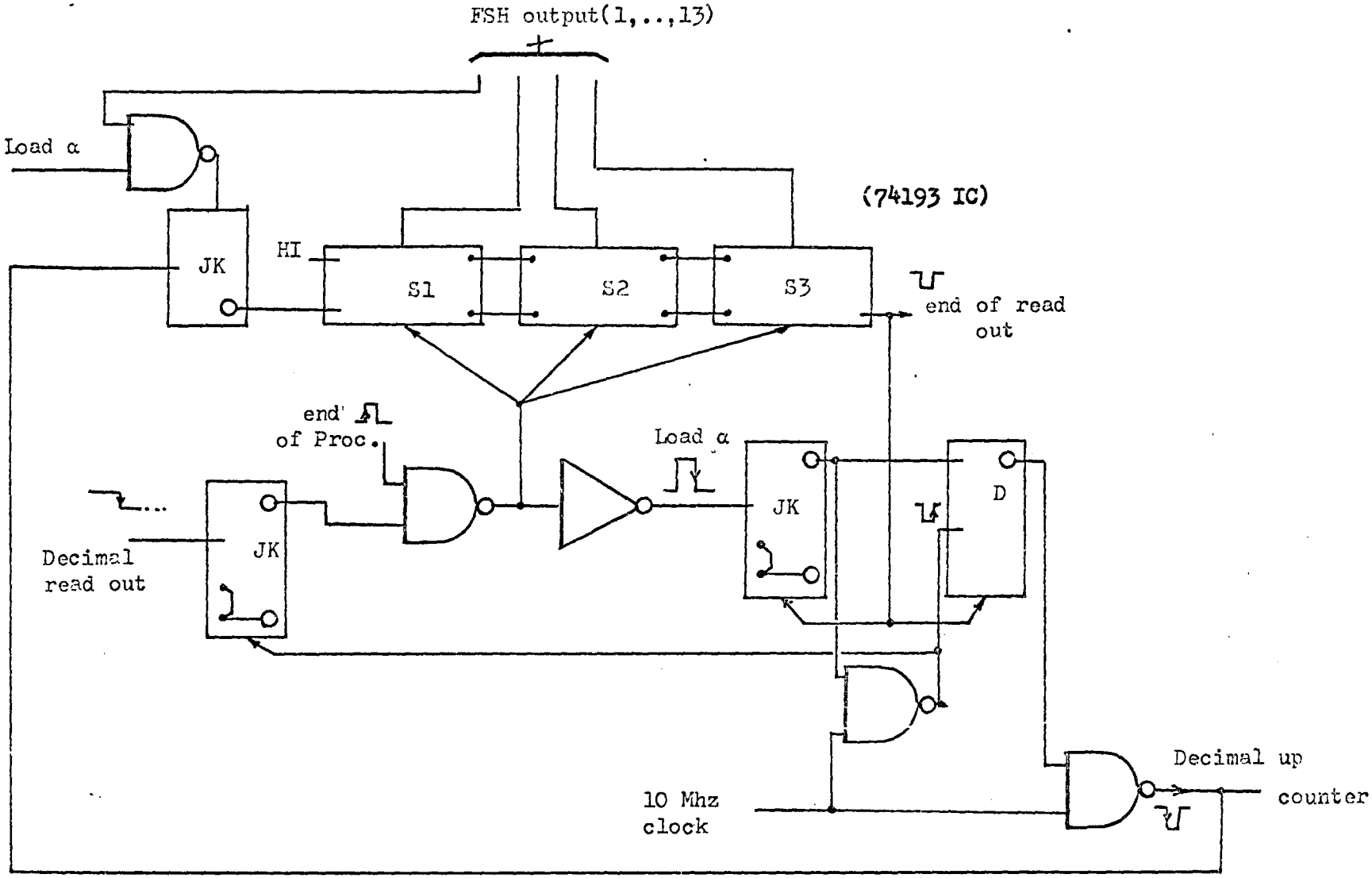

FIGURE 7-6: Decoding from binary to decimal

The minimum error due to counting is for n large, hence for zero speed:

$$e_{min} = \frac{1}{6000} \simeq 0.017\% .$$

However, to this basic error one has to add the precision of the clock. This error can be as low as possible hence, quartz crystal clocks are very stable nowadays.

Unfortunately, the biasing speed has to remain strictly constant. As no existing apparatus can reach such a precision and resolution, it was found impossible to check the constancy of the speed. However, by including a large inertia into the drum of the rotator, one can expect smoothing out higher order transients in speed, and one can suppose that the basic driving frequency is stable enough.

The present design thus presents quite an important lack for resolution purposes. The way the powers of 2 are searched, any number resulting from the division by time, and of lower order than the resolution is ignored. Therefore 0.19 rd/s as well as 0.10 rd/s will be read as 0.1 rd/s only.

Obviously, this adds to the error since the biasing speed is measured with this method. However, one should bear in mind that the error introduced is always of the same magnitude and sense. It would be quite easy to round off the result by considering the remainder which is present in the K register, as is done as a standard procedure in any desk calculator or digital measuring display.

7.9 Overall Performances

As a resumé of the performances and main advantages, one can state the following points.

- A resolution of 0.1 rd/s is obtained generally, but much better performance can be reached if wanted (say faster IC components, larger register sizes, etc.).

- A precision always less than 0.2% in a wide range, from zero to 7800 rpm is available for the digital processor part.

- A high rate of information from 1600 samples/sec at zero speed up to 16,700 samples/sec meet most requirements; besides the sampling rate increases with speed, which is advantageous.

- Zero speed is detectable without quantization noise, with a fairly high rate of information (1600/sec) and maximum accuracy (0.02%).

- Results are available directly in digital form almost instantaneously (22 μs after sampling is completed), but this delay can be brought down considerably with more elaborate techniques.

- The sampling time interval being very short (ranging from 0.6 ms to 0.068 ms), the average speed reading obtained can be considered as instantaneous in all physical systems.

- If the speed range is known, the biasing speed can be brought to the lower measured speed, so that maximum accuracy will be obtained at that level.

The relatively simple implementation of the design allows a low cost instrument presenting a much wider range of performance than any

other means known to the designer. Moreover, all the requirements of a fast transient control system are met, that is to say:

- high resolution and precision,
- high rate of information even at zero speed,
- binary result available almost instantly,
- sampling interval as small as possible to obtain instantaneous speed,
- precision increases with low speeds, and rate of information increases with the speed,
- zero speed detected with the best accuracy and with a fairly high rate of information, and
- the instrument should disturb as less as possible the actual measured system (low inertia - friction).

7.10 Compared Performances with Existing Instruments

It is rather difficult to compare two instruments, since too many factors are involved. Besides, the specific application to be used will really dictate whether or not it is appropriate to use one or the other.

The main point to stress should be the physical reality. One has to trade off precision and accuracy for readiness of information. I can be compared with Pauli's exclusion principle. Astonishing accuracies can be obtained with an integrator type of tachometer, but the number of samples have to be in accordance.

One of the main features of the new proposal is to offer a very short sampling interval, a very fast processing of the result and hence providing a large number of readings per second. Almost instantaneous sampling is realized. Thus, the accuracy of the result is comparable with usual experimental errors, say 1%.

In conclusion, most of the difficulties encountered with the BBC controller are suppressed beacuse of the very well suited performance of this digital tachometer.

Next we should show the simplifications introduced in the BBC by the completely digitalized information on speed.

CHAPTER VIII

FULLY DIGITALIZED CONTROLLER

APPLICATIONS AND MODIFICATION OF THE TACHOMETER

Although the theory of the true minimum-time controller was fully explored in Chapter IV, it was not realized practically because the speed information was not adequate. Therefore, a complicated filtering of the analogue information, the use of an A/D level converter and an analogue comparator were used. Almost all of the practical difficulties and malfunctions of the controller were caused by the analogue stage.

However, the concept of the digital tachometer giving almost instantaneous measurement of speed will change considerably the design and certainly improve it, although simplifying it.

In the following, the modifications introduced will be presented with the improvements obtained.

Some other practical applications of the digital tachometer are reviewed and the possible extension to on-line parameter identification in case of load variations is proposed.

8.1 Modifications Introduced for the B.B.C.

In Chapter IV, section 4.4.1, the general principle of the control law is kept for the control scheme. The presettable counter will still be used for the quantized position detector and measures the distance from the target. The "distance from target logic" remains the same, and generates the logic levels S_i.

However, there is no need to use a D/A level converter. The logic levels S_i have to generate digital control levels called here W_i and correspond to the switching speeds defined in Figure (4-4).

As an example, the three level controller is taken here. The truth table from Figure (8-1a) defines perfectly the words W_i and their generation shown on Figure (8-1b) is straightforward. The corresponding word W_i is stored in a 9 digit shift register, the serial output having always the highest bit.

As the tachometer provides a binary number, a parallel comparator could be used. However, the sequential logic seems to bring much better simplifications here. The tachometer gives serial output as well, and the serial output starts with the highest bit. Therefore, if the serial result called β_i is coming out, the truth table of Figure (8-2b) shows the direct comparison possible. Figure (8-2b) presents a very simple circuit to realize the operation. One should note how much simpler and more reliable this circuit is, than the D/A converter.

Once the comparison of the speed is obtained, the same circuitry as that previously designed can be used.

Figure (8-3) shows an overall block diagram of the complete controller which is now entirely digital.

8.2 Improvements and Expected Results

Suppose the motor is at standstill, and the tachometer ready to work. Figure (8-4) shows as an example, the real speed characteristic versus time, and the corresponding samples given by the tachometer.

dft.	S0	S1	S2	S3	W_i =(9 bit word)									Ω(rd/s)x10
					α9	α8	α7	α6	α5	α4	α3	α2	α1	
0	1	0	0	0	0	0	0	0	0	0	0	0	0	0
1	0	1	0	0	0	1	1	1	1	0	1	0	1	245
2	0	0	1	0	1	0	1	1	1	1	0	0	0	376
3	0	0	0	1	1	1	1	1	0	1	1	0	1	493

FIGURE 8-1-a: Three Level Digital Control Law

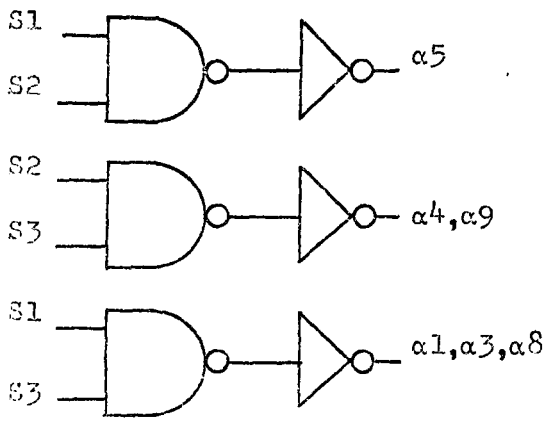

"HI"= α7,α6

"LO"= α2

FIGURE 8-1-b: Generation of the words W_i for the three level controller.

β_i	α_i	Decision (start i=13)	
0	0		explore i=i-1
1	0	W > B	store, inhibit further search
0	1	W < B	store, inhibit comparison
1	1		explore i=i-1

digital comparison

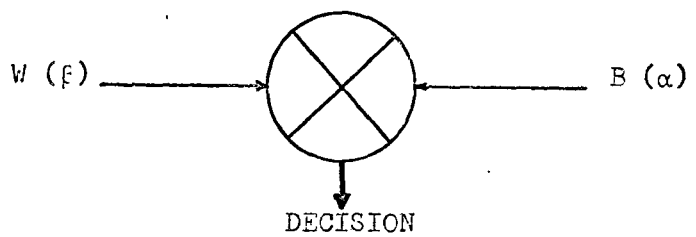

FIGURE 8-2-a : Comparison of two binary numbers W and B

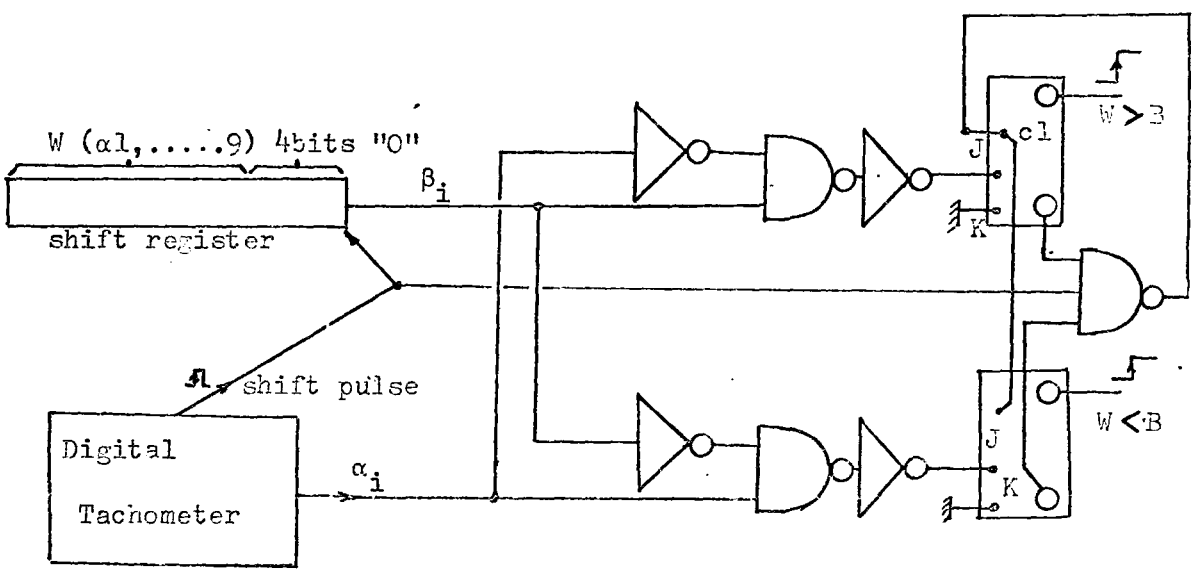

FIGURE 8-2-b: Practical implementation realising the comparison

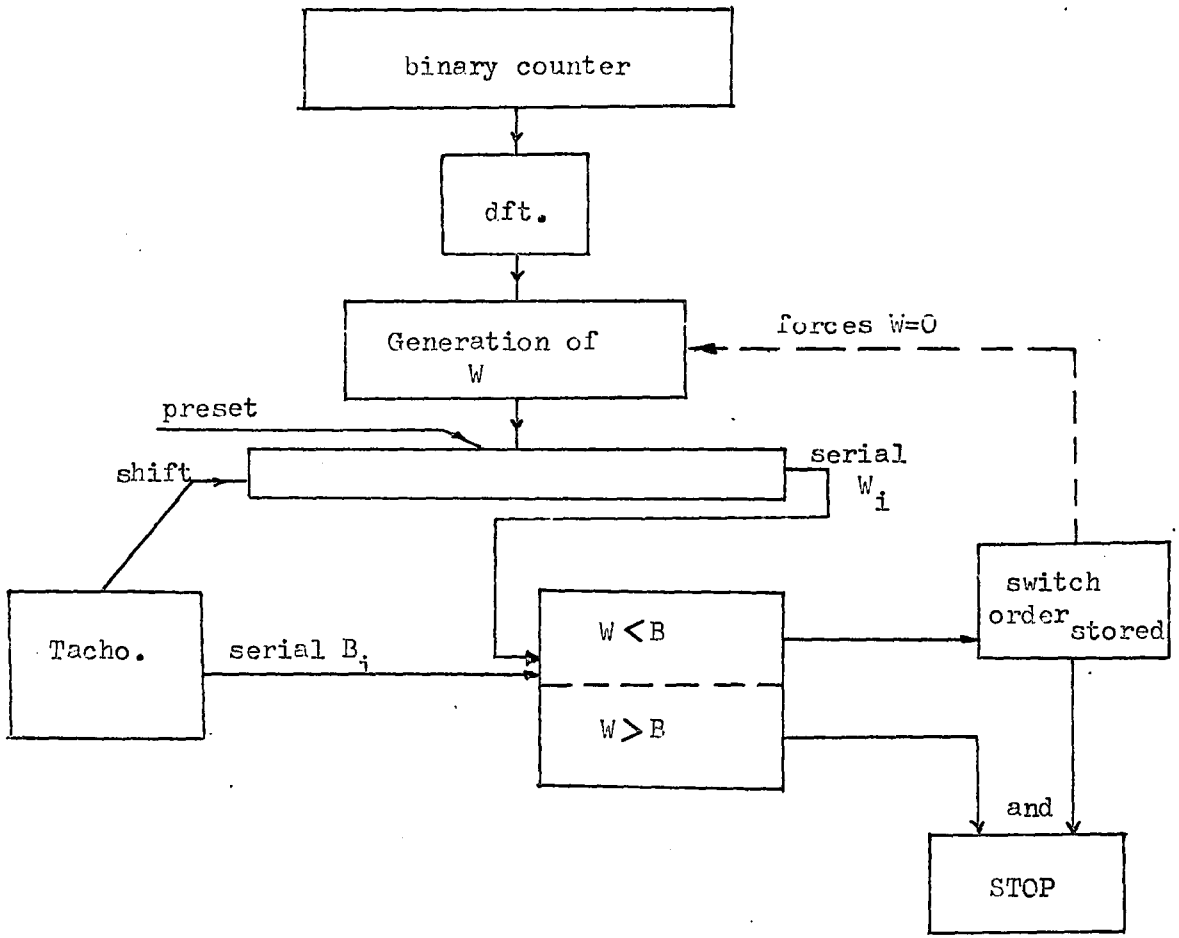

FIGURE 8-3 : Fully digitalized BBC.

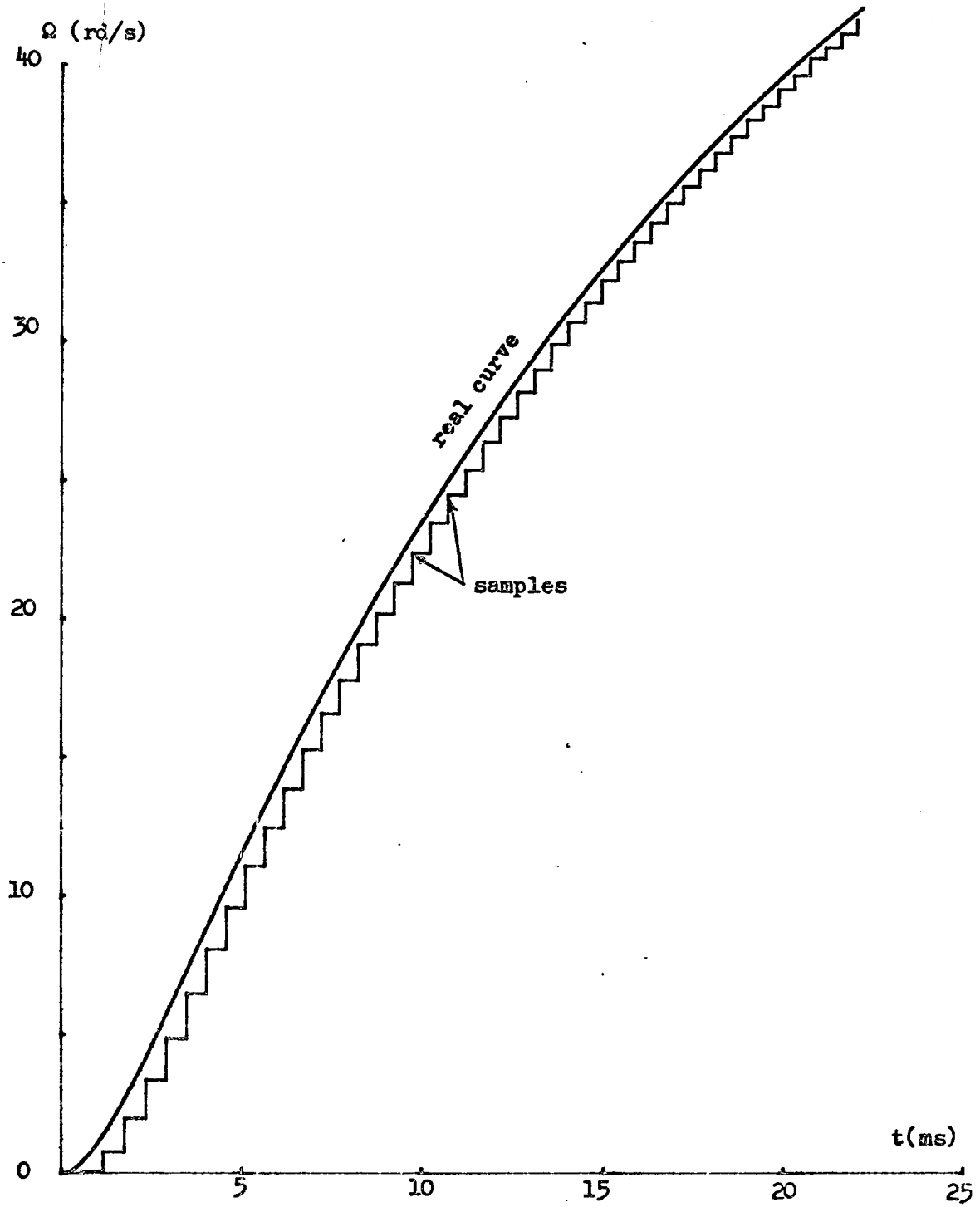

FIGURE 8-4 : Tachometer sampling the starting curve of the PM motor

Here, very large accelerations take place, and therefore, although the sampling time of the tachometer is less than .5 ms, the average over that time interval differs with the real curve.

However, it has to be noticed that the curve read by the tachometer is very close to the real one, and no other existing device could provide such an information.

Figure (8-5) is a blow up of the part of the same characteristic, around the first switching level for the 3 level controller, previously quoted.

It has to be noticed at that point that if the level is set as precalculated, because of the very high acceleration and quantized samplings, the speed readings are always below the real curve. Therefore, the switching order is given only at a real speed of 25.3 rd/s instead of 24.5 rd/s. As the sense of the error is always known, the switching level preset on the controller should be modified and decreased by a certain amount, say 23.6 rd/s, hence the switching will occur at around 24.3 rd/s which is very close to the theoretical switching level of the control law.

The equivalent r.m.s. noise, due here to quantization noise primarily, would be less than 1%, which obviously cannot be reached with any other existing device associated with filtering.

Hence, the modifications introduced in the B.B.C., making it fully digital, are above expectations.

First of all, the performances are much better (a 1% rms noise does not use the checking loop as presented earlier, unless load

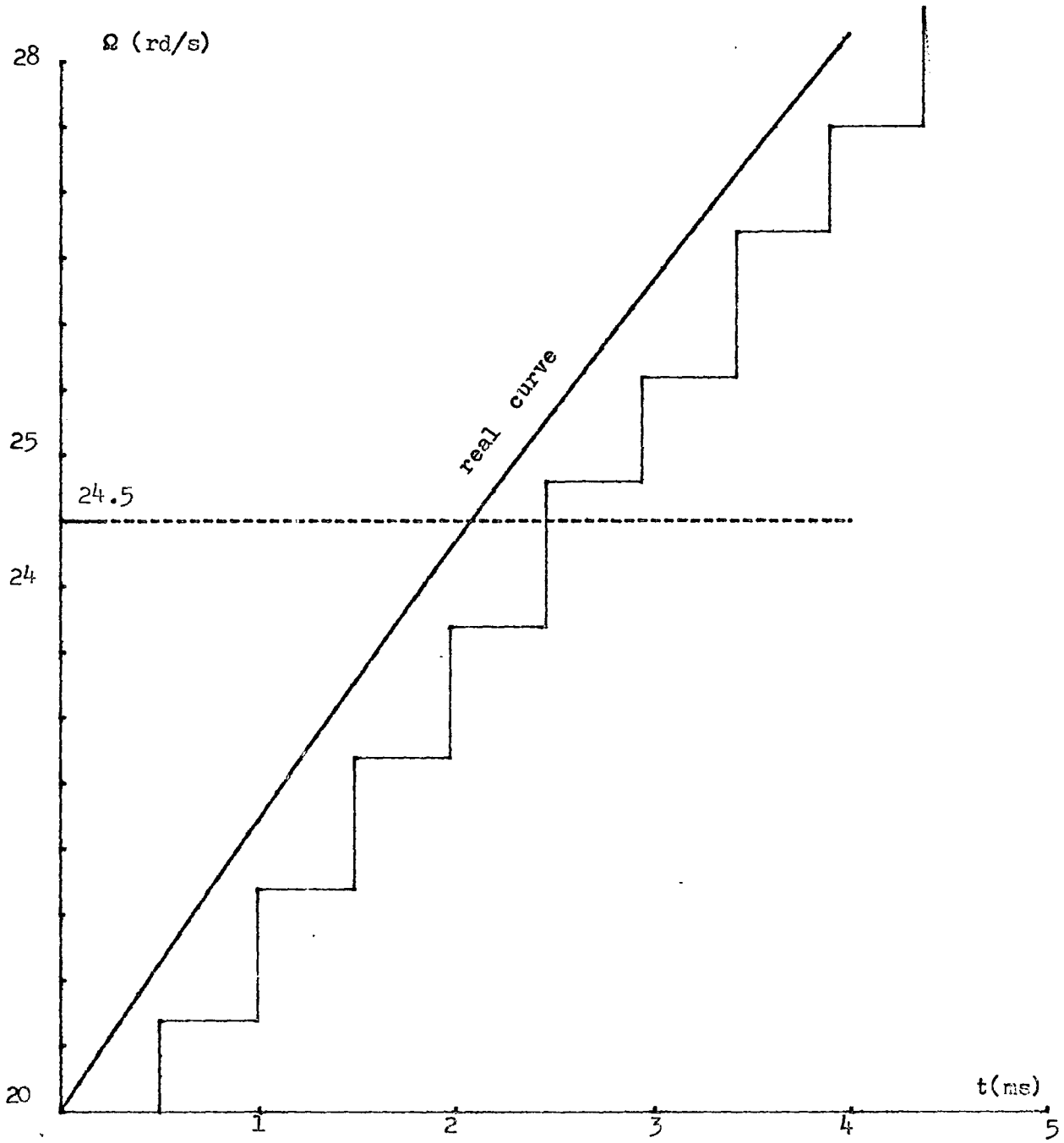

FIGURE 8-5 : STAIR CASE TACHOMETER READINGS AROUND A SWITCHING LEVEL

disturbance appears), however, on the other hand, the whole D/A conversion stage is suppressed and replaced by a very simple digital circuit, much more reliable and easier to handle (for instance, it is not heat sensitive).

8.3 Possible Applications

Some applications of the B.B.C. have already been discussed. It is obviously much more efficient in its modified fully digital form.

The tachometer built here has many other applications.

8.3.1 Frequency Meter

The tachometer can be used, for example, as a basic low-frequency meter, say in a range from 20 Hz to 1 KHz but obviously, if used in this manner, some modifications could enlarge considerably this range. It has to be noted that this range is around the standard 60 Hz used in power systems.

As a main advantage, instead of measuring an average over a relatively long time as most of the frequency meters on the market do, an average frequency over a very short time interval is provided and the result available directly digitally.

Unfortunately, due to the upper frequency limit of the counters and the register sizes used, only low frequencies can be measured, unless accuracy and resolution are abandoned for speed of resolution and information rate.

8.3.2 Speed Controller

In the case of a variable speed around a steady state (say, paper mills), the biasing speed f_o can be set at the lower limit of permissible speed drop. This procedure permits one to bias the system so that the relative speed is low. As seen, the accuracy is the best at zero speed. Hence, if the speed variation is small, say 10 rps maximum, one could design the tachometer to use the number sizes considered, but the resolution can be now 0.01 rd/s; even 0.001 rd/s if desired.

If such a high resolution is desired for transients, it is advisable to push the clock frequency to extreme limits, say 20 MHz or even 50 MHz. This would enable a precision of measurement compatible with the desired resolution.

Obviously prices would increase considerably for such a sophisticated design because of the cost of special components: 50 MHz I.C.'s for example, but such special performances should not be necessary in most practical applications.

8.3.3 Transient Response Tachometer

If the whole range 0-7800 rpm is expected, this tachometer meets all the requirements of digital control system specifications:

- Digital result (serial output and final output)
- Information available very fast after sampling
- Very large number of informations per second
- Rate of information increases with the speed to be measured.

The only serious limitation would be with the biasing speed, however, a special clocked power supply could provide as accurate a speed as possible, since very limited load is used.

8.3.4 Kinetic Energy Meter

The speed, obtained digitally, can be squared very easily, and provides a number proportional to the kinetic energy of the shaft in rotation. In position control systems where heavy inertia is involved, like elevators, etc., this can be of great use.

8.3.5 Test Equipment and Digital Control

Obviously the tachometer provides a fantastic test instrument. Besides providing digital output, it enables direct connection with digital recording, digital controllers, or computer controlled processes.

8.4 Proposed Modifications in the Tachometer

8.4.1

When examining on Figure (8-4) the theoretical speed characteristic and the samples given by the tachometer, one immediately notices the fact that in case of high acceleration rates the average speed read falls always below the real curve, by an amount much larger than the tachometer's resolution.

One could assume that during the sampling interval, always less than .6 ms, the speed varies linearly with time. This is almost true

for any practical purpose, unless very small motors, with very low inertia are used, but in that case only position is of interest anyway.

Hence, one can assume that each reading provided by the tachometer is the average speed over the previous sampling interval. If the information provided by the tachometer at the k^{th} sampling interval is called F_k^r, the corrected real speed F_k^c at the end of the k^{th} sampling would be given by the recursive equation

$$F_k^c = 2F_k^r - F_{k-1}^c \qquad (8\text{-}1)$$

starting at $F_o = 0$.

The same starting characteristic as depicted by Figure (8-4) is sampled, but samples are corrected with the above exposed scheme.

The result of the sampling is shown on Figure (8-6), and considering the scales which are rather expanded, an amazingly accurate discrete sampling is performed. However, due to the use of integral numbers, and mainly due to the accumulative error introduced by the equation (8-1), a fluctuation of the error appears. But one can immediately picture that the averaging process is self correcting and that the deviations due to cumulative errors are always brought back within a reasonable range. On overall basis a smoothing out of the curve obtained will lead to the true characteristic.

8.4.2

The implementation of the linear averaging correction is straightforward with the present tachometer design. Figure (8-7) shows

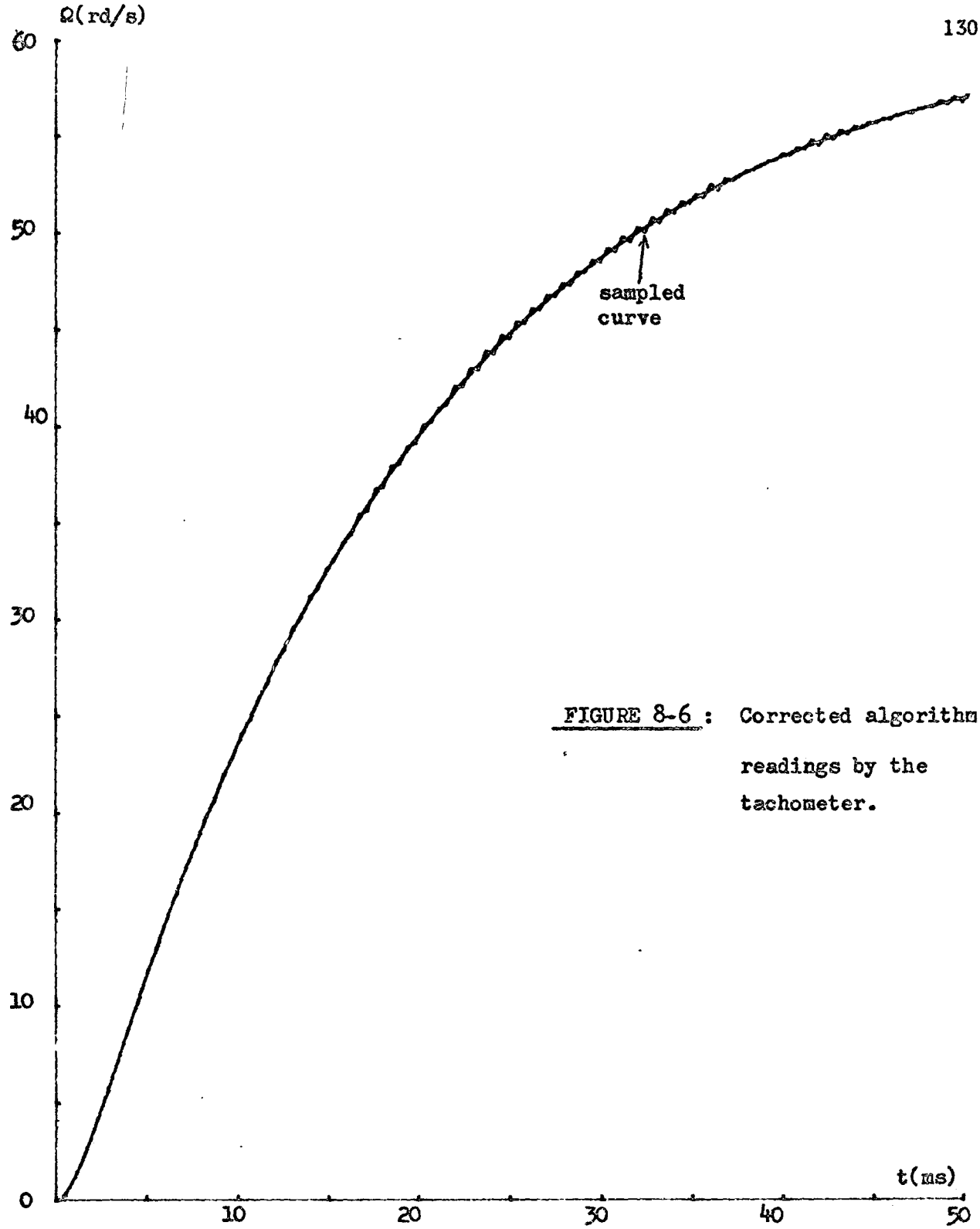

FIGURE 8-6 : Corrected algorithm readings by the tachometer.

the general block diagram of the implementation of equation (8-1).

The register FSH receives as described, a 13-bit number which represents F_k^r. This number is fed into the 13 highest bits of the input of the binary parallel adder, the lowest bit being at state "0" (realizing the multiplication by 2).

A 13-bit register RES contains F_{k-1}^c and its complementary output is fed into the 13 lowest bits of the second input of the adder, the highest being at state "1". Hence, the result on the adder, after about 200 ns appears as the quantity F_k^c, which can be transferred into register RES and represents the corrected speed sample after the kth sampling. The cost of the operation is very low, only a 14-bit parallel adder associated with a 13-bit memory which is useful anyway, for storing the information till the next sample arrives.

The transfer pulse can be the pulse "END OF PROCESSING" which is delayed already by the desired amount of time.

8.5 Tachometer Modified as Accelerometer

As discussed in section 7.5, the biasing speed can be preset using the tachometer itself. This is done by inhibiting the first transfer during cycle II of the processor. This scheme can be adapted to preset any speed as biasing speed.

Suppose one needs only a speed band for speed regulation, hence the disc is rotated with the lowest speed of the band to be studied, and this will become the biasing speed. Hence only differences with biasing speed are read by the tachometer.

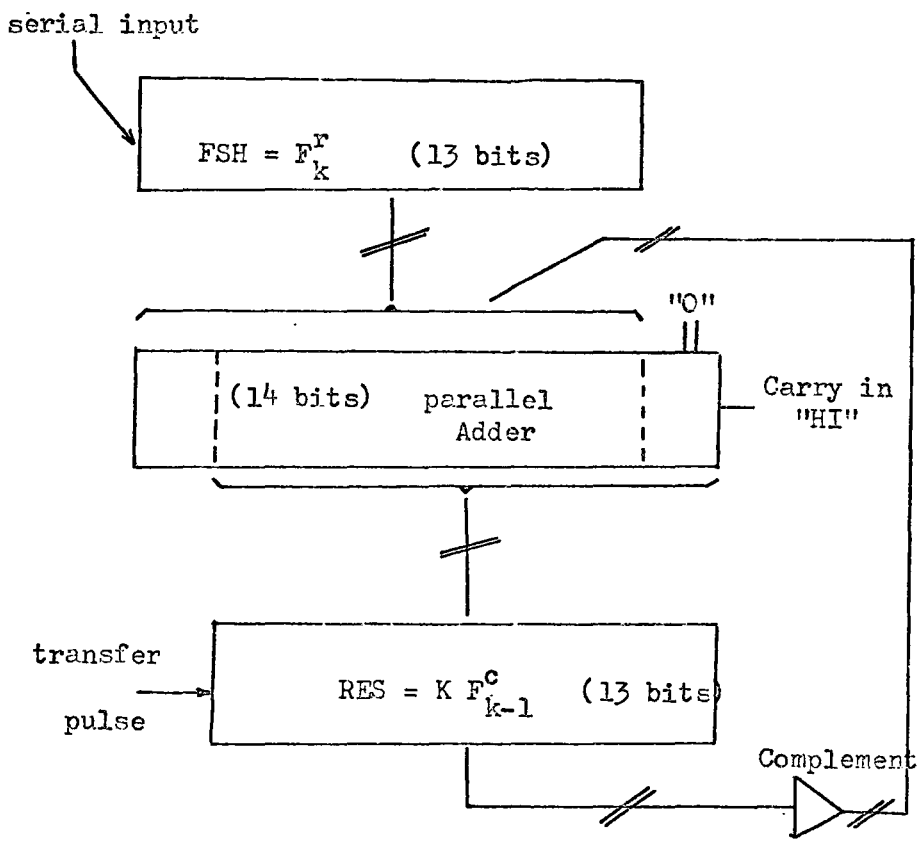

FIGURE 8-7 : "Averaging"algorithm implementation

Moreover, the sampling rate for the accelerometer does not need to be as frequent as for the speed because any mechanical system cannot have any appreciable change in acceleration within 0.6 ms. Therefore, once the sampling rate is decided, every time a sampling pulse arrives, the contents of the final register can be transferred into the auxilliary register as discussed previously. Hence, the tachometer reads the variation of speed since the last pulse. If the sampling period is known, the reading provides directly the average acceleration during this period.

The advantage of this accelerometer over the existing ones is derived from the performance of the tachometer. The increase of speed registered does not represent the difference between two average speeds, but effectively the increase of instantaneous speeds.

Unfortunately, a problem may be caused by the fact that it is very unlikely that an "acceleration pulse" will coincide with a "rotator pulse". This difficulty may be overcome if the sampling interval for the accelerometer is chosen sufficiently large, say 10 to 100 ms, so that the influence of non-coincidence becomes negligible. It may be added however, that even this represents a considerable improvement over existing accelerometers.

8.6 Case of Slowly Variable, Unknown Mechanical Loads

In the case of the permanentic motor starting with a certain load, it has been shown that equations (3-21) are a good representation in phase plane of the trajectory. This trajectory during acceleration,

has been shown dependent only on three auxilliary parameters, (σ, μ, Ω_f), obviously depending themselves on the three mechanical parameters. But the knowledge of these three auxilliary parameters is sufficient to reproduce the starting trajectory in phase plane.

On the other hand, the equation of the switching predictor for reverse voltage braking has been described by equation (3-29). The angle θ_{brake} is a function of A_2, B_2 and s_1.

As shown by the equations (3-24-1) and (3-24-2) A_2 and B_2 are functions of σ, μ and the load parameters (a, b, J), as well as Ω_{switch}.

The following will attempt to find a closed-form solution, as accurate as possible, relating A_2 and B_2 only to the auxilliary parameters (σ, μ, Ω_f) and Ω_{switch}.

From the determinant of the system (3-15) given by equation (3-16), one can immediately write the poles as:

$$s_1 + s_2 = -\frac{R}{L} - \frac{a}{J} \tag{8-2}$$

$$s_1 \times s_2 = \frac{aR + K^2}{JL} \quad . \tag{8-3}$$

From (8-2) and (8-3)

$$\frac{s_1 + s_2}{s_1 s_2} = \frac{1}{s_1} + \frac{1}{s_2} = \frac{-aL + RJ}{aR + K^2} \tag{8-4}$$

Let us call the inverses of the time constants s_1 and s_2, X and Y respectively.

If one supposes that additive armature resistance is not added to the circuit, the value of R is very close to the value of K^2, hence, from equations (8-3) and (8-4)

$$X + Y \simeq \frac{-aL}{(a+1)R} - \frac{J}{a+1} \tag{8-5}$$

$$XY \simeq \frac{J}{a+1} \times \frac{L}{R} \tag{8-6}$$

Usually $|s_1| << |s_2|$ because of the differences in the mechanical and electrical time constants. Hence,

$$X >> Y$$

But practically

$$\frac{J}{a+1} >> \frac{aL}{(a+1)R}$$

Let

$$X = -\frac{J}{a+1}(1-\varepsilon) \qquad \text{with } \varepsilon << 1 \tag{8-7}$$

From equation (8-6) one obtains a first order approximate

$$Y = \frac{-L/R}{1-\varepsilon} \simeq -\frac{L}{R}(1+\varepsilon) \tag{8-8}$$

Combined with (8-5)

$$X+Y = \frac{-J}{a+1}(1-\varepsilon) - \frac{L}{R}(1+\varepsilon) = \frac{-aL}{(a+1)R} - \frac{L}{a+1} \tag{8-9}$$

and

$$\varepsilon \simeq \frac{1}{\frac{JR}{L} - (a+1)} \tag{8-10}$$

An exact representation of σ and μ versus the load parameters (a, J) is shown on Figure (8-8). The load parameters are varied in a wide range far above usual practical applications.

$\frac{JR}{L}$ has a value of 15 at the minimum and increases proportionally with J. The quantity a+1 is 1.01 at the minimum and 1.1 at the maximum. Hence,

$$\varepsilon \simeq \frac{L}{JR} \quad . \tag{8-11}$$

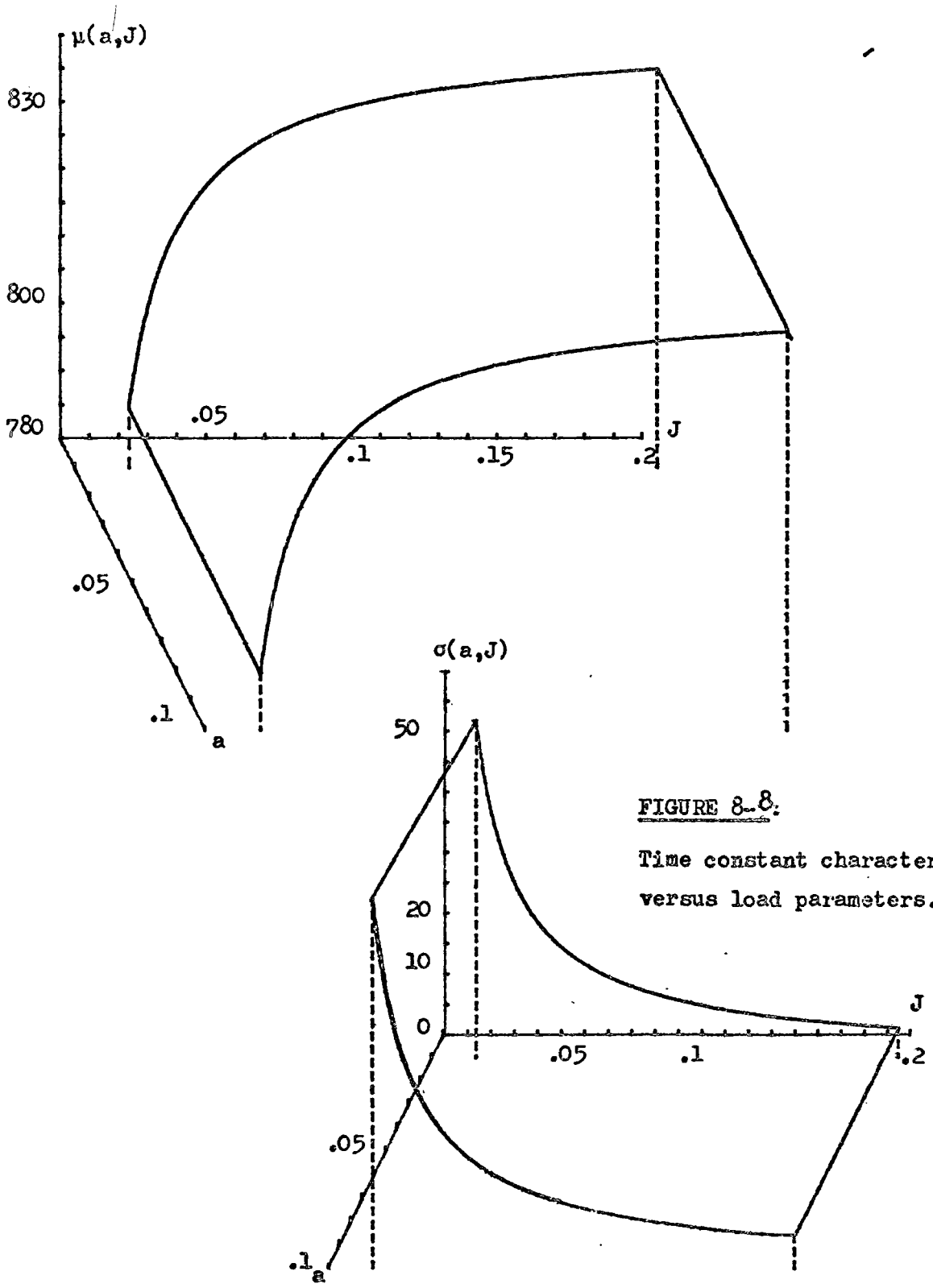

FIGURE 8.8.

Time constant characteristics versus load parameters.

The approximate values of the time parameters are given now by equations (8-7) and (8-5) as

$$s_1 \simeq \frac{a+1}{\frac{L}{R} - J} \tag{8-12}$$

$$s_2 \simeq -\frac{R}{L} + \frac{1}{J} \tag{8-13}$$

However, a comparison with the curves from Figure (8-9) shows that a good approximation can still be obtained by reducing equation (8-12) to

$$s_1 = -\frac{a+1}{J} \tag{8-12'}$$

Back to equation (3-24-2), B_2 can be expressed as a linear function of Ω_{sw}

$$\left.\begin{aligned} B_2 &= \alpha\, \Omega_{sw} + \beta \\ \text{with} \quad \alpha &= \frac{s_2 + \frac{a}{J}}{s_1 - s_2} \\ \beta &= \frac{-\frac{b}{J} + s_2\, A_2}{s_2 - s_1} \end{aligned}\right\} \tag{8-14}$$

(A_2 does not depend on Ω_{sw} as shown by equation (3-24-1)).

Hence, from (8-2) one can write immediately

$$\alpha = \frac{\frac{R}{L} - \sigma}{\mu - \sigma} \tag{8-15}$$

From equations (3-24-1) and (3-19-1)

$$\Omega_f - A_2 = 2\left(\frac{KU}{aR + K^2}\right) \tag{8-16}$$

which can be finally simplified into

$$\Omega_f - A_2 = \frac{2KU(\frac{R}{L} - \mu)}{L\sigma\mu} \tag{8-17}$$

Hence, A_2 is expressed as a function of the auxilliary variables as

$$A_2 = \Omega_f - 2KU \frac{\frac{R}{L} - \mu}{L\sigma\mu} \tag{8-17'}$$

Likewise the quantity b/J can be written as

$$\frac{b}{J} = \frac{b}{J} \times \frac{(L\sigma\mu R)}{(L\sigma\mu R)} = \frac{bL\sigma\mu R}{(aR+K^2)R} \tag{8-18}$$

and from (3-19-1)

$$\frac{bR}{aR+K^2} = \frac{KU}{aR+K^2} - \Omega_f \tag{8-19}$$

Combining equations (8-18) and (8-19) from (8-14) one can derive easily

$$\beta = (\frac{\mu}{\mu-\sigma}) \left[\Omega_f(\frac{L\sigma}{R} - 1) + \frac{(\frac{R}{L} - \mu)}{L\sigma\mu} (2 - \frac{L\sigma}{R}) \right] \tag{8-20}$$

It has been demonstrated here that once the auxilliary parameters σ, μ, Ω_f are defined, the switching predictor can be calculated directly using the given sequence

α by equation (8-15)

A_2 by equation (8-17')

β by equation (8-20)

Hence $$\phi(\Omega_{sw}) = \frac{\alpha\Omega_{sw}+\beta}{-A_2}$$

can be sampled and $\theta_{brake}(\phi)$ is calculated by equation (3-31).

8.7 On-line Parameter Estimation - Computer Control

The control of variable unknown loads is a very sophisticated problem. In the case of slowly varying loads (that means that the load does not vary within control time), the digital tachometer provides a means to reach a good minimum-time control without requiring a time consuming complicated learning-process.

Since a digital computer is used anyway, the only information required will be the sampling time T given by the "Rotator". The computer will read the time T and hence will perform the calculation of the speed estimate much faster and with more accuracy than the tachometer's processor.

Hence, an on-line identification of the parameters (σ, μ, Ω_f) can be performed as a lot of samples of the curve are available. Besides, the range of variations for the load are fairly limited, therefore convergence for the optimization of the estimates should be fairly fast.

Every time the computer can compare the actual speed with the predicted switching level calculated as presented in section 8.6.

Figure (8-9) gives a block diagram of the general controller using a digital computer for parameter estimation, evaluation of the predictor, and switching decision.

It has to be noted that the computer registers could be used directly for counting the time T, and a clock of much higher frequency could then be used.

FIGURE 8-9 : Computer minimum time control

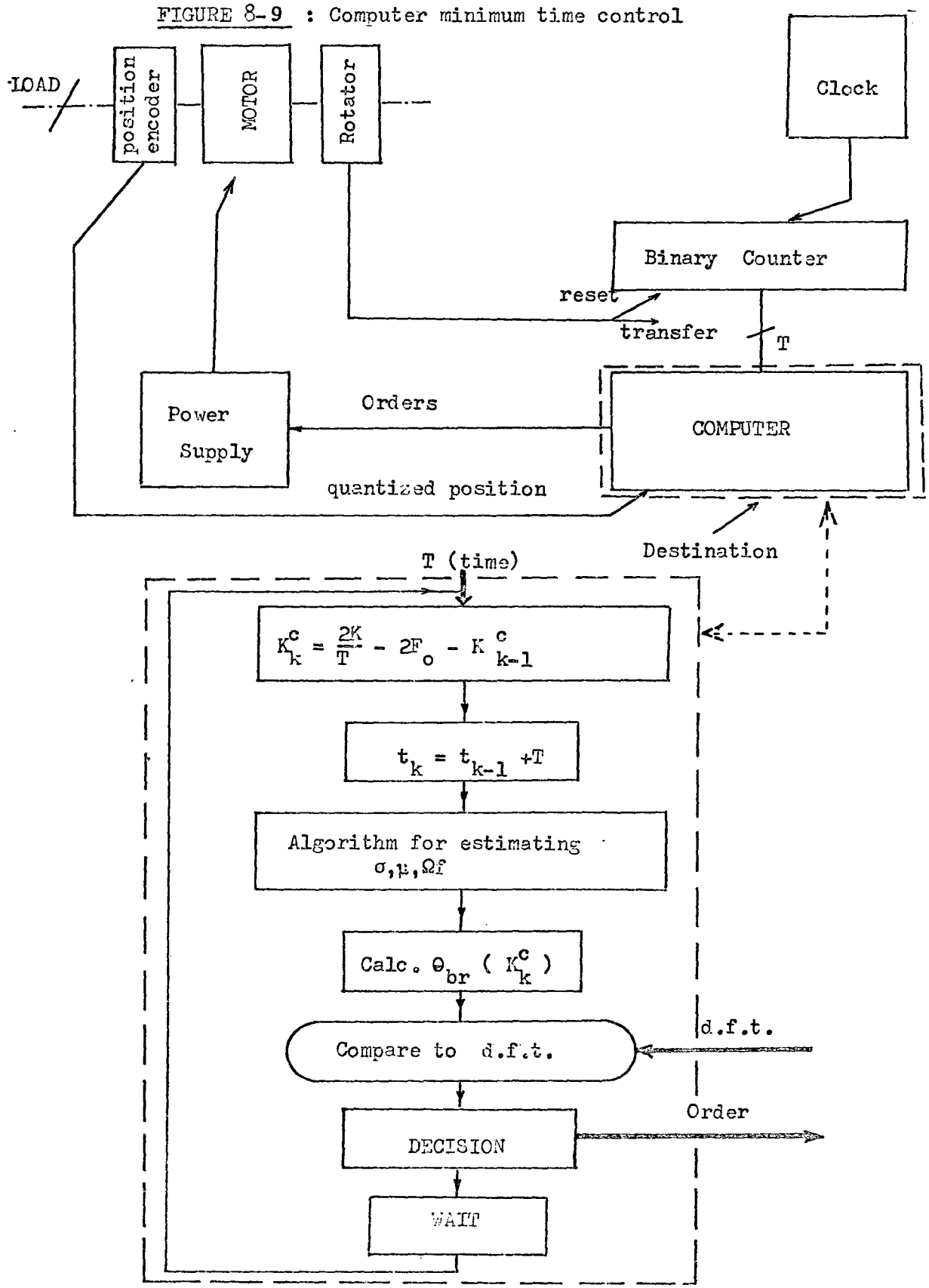

To illustrate the capability of sampling a curve with the "Rotator" pulse only and letting the computer define the estimate of the speed, an oscillatory speed around a steady-state is sampled.

A very stringent case is considered with a sinusoidal speed of 50 Hz frequency and an amplitude of 10 rd/s, around a speed of 10 rd/s.

A 20 MHz clock is used to sample the curves, and the result is given by Figure (8-10). It has to be noticed how well the curve is defined, presenting a ripple only in the sudden changes of slope. However, the higher the speed, the smoother the result will be, since the sampling rate increases considerably.

8.8 Comparisons of Results When Sampling Curves

The very stringent condition of the previous sinusoidal speed is studied now. Figure (8-11) shows the characteristics obtained as the sampling proceeds. In the first case, the tachometer without corrected averaging is used. One can immediately see that the registered curve is a true replica, without too much of a ripple, however, a time lag exists between the true characteristic and the resulting one. The next case studies the performance of the corrected algorithm. It has to be noted here, that a ripple appears, although the mean value of the error is found to be zero. This ripple comes mainly from the limited size of numbers used. In the case of the computer performing the algorithm and allowing a 20 MHz clock, the error can be shown to be much less.

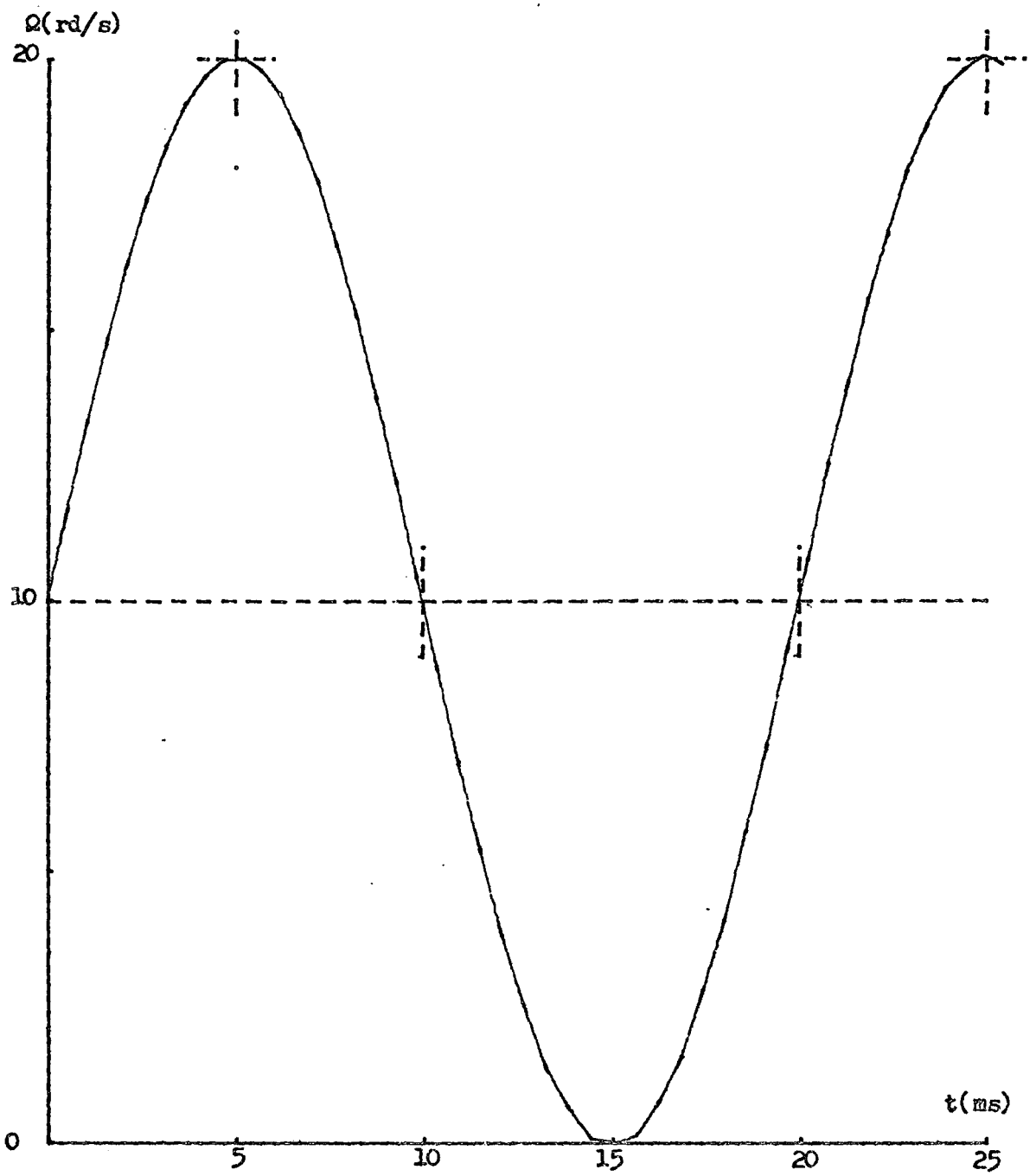

FIGURE 8-10 : Computer processing (20 Mhz clock) sampling $\Omega = 10\,(1 + \sin 100\pi t)$

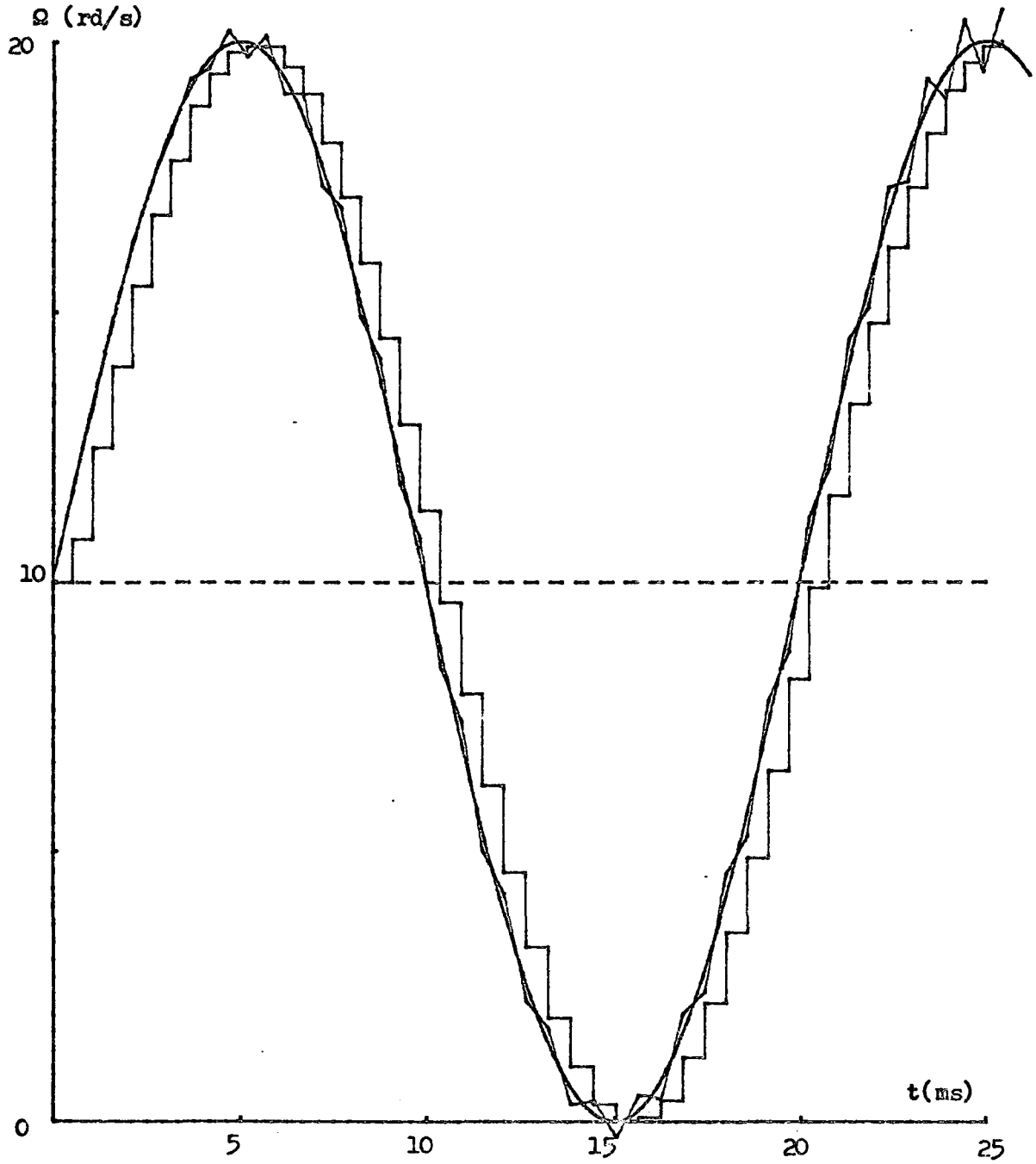

FIGURE 8-11 : Tachometer sampling, normal, and corrected algorithm.
Sampling $\Omega = 10(1+\sin 100\pi t)$

In conclusion one could state that both corrected and non-corrected algorithms can be found to be very useful.

In the case of parameter identification, the corrected version seems to be of better use. However, rapid acceleration transients could result in ripples which have to be smoothed out.

In the case of a rapid digital control, if the time lag is known, for example with the BBC, a modification of the switching threshold is obvious. If this cannot be done, then the corrected version has to be used.

CHAPTER IX

SUMMARY

Most of the control system applications have somewhere a position control, even if in only a minor loop. This very important control problem has been solved in many ways, however, the approach was always more or less empirical. Besides, the minimum-time problem has never had a closed-form solution that is very useful in practice.

In this work, the permanent magnet d.c. motor has been shown to be very well suited for the minimum-time position control, especially when very high acceleration rates and torques are involved.

An approximate closed-form solution of the minimum-time switching characteristics has been presented and allows the calculation of the switching instant very easily at any moment along the trajectory. However, the increase of digital control has directed the search towards a digitalized controller. The quantization of the switching predictor has led to a function, somewhat similar to a true stepper.

An original design, realizing a bang-bang controller has been developed and tested. The objective of the design was to realize an easy, cheap system realizing very constringent conditions.

Electrical braking is found to apply very high decelerations, therefore, the control cycle is very short, within 100 ms generally. The simple implementation and realization of the bang-bang controller has led to a series of discussions and a major difficulty

has been pointed out. There is no actual device which can provide sufficiently accurate informations about the instantaneous velocity of a rotating shaft. Analogue instruments have noise components in the frequency range to be measured, hence unfiltrable, unless the initial signal be degraded.

Digital instrumentation, although noise free, does not provide instantaneous speeds, and moreover, zero speed cannot be detected because of quantization noise. In any case, the rate of informations are far too slow for the purpose of fast speed transients.

Therefore a new line of research had to be investigated, and a digital instrument, based on an entirely new concept has been developed. This digital tachometer, although relatively inexpensive and simple, meets all the requirements of control systems. The sampling time is reduced to less than 600 μs, hence the speed reading can be considered instantaneous for mechanical loads. Besides the rate of information is always between 1600 and 14,000 samples/sec, with a very accurate zero detection. A resolution of .1 rd/s and precision of less than .2% add to the quality of this instrument.

With this new tachometer the bang-bang controller becomes fully digital, with noise free signals, and enables it to function exactly according to the theoretical control law.

The effective control differs from the optimum by only a few milliseconds, and the cycle of the trajectory is very near from the rectangular response.

Many applications can be found for such a position controller, and some were discussed more thoroughly, but it has to be pointed out that the development of the new digital tachometer opens up wide areas of research where the lack of velocity informations inhibit the work.

Very fast transients can be studied, allowing direct computer control, since digital informations are provided. Optimum control loops with on-line parameter identifications are possible now, and avoid very complicated learning procedures.

Hopefully, the development of such a new instrument will direct further research in computer control of rotating shafts, especially when load variations or unknown loads are present, a problem which had no practical solution up until now.

APPENDIX A

A SCHMIDT-TRIGGER FOR DRIVING STANDARD I-C PACKAGES

Because of the low input impedance associated with integrated-circuit packages it is difficult to cascade these with normal transistorized Schmidt-triggers without affecting the sharpness of the trailing edge of the pulse. Moreover, the transistor switching is too slow if the information is fed into a clock, the standard requirement being a rise-time smaller than 3 microseconds.

The following scheme, using integrated-circuit inverters, solves the problem of switching-time and presents the advantage of requiring a single 5-volt source, and also provides a very clean pulse sharp at both edges. Figure AP1 shows the circuit used. The ratio r_1/R_0 determines the hysteresis levels and R_0 should be less than 1.5K in order to match the input impedance of the inverter I1.

The operation of the circuit will now be explained. Suppose that v is zero or negative. The output of I1 is then forced to be the state "1" and the output of I2 is the state "0". Hence, the voltage at B is 0 volts, maintaining stable equilibrium. As long as the voltage at A is below 0.175 V (the switching theshold of the IC package), stable equilibrium is maintained. If v rises so that the voltage at A reaches the threshold value, the output of I1 decreases, causing the voltage at B to rise, which in turn, forces the voltage at A to increase rapidly due to the positive feedback. The new equilibrium point is reached within

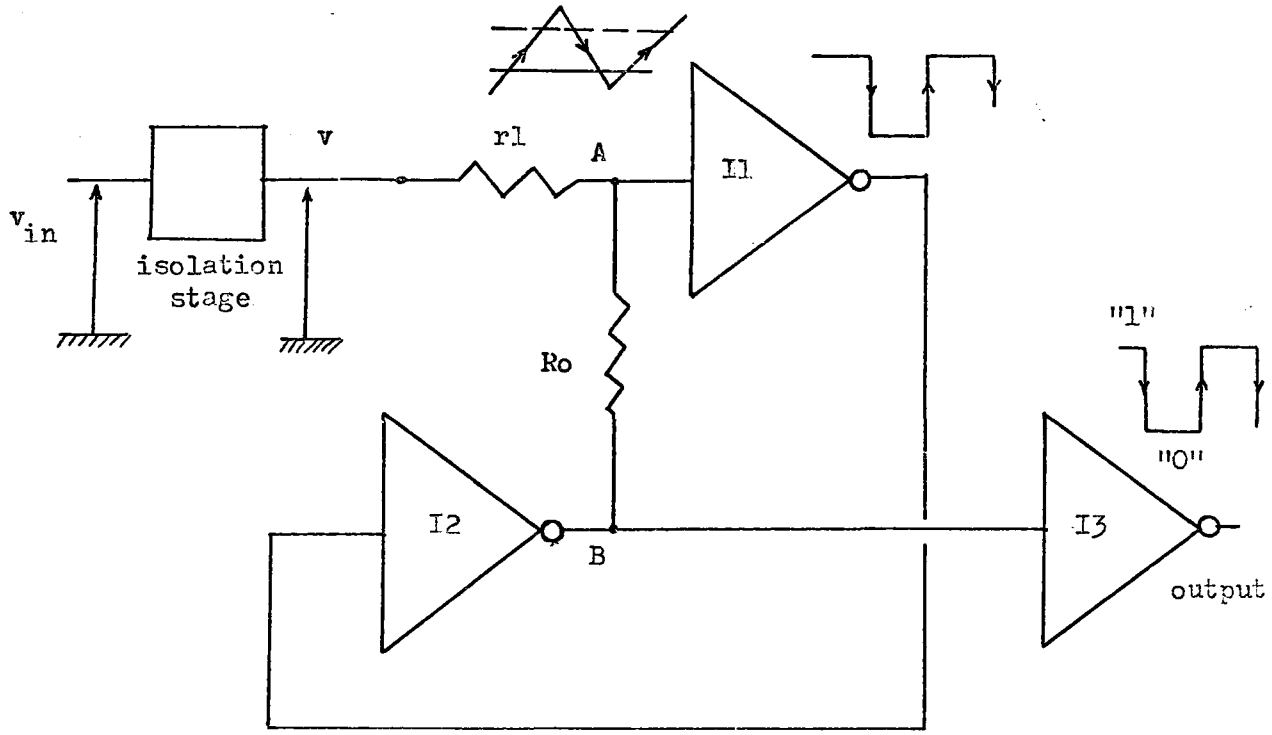

FIGURE AP1 : Schmidt-Trigger implementation

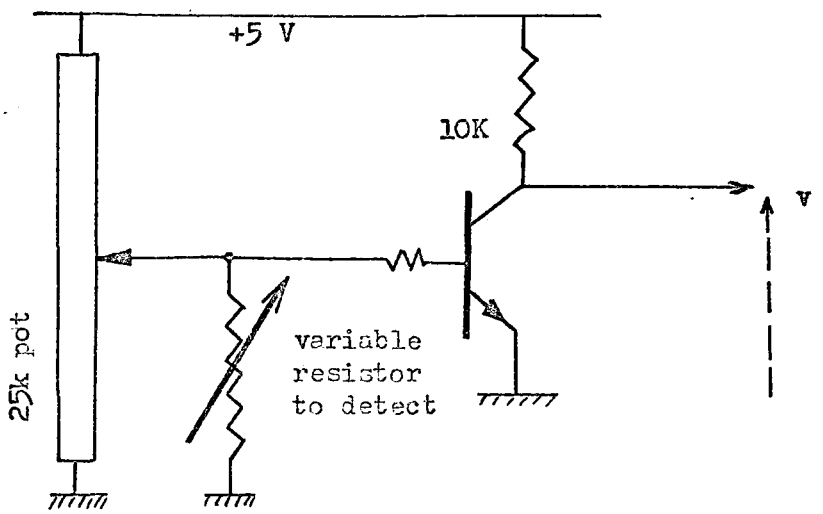

FIGURE AP2 : typical isolating stage

50 to 100 nanoseconds with the voltage at B equal to +4V, and a stable equilibrium is maintained. In order to switch I1 again, the voltage at A has to drop below another level. This will cause the output of I1 to increase, forcing the output of I2 to zero realizing another positive feedback. This double feedback characteristic is one of the main features of this circuit.

The inverter I3 is used here only to smooth out the "high" and "low" final levels and also serves to isolate the output impedance-wise.

The main advantages of the circuit are the following:

i) It is very economical. For example, one IC7404 package provides 2 Schmidt triggers costing less than $2.00.

ii) The switching time is very small, between 50 to 100 nanoseconds.

iii) Its output can be connected directly to IC digital logic components.

iv) It requires a single 5-volt supply.

The main drawbacks are the following:

i) As with a normal transistorized Schmidt trigger, the calculations for the switching levels are complicated and one required the switching characteristics of the inverters as well as their input impedances.

ii) An isolating stage has to be used for the input voltage unless the voltage source has negligible internal impedance.

Figure AP2 proposes an isolating stage to detect a variable resistor, like a photodiode, contaminated with noise. The hysteresis of the Schmidt trigger allows precise threshold detection.

BIBLIOGRAPHY

A. On Stepping Motors

[1] A.G. Thomas and J.F. Fleischauer, "The power stepping motor - a new digital actuator", Contr. Engrg., vol. 4, pp. 74-81, January 1957.

[2] S.J. Bailey, "Incremental servos - Introduction", Control Engrg., vol. 7, pp. 123-127, November 1960.

[3] ———— "Operation and analysis", Control Engrg., vol. 7, pp. 97-102, December 1960.

[4] ———— "Applications", Control Engrg., vol. 8, pp. 85-88, January 1961.

[5] ———— "Industry survey", Control Engrg., vol. 8, pp. 133-135, March 1961.

[6] ———— "Interlocking steppers", Control Engrg., vol. 8, pp. 116-119, May 1961.

[7] J.P. O'Donahue, "Transfer function for a stepper motor", Control Engrg., vol. 8, pp. 103-104, November 1961.

[8] A.E. Snowden and E.M. Madsen, "Characteristics of a synchronous inductor motor", Trans. AIEE (Application and Industry), vol. 8, pp. 1-5, March 1962.

[9] N.L. Morgan, "Verstile inductor motor for industrial control problems", Plant Engrg, vol. 16, pp. 143-146, June 1962.

[10] J. Proctor, "Stepping Motors move in", Product Engrg., vol. 34, pp. 74-78, February 1963.

[11] A.O. Morreale, "Theory and operation of step-servo motor", Elec. Design News, July 1963.

[12] R.B. Kieburtz, "The step motor - the next advance in control systems", IEEE, vol. AC-9, pp. 98-104, January 1964.

[13] G. Baty, "Control of stepping motor positioning systems", Electromech. Des., vol. 9, pp. 28-39, December 1965.

[14] T.R. Fredriksen, "Closed-loop stepping motor application", Proc. 1965 JACC, pp. 531-538.

[15] ———— "New developments and applications of the closed-loop stepping motor", Proc. 1966 JACC, pp. 767-775.

[16] ———— "Direct digital processor control of stepping motors", IBM J Research and Develpt., vol. 11, March 1967.

[17] ———— "Stepping motors come of age", Electrotechnology, vol. 80, pp. 36-41, November 1967.

[18] ———— "Applications of the closed-loop stepping motor", IEEE Trans., vol. AC-13, pp. 464-474, October 1968.

[19] ———— "The closed-loop stepping motor, an ideal actuator for process control", Automatica, vol. 5, pp. 61-65, 1969.

[20] Philips Product News, "Stepper motors", 1969.

[21] M.A. Delgado, "Mathematical model of a stepping motor operating as a fine positioner around a given step", IEEE Trans., vol. AC-14, pp. 394-397, August 1969.

[22] K. Venkataratnam, S.C. Sarkar and S. Palani, "Synchronizing characteristics of a step motor", IEEE Trans., vol. AC-14, pp. 510-517, October 1969.

[23] R.F. Mathams, "Phase-plane analysis of a permanent-magnet stepping motor", Electronics Letters, vol. 4, March 22, 1968.

[24] B.C. Kuo, G. Singh and R. Yackel, "Modelling and simulation of a stepping-motor", IEEE Trans., vol. AC-14, pp. 745-747, December 1969.

[25] ———————————— "Time-optimal control of a stepping motor", IEEE Trans., vol. AC-14, pp. 747-749, December 1969.

[26] A.J. Bianculli, "Stepper motors: Application and selection", IEEE Spectrum, pp. 25-29, December 1970.

B. Permanentic Motors

[1] E. Arnold, "La machine dynamo à courant continu", Béranger Ed., tomel, 1904.

[2] A.E. Fitzgerald and C. Kingsley, "Electric machinery", 2nd Edit., McGraw-Hill.

[3] D. Ginsberg and L.S. Misenheimer, "Design calculations for permanent magnet generator", AIEE Trans., vol. 72, Part II, 1953.

[4] D.D. Hershberger, "Design considerations of fractional horsepower size permanent magnet motors and generators", AIEE Trans., vol. 72, part III, 1953.

[5] A. Langsdore, "Principles of d.c. machines", 5th Edit., McGraw-Hill, 1940.

[6] E. Pillet, "Machines à courant continu", tome 1, ENSEHRG, Grenoble, 1962.

[7] E. Pillet et M. Sylvestre-Baron, "Complément à l'étude de la réaction magnétique d'induit dans les machines à courant continu", Compte rendu des séances de l'Académie des Sciences, tome 254, séance du 25 juin 1962, pp. 4442-4443.

[8] ———————————— "Réaction magnétique d'induit dans les machines à aimants permanents", Compte rendu des séances de l'Académie des Sciences, tome 256, séance du 18 mars 1963, pp. 3038-3041.

[9] M. Sylvestre-Baron, "Réaction magnétique d'induit dans les machines à aimants permanents", ENSEHRG, Grenoble, Thèse de Doctorat, 1963.

[10] B. Szabados, "Precise mathematical models for electromagnetic and permanentic motors", M.Eng. Thesis, McMaster University, Hamilton, Ontario, January 1969.

[11] B. Szabados, C.D. diCenzo and N.K. Sinha, "Dynamic measurements of the main electrical parameters of a D.C. machine", IEEE Trans. Industry and General Applications, vol. IGA-7, No. 1, pp. 109-115, February 1971.

[12] B. Szabados, N.K. Sinha and C.D. diCenzo, "Comparison of mathematical models for d.c. motors", Part I, "Definition and measurement of the main parameters", to be published in Control Engineering.

[13] ———————————— Part II, "Establishment of mathematical models for d.c. motors", to be published in Control Engineering.

[14] B. Szabados, N.K. Sinha and C.D. diCenzo, "Practical switching characteristics for minimum-time position control using a permanent-magnet motor", ready for publication.

[15] ———————— "Stepping motors versus permanent-magnet motors for control application", ready for publication.

[16] ———————— "A time-optimal digital position controller using a permanent-magnet d.c. servomotor", ready for publication.

[17] M.S. Garrido, "Eléments d'une théorie dynamique des machines électriques", Revue Générale de l'Electricité, tome 77, no. 1, pp. 27-33, janvier 1968.

C. General References

[1] R.C. Dorf, "Modern control systems", Addison-Wesley Publ. Co., pp. 34-37, 1967.

[2] S.S. Kuo, "Numerical methods and computers", Addison-Wesley 3955, pp. 115-123, 1966.

[3] "360 Scientific Subroutine Package", RKGS, pp. 118-121.

[4] A.P. Sage, "Optimum Systems Control", Chapter 4 (Prentice-Hall Inc.) 1968.

[5] G. Hoffmann de Visme, "Digital processing unit for evaluating angular acceleration", Elect. Engrg., April 1968, pp. 183-188.

[6] A. Dunworth, "Digital instrumentation for angular velocity and acceleration", IEEE Trans., vol. IM-18, June 1969.

[7] N.K. Sinha, B. Szabados and C.D. diCenzo, "New high precision digital tachometer", Electronics Letters, vol. 7, no. 8, pp. 174-176, April 1971.

[8] R.E. Locher, "On switching inductive loads with power transistors", General Electric Co., Auburn, N.Y., pp. 256-262.

[9] R.C.A. Silicon Power Circuits Manual, Technical series SP-50, 1967.

[10] Christofides and Adkins, "Determination of load losses and torques in squirell cage induction motors", Proc. IEE, December 1966.

[11] I. Tiroshi and J. Ben-Uri, "Analysis of an up-down counter used as velocity-servo error register", IEEE Trans., vol. AC-13, pp. 93-96, February 1968.

[12] J.M. Stephenson, "New low-noise tachogenerator", Proc. IEE, vol. 116, no. 11, pp. 1981-1983, November 1969.